https://ntrs.nasa.gov/search.jsp?R=20010093211 2018-05-14T14:49:11+00:00Z

NASA/CR—2001-211112



Probabilistic Structural Analysis and Reliability Using NESSUS With Implemented Material Strength Degradation Model

Callie C. Bast, Mark T. Jurena, and Cody R. Godines
University of Texas, San Antonio, San Antonio, Texas

Prepared under Grant NAG3–2060

National Aeronautics and
Space Administration

Glenn Research Center

July 2001

Acknowledgments

The authors gratefully acknowledge the guidance and encouragement of Drs. Christos C. Chamis and Shantaram Pai and the support of NASA Glenn Research Center and the Minority University Research and Education Program, NASA Headquarters. Professors Lola Boyce, David Crane, and Randall Manteufel are recognized for their participation and contributions to the summer courses. Also acknowledged is Mr. Henock Perez, Undergraduate Research Assistant during Year 2, for his "behind the scenes" contributions to this project.

Contents were reproduced from the best available copy as provided by the authors.

Available from

NASA Center for Aerospace Information
7121 Standard Drive
Hanover, MD 21076

National Technical Information Service
5285 Port Royal Road
Springfield, VA 22100

Available electronically at http://gltrs.grc.nasa.gov/GLTRS

TABLE OF CONTENTS

SECTION PAGE

LIST OF TABLES iv

LIST OF FIGURES v

NOMENCLATURE vi

1.0 RESEARCH

1.1 INTRODUCTION 1

1.2 NESSUS 3

1.3 RELIABILITY 7

1.4 TURBOPUMP BLADE AND DATA FILES 17

1.5 RELIABILITY RESULTS 25

1.6 SENSITIVITY FACTOR RESULTS 29

1.7 DISTRIBUTION TYPE ANALYSIS 31

1.8 CONCLUSIONS 39

2.0 EDUCATION

2.1 INTEGRATION OF RESERCH AND EDUCATION OBJECTIVES 41

2.2 1998 AND 1999 SUMMER COURSES 41

2.3 NESSUS STUDENT USER'S MANUAL 42

3.0 ACCOMPLISHMENTS

3.1 ACCOMPLISHMENTS: RESEARCH 43

3.2 ACCOMPLISHMENTS: EDUCATION 45

3.3 STUDENT ACHIEVEMENTS 45

5.0 REFERENCES 47

APPENDIX I 49

APPENDIX II 53

APPENDIX III 91

APPENDIX IV 129

LIST OF TABLES

Table 1.4.1 Random Inputs for Stress 19

Table 1.4.2 Random Inputs for Strength 22

Table 1.4.3 Sample NESSUS Input File 23

Table 1.4.4 Sample NESSUS Output File 24

Table 1.5.1 Comparison of Probabilities of Failure and Reliability 25

Table 1.6.1 Ordered Sensitivity Factors 29

Table 1.7.1 Effect of Distribution on Probabilities of Failure 33

LIST OF FIGURES

Figure 1.3.1 Strength and Stress Probability Plot 9

Figure 1.3.2 Limit State Diagram 10

Figure 1.3.3 Overlap of Strength - Stress 11

Figure 1.3.4 Limit State in u-Space for Two Random Variables 12

Figure 1.4.1 Drawing of the Physical Turbopump Blade 17

Figure 1.4.2 Drawing of the Blade's Constraints and Forces 18

Figure 1.5.1 Overlap of the Strength and the Stress Plots 26

Figure 1.5.2 Reliability Plots on Normal Probability Paper 27

Figure 1.6.1 Sensitivity Factors for the Random Variables 30

Figure 1.7.1 Probability Density Plot for the Centrifugal Loading (DLOAD) 32

Figure 1.7.2 Effect of Distribution on Loading (DLOAD) 34

Figure 1.7.3 Effect of Distribution on Strength (SO) 35

Figure 1.7.4 Effect of Distribution on Density (DMOD) 36

Figure 1.7.5 Effect of Distribution on Thickness (THICK) 37

NOMENCLATURE

A_i	current value of the i^{th} effect
A_{iU}	ultimate value of the i^{th} effect
A_{iO}	reference value of the i^{th} effect
a_i	i^{th} value of the empirical material constant
C_{XiXj}	variance-covariance matrix
DMOD	random variable input name for mass density
DLOAD	random variable input name for centrifugal loading
EMOD	random variable input name for modulus of elasticity
n	number of effects (product terms) in the model
N	random variable input name for current value of high cycle mechanical fatigue cycles
N	current value of high cycle mechanical fatigue cycles
N'	current value of low cycle mechanical fatigue cycles
N''	current value of thermal fatigue cycles
NU	random variable input name for ultimate number of high cycle mechanical fatigue cycles
N_U	ultimate value of high cycle mechanical fatigue cycles
N'_U	ultimate value of low cycle mechanical fatigue cycles
N''_U	ultimate value of thermal fatigue cycles
NO	reference number of high cycle mechanical fatigue cycles random variable input name
N_O	reference value of high cycle mechanical fatigue cycles
N'_O	reference value of low cycle mechanical fatigue cycles
N''_O	reference value of thermal fatigue cycles
PMOD	random variable input name for Poisson's ratio
QQ	random variable input name for the empirical material constant for temperature
q	material constant for temperature
w	material constant for high cycle mechanical fatigue
r	material constant for low cycle mechanical fatigue
S	current value of material strength
S_O	reference value of material strength
T	current value of temperature

NOMENCLATURE (continued)

T	random variable input name for current temperature
T_U	ultimate value of temperature
TU	random variable input name for ultimate value of temperature
T_O	reference value of temperature
t	current value of creep time
t_U	ultimate value of creep time
t_O	reference value of creep time
u	material constant for thermal fatigue cycles
v	material constant for creep time
W	random variable input name for empirical material constant for high cycle mechanical fatigue cycles
μ	mean
σ	standard deviation
ρ_{ij}	correlation coefficient

1.0 RESEARCH

1.1 INTRODUCTION

Probabilistic structural analysis methods are particularly useful in the design and analysis of space propulsion systems operating in severe and uncertain environments. By quantifying the uncertainties associated with the design, these methods play a critical role in establishing increased performance and reliability for such systems, both current and future. A prime example of a current space propulsion system is the Space Shuttle Main Engine (SSME). For this project, a fuel turbopump blade, a component of the SSME, was analyzed using a probabilistic finite element code, NESSUS, along with an embedded Material Strength Degradation (MSD) model.

The use of NESSUS and the MSD model are dictated by the dispersion of the physical quantities involved. The considerable scatter of experimental data and the lack of an exact description of the underlying physical processes for the combined mechanisms of fatigue, creep, temperature variations and so on, make it natural, if not necessary to consider probabilistic models for a strength degradation model. This engine operates in a harsh environment with high loads and temperature extremes. As noted from C.C. Chamis and D.A. Hopkins *". . . hot rotating structural components are relatively small. Fabrication tolerances on these components which in essence are small thickness variations, can have significant effects on the component structural response. Fabrication tolerances by their very nature are statistical. Furthermore, the attachment of components in the structural system generally differ by some indeterminate degree, from that assumed for designing the component. In summary, all four fundamental aspects: (1) loading conditions, (2) material behavior, (3) geometrical configuration and (4) supports on which structural analysis are based, are of a random nature. The direct way to formally account for all these uncertain aspects is to develop probabilistic structural analysis methods where all participating variables are described by appropriate probabilistic density functions. [1]"* The SSME fuel turbopump blade discussed here is a prime example of a small component whose variations in thickness, strengths, etc., significantly affect its structural response.

The main objective of this project was to determine which input parameters most influence the structural response of the turbopump blade. A finite element model of a turbopump blade, composed of Inconel 718, a material for which the MSD model is calibrated, was analyzed for the effects of high temperature and high cycle mechanical fatigue. Section

1.2 presents NESSUS and the newly implemented MSD model. An overview of statistical terminology and definitions concerning structural reliability are provided in Section 1.3.

Section 1.4 characterizes the SSME fuel turbopump blade as well as outlines NESSUS input and output data files. Sections 1.5 through 1.7 present analysis results. In Section 1.5 reliability results are presented and comparisons between the Advanced Mean Value (AMV) method and the well-known Monte Carlo Simulation method are summarized. Section 1.6 discusses sensitivity factor results. Also discussed is the effect on sensitivity factor results for a change in the blade thickness random field from a single correlated random variable to a partially correlated random variable. Section 1.7 examines how changing the distribution type on a single random variable influences both reliability and sensitivity factor results. Conclusions drawn from these results are presented in Section 1.8.

1.2 NESSUS

Historically, NESSUS has provided probabilistic structural analysis for the response of engineered structures. It integrates both probabilistic analysis and finite element methods to produce a useful tool for both design and analysis of critical structural components. NESSUS allows for both random and deterministic descriptions of input and output quantities. For example, input parameters for material properties such as Young's modulus, Poisson's ratio, and mass density can be modeled as random variables wherein the user provides the appropriate statistics, namely mean, standard deviation and distribution type [2]. In addition, random input can include random fields, as well as random variables. Distributions such as Gaussian, Weibull, or lognormal may be selected. Other input parameters, such as loading type, geometry, boundary conditions and initial conditions can also be considered random. Then, probabilistic analysis yields the cumulative distribution functions (CDF's) of the output random variables, e.g., stresses, strains, displacements, etc.

Code Organization

NESSUS is divided into ten parts. The preprocessor, NESSUS/PRE, provides for the representation of random fields. NESSUS/PRE computes a set of independent random variables from the random fields using an eigenvalue decomposition [3]. PFEM is the module for coordinating the operations between the finite element code and FPI. Next, a deterministic finite-element module, NESSUS/FEM, generates the deterministic responses of the finite-element structural model to a number of prescribed perturbations of the input variables. NESSUS/FEM contains a mixed iterative procedure to obtain the response of a structure. A Newton-Raphson iterative procedure based on a mixed variational principle can be used in NESSUS/FEM. Besides FEM, BEM, the boundary element module is used for structural analysis. These deterministic solutions provide the data from which a first or second-order Taylor series of the response is fit that defines the explicit functional relationship between the input random variables and the response of interest. The postprocessor, NESSUS/FPI (Fast Probability Integration), performs the probability calculations. The postprocessor also includes a choice of probabilistic analysis methods other than FPI, including for example, Adaptive Importance Sampling (AIS) and Monte Carlo simulation [4,5]. SIMFEM however, contains the driving module for the Monte Carlo as well as the Latin Hypercube sampling of the structure. There are also other packages for specialized analysis such as the RISK, SYSTEM and SYSRSK modules. The RISK module computes the risk with respect to cost or a user defined criteria. The SYSTEM module is an alternate system reliability method for probabilistic fault tree analysis. The SYSRSK module computes the system risk by combining the cost of failure, in terms of replacement, inspection, repair or other criteria of individual

components of the system with their probability of failure. The current version of NESSUS provides these ten component parts in an integrated package. These modules can be used in various combinations as the user desires.

This project required the use of the PRE, PFEM, FEM and FPI modules. For the random thickness field, PRE was used to compute a set of independent random variables from the random field thickness input using an eigenvalue decomposition. The resulting file was then used by the PFEM, FEM and FPI modules for further analysis.

The AMV method is a mean-based predictor-corrector method which uses local gradients to project the results for the entire CDF then corrects the prediction with a re-analysis of the structural model at each predicted point. The local gradients are usually, but not necessarily, taken about the mean values of the random variables. The AMV method with iterations, termed AMV+, is an extension of the AMV method. It involves new gradient computations about the previously predicted results. These new gradients are then used to compute an improved result. Both AMV and AMV + results can either be specified as an automatic CDF analysis, a number of probability levels or a specified response corresponding to a specified probability [6]. Convergence to a specific tolerance can be specified by the user. The FEM module then calculates the deterministic response where the Newton-Raphson iterative procedure is enabled. Finally the FPI module calculates the structural reliability of the turbopump blade.

Material Strength Degradation (MSD) Model

The enhanced version of NESSUS reported in this document, includes a previously developed probabilistic material strength degradation (MSD) model [7]. The MSD model in the form of a postulated randomized multi-factor equation provides for quantification of uncertainty in the lifetime strength of components subjected to a number of diverse random effects. Presently, the model includes five effects that typically reduce lifetime strength:

- high temperature
- high-cycle mechanical fatigue
- low-cycle mechanical fatigue
- creep
- thermal fatigue

The MSD model was calibrated for INCONEL 718 by appropriate curve-fitted least squares linear regression of experimental data. Linear regression of the data for each effect resulted in estimates for the empirical material constants, as given by the slope of the linear fit. These estimates, together with ultimate and reference values, were used to calibrate the model specifically for Inconel 718 [8]. Lifetime material strength results, in the form of cumulative

distribution functions (CDF's), illustrate the sensitivity of lifetime strength to any one, or a combination of, the five effects. The mathematical expression for this MSD model is:

$$\frac{S}{S_O} = \prod \left[\frac{A_{iU} - A_i}{A_{iU} - A_{iO}} \right]^{a_i} \tag{1.2.1}$$

where, A_i, A_{iU} and A_{iO} are the current, ultimate and reference values, respectively, of a particular effect; a_i is the value of the calibrated empirical material constant for the i^{th} effect terms of the variables in the model; and S and S_O are the current and reference values of material strength. Each term has the property that if the current value equals the ultimate value, the lifetime strength will be zero. Also, if the current value equals the reference value, the term equals one and strength is not affected by that value. The product form of equation (1.2.1) assumes independence between individual effects. This equation may be viewed as a solution to a separable partial differential equation in the variables with the further limitation or approximation that a single set of separation constants, a_i, can adequately model the material properties.

The multifactor equation for material strength degradation (MSD) was implemented in NESSUS using the NZFUNC subroutine that was initially developed for predefined resistance models[9]. All input from the MSD model is in the NESSUS/PFEM input deck using a keyword interface consistent with previous versions of NESSUS.

The model is currently set up for five fixed effects and twelve general effects that can be defined by the user. The fixed effects include: Temperature, High cycle mechanical fatigue, Low cycle mechanical fatigue, Creep, Thermal fatigue. When expanded for all effects, the equation is as follows:

$$S = S_O \left[\frac{T_u - T}{T_u - T_o} \right]^q \left[\frac{N_u - N}{N_u - N_o} \right]^w \left[\frac{N'_u - N'}{N'_u - N'_o} \right]^r \left[\frac{t_u - t}{t_u - t_o} \right]^v \left[\frac{N''_u - N''}{N''_u - N''_o} \right]^u \left[\frac{A_u - A}{A_u - Ao} \right]^a, \tag{1.2.2}$$

Temperature HCF LCF Creep Thermal Fatigue General

where T is temperature, N is cycles, t is time, and A is a user-defined effect. The lower case exponents are the empirical material constants for each effect. The subscript, u, refers to an ultimate value, the subscript, o, is the reference value, and the non-subscripted term is the current value for the effect.

To increase model sensitivity for the effect, a logarithmic base ten transformation is introduced. For Inconel 718, all effects except temperature require the logarithmic

transformation and have the following form.

$$S = S_o\left[\frac{LOG(A_{iU}) - LOG(A_i)}{LOG(A_{iU}) - LOG(A_{iO})}\right]^a \qquad (1.2.3)$$

For other materials, the nature of the data will dictate the use of the log transformation. The effects to be used and the model type (log transformation) are defined in the g-function definition section of the PFEM input file. Any combination of effects can be selected and any of the terms can be considered random if desired. The form of the g-function used by NESSUS is

$$g = S_O\prod_i\left[\frac{A_{iU} - A_i}{A_{iU} - A_{iO}}\right]^{a_i} - \sigma \quad , \qquad (1.2.4)$$

where S_O is the reference value of material strength, A_{iU} is the ultimate value of the particular effect, A_{iO} is the reference value of the particular effect, A_i is the current value of the particular effect, a_i is the empirical material constant for the particular effect, and σ is the structural response as calculated by NESSUS/FEM, i.e. stress. The equation expanded for the two effects of high temperature and high-cycle mechanical fatigue is shown in equation 1.2.5 below:

$$z = S_o\left[\frac{T_u - T}{T_u - T_o}\right]^q\left[\frac{LOG(N_U) - LOG(N_i)}{LOG(N_U) - LOG(N_O)}\right]^w - \sigma, \quad (1.2.5)$$

With the implementation of the MSD model, NESSUS can now determine the reliability of a structural component utilizing its material strength variability. Thus for example, NESSUS now produces statistical distributions for the component material strength, S, as well as a statistical distribution of component stress, σ.

1.3 RELIABILITY

Structural reliability calculations can be made using the Material Strength Degradation (MSD) model combined with the stress output from the FEA model. Structural reliability is the probability that the strength exceeds the stress as defined by equation 1.3.1 below:

$$R = P(S > \sigma) \quad , \tag{1.3.1}$$

where R is the structural reliability and P(S > σ) is the probability that the strength is greater than the stress. The von Mises stress term is used in this project since it represents a three-dimensional state of stress and is considered a good indicator for the onset of mechanical failure for ductile materials [10]. The equation for Von Mises stress is given below:

$$\sigma' = \left[\frac{(\sigma_1 - \sigma_2)^2 + (\sigma_2 - \sigma_3)^2 + (\sigma_1 - \sigma_3)^2}{2} \right]^{1/2} \tag{1.3.2}$$

where σ_1, σ_2 and σ_3 are the principal stresses. These principal stresses are the roots to the following cubic equation [11]:

$$\begin{aligned} &\sigma^3 - (\sigma_x + \sigma_y + \sigma_z)\sigma^2 + (\sigma_x\sigma_y + \sigma_x\sigma_z + \sigma_y\sigma_z - \tau_{xy}^2 - \tau_{yz}^2 - \tau_{zx}^2)\sigma \\ &\quad - (\sigma_x\sigma_y\sigma_z + 2\tau_{xy}\tau_{yz}\tau_{zx} - \sigma_x\tau_{yz}^2 - \sigma_y\tau_{zx}^2 - \sigma_z\tau_{xy}^2) = 0 \end{aligned} \tag{1.3.3}$$

In short, von Mises stress is a scalar value representing a three-dimensional state of stress. The distortion-energy theory predicts that yielding will occur whenever the distortion energy per unit volume equals the distortion energy in the same volume when yielded in a simple tensile test as shown in equation 1.3.4 below [12].

$$\sigma' \geq S_Y \tag{1.3.4}$$

The reliability approach is a departure from the factor of safety approach widely used in engineering design. Input of the usual physical quantities as either random variables or random fields has many advantages including:

- probability of failure- quantifies reliability
- sensitivity-identifies important variables
- importance

Using the probabilistic approach, an analysis of the turbopump blade model yielded a reliability of 0.999. Initially all of the random variables were modeled as normal distributions and the blade thickness was modeled as a fully correlated random field. Taking the median

value of the strength and the deterministic value of the stress from NESSUS, the factor of safety is:

$$N = \frac{S}{\sigma} = \frac{1.16107E05}{1.0554E05} = 1.10 \qquad (1.3.5)$$

The reliability measure of 0.999 denotes a failure for 1 in every 1000 uses. The factor of safety, N=1.10, implies the structure can withstand 1.1 times its nominal load. This may give the engineer a false sense of security. The factor of safety approach requires engineering judgement that results from experience.

The structure is also under high cycle fatigue. To this end the Goodman Equation is used [13] as given by Equation 1.3.6:

$$\frac{\sigma_a}{S_e} + \frac{\sigma_m}{S_{ut}} = \frac{1}{n}, \qquad (1.3.6)$$

where σ_m is the mean stress due to cyclic loading, σ_a is the average stress, S_{ut} is the ultimate strength of the material and S_e is the endurance limit of the material. This results in a factor of safety of 1.11 as shown below.

$$n = \left[\frac{32.5 \text{ ksi}}{111 \text{ ksi}} + \frac{105.5 \text{ ksi}}{173 \text{ ksi}}\right]^{-1} = 1.11 \qquad (1.3.7)$$

Reliability has advantages in that it quantifies the uncertainty of material properties and provides for the driving variables for design. While the reliability method has its advantages, it is at the expense of being more complex requiring a background in statistics and the comprehension of terms such as the performance function.

The performance function is a user-defined function. In this particular case, the performance function is defined as the equation:

$$Z = S - \sigma, \qquad (1.3.8)$$

where Z is a measure of performance such as stress, strain or displacement, S is the strength and σ is the von Mises stress [14]. The strength value resulting from the combined effects of high cycle fatigue and high temperature was defined previously in the MSD model. The von Mises stress, is used to compare with material strength and estimate failure or nonfailure.

The limit state is the surface that separates the density space into safe and fail regions where the performance function is zero. This limit state is termed g, as in the

following equation:

$$g(X) = S(X) - \sigma(X) = 0 \quad , \tag{1.3.9}$$

where g(**X**) is the limit state, defined on the domain of the vector of random variables **X**, S(**X**) is the strength and σ(**X**) is the stress. When σ and S are independent, i.e. no common random variables, their two distributions are as shown in Figure 1.3.1. Note that there is some overlap between the stress and the strength. The region where this overlap occurs is the probability of failure. For most design cases, attempts are made to minimize this overlap for a smaller probability of failure.

Within the vector **X** of equation 1.3.9, there are 13 random variables and 1 random field. These are further divided into 9 random variables for the MSD model and 5 for the stress side. The MSD model utilized includes the effects of: High-Cycle Fatigue (HCF) and High Temperature. The stress side's random variables are the loading, modulus of elasticity, Poisson's ratio, mass density and the thickness random field. The HCF components are the ultimate number of cycles, designated number of cycles, reference number of cycles and an empirical material constant (exponent). The temperature side of the strength includes the ultimate temperature, designated temperature, reference and an exponent. The remaining variable is the material's initial strength. These 13 random variables and 1 random field result in a complex failure hypersurface which is not easy to visualize. Fortunately NESSUS resolves this problem for the user.

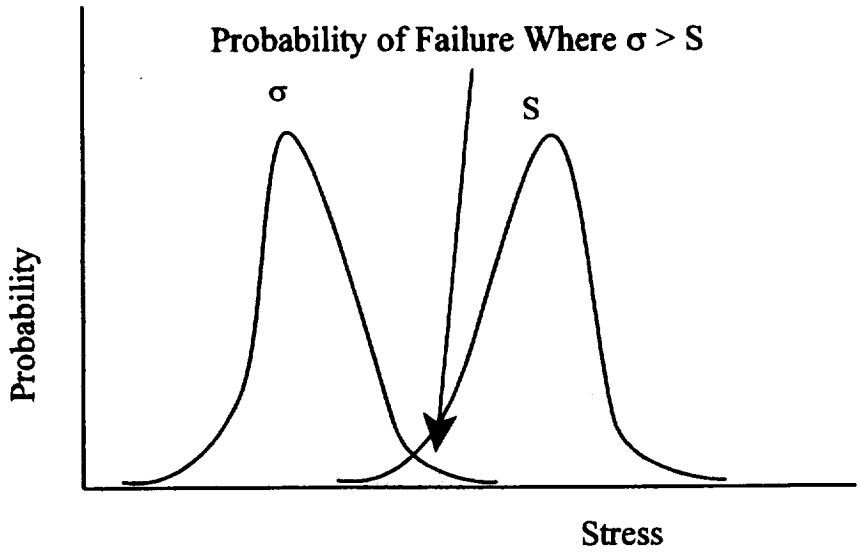


Figure 1.3.1 Strength and Stress Probability Plot

For the case of only two random variables included in a structural reliability analysis, the Joint Probability Density Function (JPDF) can be visualized. The probabilities are contours that are arranged such that the lowest probability is the biggest ellipse and the highest probability is the smallest ellipse. Thus the highest probability occurs at the center of the innermost ellipse in Figure 1.3.2. Recall that the limit state function is where the performance function equals zero, i.e. g = 0. This limit state function is usually desired to be some distance away from the location of the highest probability as shown in Figure 1.3.2. The probability that the structure will fail is upward and to the right and above the performance function.

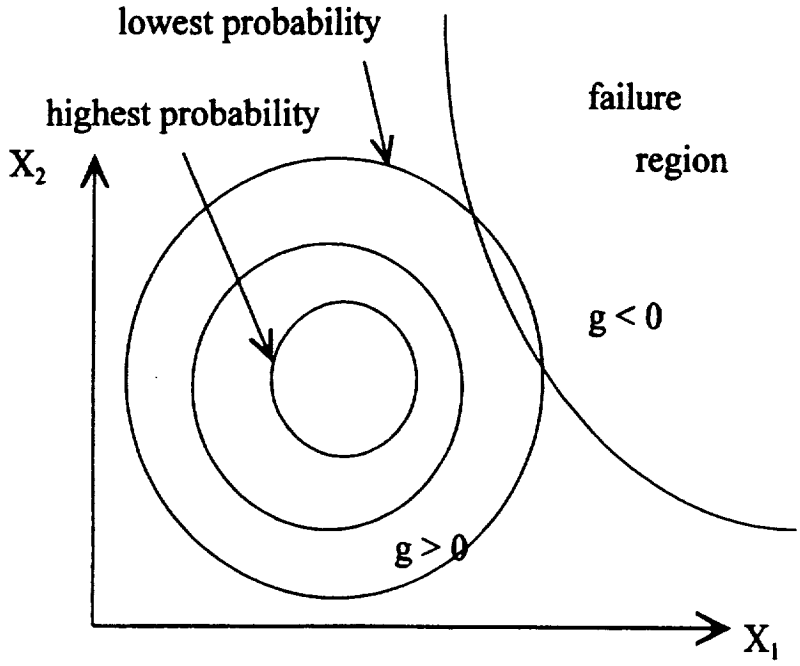


Figure 1.3.2 Limit State Diagram

Structural reliability is the probability that the structure will not fail. This is given by the following equation:

$$\text{Re}liability = P(g > 0) \qquad (1.3.10)$$

where P is the probability. NESSUS output results yield the probability of failure, p_f. In terms of this failure, the reliability is calculated from equation 1.3.11 below:

$$\text{Re}liability = 1 - P(g < 0) \quad , \qquad (1.3.11)$$

where P(g<0) is the probability of failure. Thus, the area to the right of the origin in Figure 1.3.3 is the reliability of the particular structure and the shaded area to the left is the failure region.

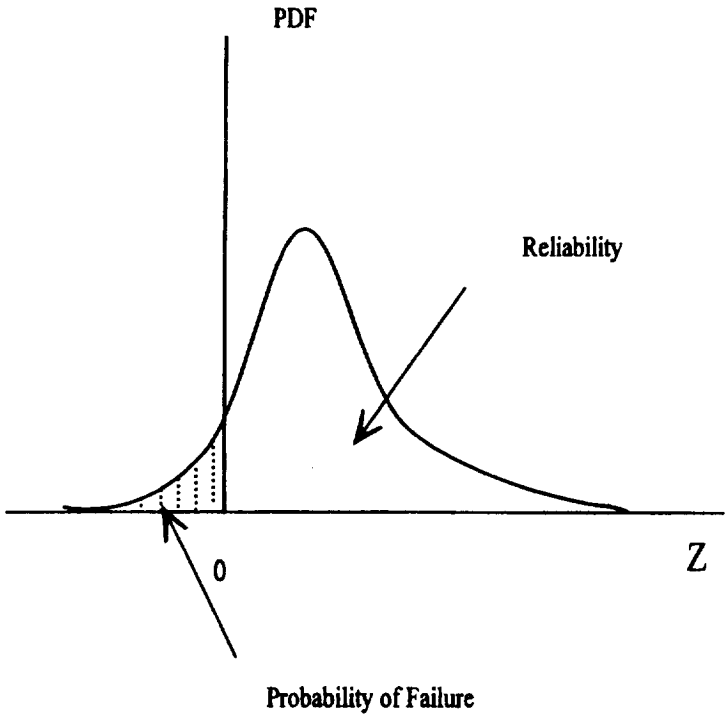
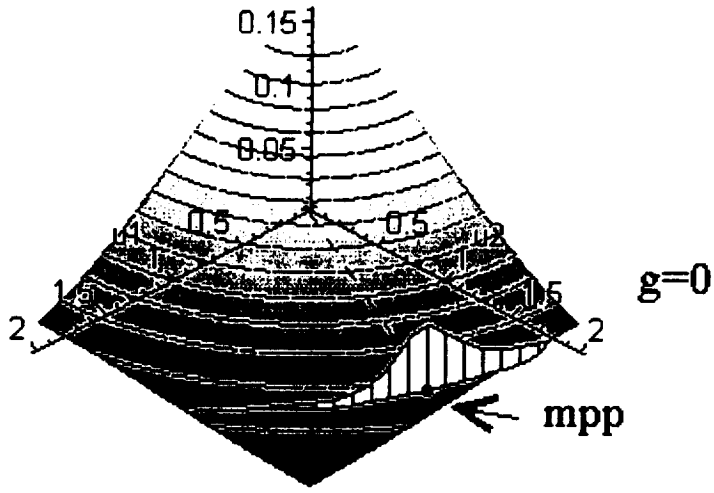


Figure 1.3.3 Overlap of Strength - Stress

Most Probable Point (MPP)

The Most Probable Point (MPP) is the point on the limit state with the highest joint probability as shown in Figure 1.3.4. Note that this joint PDF is three-dimensional and is now centered about the origin. This is due to the Rosenblatt transformation. The Rosenblatt transformation can be used for correlated random variables and is a transformation whereby distributions are transformed from one distribution to another [15]. In NESSUS, the Rosenblatt transformation is impractical because the available data is often insufficient to establish the joint and the conditional probability distributions In this case the usual random variables are transformed from an original input distribution into a standard normal distribution. This is where the mean of the distribution is zero and the standard deviation is one.



Cut volume = P(Z<=0)

Figure 1.3.4 Limit State in u-Space for Two Random Variables

Beta

As the random variables are transformed into the standard normal distribution, the resulting distance from the origin to the MPP, termed beta, is defined by equation 1.3.12 .

$$\begin{aligned} \beta^2 &= (u)_1^2 + (u)_2^2 + (u)_3^2 + \cdots (u)_n^2 \\ &= \sum_{i=1}^{n} (u)_i^2 \end{aligned} \tag{1.3.12}$$

where the $\mathbf{u}_i$ are the transformed random variables in standard normal space at the limit state. The probability of failure is approximately the value of the joint probability at the MPP as seen in the equation below:

$$P_f \cong \Phi(\beta) \approx \int \ldots \int_{g_{aprox}(u) \le 0} f_u(u) du \tag{1.3.13}$$

where f_u is the joint probability distribution function and $g_{approx.}$ is the approximation of the limit state g. This approximation of g can be a polynomial, usually either a linear or quadratic equation.

Sensitivity Factors

The sensitivity factors are a ranking of which random variables "drive" or most influence the output results, e.g. probability of failure. These are useful in the assessment of which random variables need to be changed for design optimization.

These sensitivity factors are defined as the direction cosines to the MPP of the input random variables for NESSUS. The sensitivity factor, α, is given by equation 1.3.14 below.

$$|\alpha_i| \propto \left(\frac{\partial g}{\partial X_i} \right) \sigma_i \tag{1.3.14}$$

where α_i is the sensitivity factor, i indexes the random variable number, $\frac{\partial g}{\partial X_i}$ is the gradient of the limit state with respect to the particular random variable X_i, and σ_i is the standard deviation of the ith random variable. When the limit state is taken as a linear approximation, the following equation holds:

$$\alpha_i = \frac{\partial [g(X)]}{\partial (X_i)} = \frac{\partial \left[a_o + \sum_{i=1}^{n} a_i u_i \right]}{\partial (X_i)} , \tag{1.3.15}$$

where g is the linear approximation of the limit state, n is the number of random variables, and a_o and a_i are constants determined by Taylor's series expansion NESSUS [16].

Distribution Types

The lognormal and Weibull distributions are derived from the normal distribution. The lognormal distribution was calculated using the following equations [17]:

$$C_x = \frac{\sigma_x}{\mu_x} \quad , \tag{1.3.16}$$

where C_x is the coefficient of variation, σ_x is the standard deviation and μ_x is the mean from the normal distribution. Likewise for the median the equation is:

$$\tilde{X} = \frac{\mu_x}{\sqrt{1+C_x^2}} \quad , \tag{1.3.17}$$

where is the median of the distribution.

The Weibull distribution was calculated using the following equations:

$$f_x = \left(\frac{\alpha}{\beta}\right)\frac{x^{\alpha-1}}{\beta}\exp\left[-\left(\frac{x}{\beta}\right)^{\alpha}\right] \quad x>0,\ \alpha>0,\ \beta>0 \quad , \tag{1.3.18}$$

where α is defined as;

$$\alpha = C_x^{-1.08} = \left(\frac{\sigma_x}{\mu_x}\right)^{-1.08} \quad , \tag{1.3.19}$$

β is defined as;

$$\beta = \frac{\mu_x}{\Gamma\left(\frac{1}{\alpha}+1\right)} \quad , \tag{1.3.20}$$

and Γ is defined as the integral;

$$\Gamma(x) = \int_0^{\infty} t^{x-1}e^{-t}dt \tag{1.3.21}$$

Monte Carlo Simulation

Reliability results were calculated using the Advanced Mean Value Method (AMV) and the well-known Monte Carlo Simulation method. Using the Advanced Mean Value Method requires several steps: computing sensitivities by perturbing each random variable and recomputing the response; using the Fast Probability Integration (FPI) to compute the Mean Value (MV) cumulative distribution function (CDF.) and associated Most Probable Point (MPP); the response at the predicted MPP for each probability level; and computing the sensitivities about the predicted MPP. The last two steps are AMV and AMV+ respectively. Once these last two steps are performed, the run proceeds through FPI to compute the response at each probability level and new MPP [18]. With the FPI calculated the convergence criteria is

measured at each probability level. If the response does not converge, the data is run through the AMV and AMV+ steps until convergence is reached [19].

Monte Carlo Simulation is a more widely accepted method for calculating reliability results. The method is more robust than AMV+ in that it is independent of the number of random variables. Monte Carlo Simulation uses random samples from the probability distributions of each random variable and computes the response. The probability of failure is determined by counting the number of failures and dividing by the total number of samples. The method is exact as the number of simulations approaches infinity. The major disadvantage of this method is the computing time required for large sample sizes. Thus the number of simulations (samples) must be given careful consideration. In many "quick and dirty" calculations, a very simple equation for determining the sample size is shown in equation 1.3.22 below [20]:

$$N \geq \frac{10}{p_f} \tag{1.3.22}$$

where, N is the number of samples for the Monte Carlo simulation required for the given probability of failure; p_f The Shooman equation gives a more accurate assessment of how many points are necessary for a given probability of failure. The Shooman equation is that given by Equation 1.3.23 [20]:

$$\%error = 100 \cdot \Phi^{-1}[(1-\alpha)/2] \cdot \sqrt{\frac{1-p_f}{k-p_f}} \quad , \tag{1.3.23}$$

where (1- α) is the confidence desired and $\Phi^{-1}[(1-\alpha)/2]$ is the inverse probability of the confidence divided by two. For calculating the number of points for a 95% confidence the Shooman equation is as follows:

$$N = \frac{1-p_f}{p_f} \cdot \left(\frac{200}{\%error}\right)^2 \quad , \tag{1.3.24}$$

where the %error could be some reasonable value, usually between 5% and 20%.

1.4 TURBOPUMP BLADE AND DATA FILES

Previously, the probabilistic analysis of a single structural member, a MAR-M246 SSME turbopump blade was undertaken [21]. The finite element model used is a reasonably realistic representation of the Space Shuttle Main Engine fuel turbopump blade shown below in Figure 1.4.1.

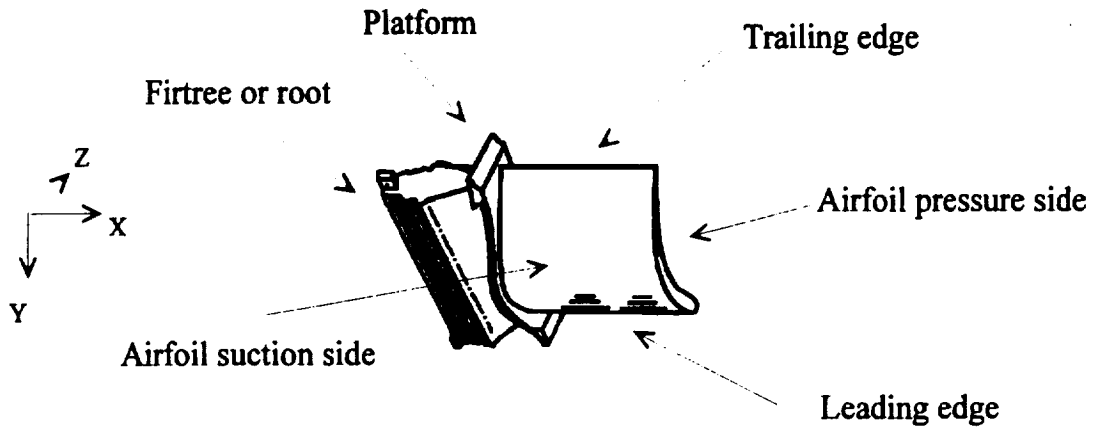


Figure 1.4.1 Drawing of the Physical Turbopump Blade

Note the overall shape of the structure that was modeled. It has a curved shape toward the tip of the aerodynamic surface and a less noticeable twist along the length of the turbopump blade. The various parts of the blade should be noted. They are the firtree root, the platform, the trailing edge, the leading edge, the airfoil suction side and the airfoil pressure side. The firtree root, sometimes called just the root attaches the turbopump blade to the rotor. Above the root is the platform. It separates the root and nonaerodynamic parts of the rotor from the fluid flow of the blade. Important to the fluid flow are the leading edge and the trailing edge. These parts are where the fluid flows toward and away from the blade, respectively. As mentioned before, this blade has curvature like a wing. Hence, to one side of the blade there is an area of high pressure and low velocity relative to an area with low pressure and high velocity. The high pressure side is called the airfoil pressure side and the low pressure side is called the airfoil suction side. At the right side, note that the thickness of the blade starts to decrease from the leading edge to the trailing edge. This is an important attribute to keep in mind when analyzing the resulting stresses. Figure 1.4.2 shows the boundary conditions and forces on the blade.

Note that on the left-hand side of the blade there is a cantilever on the center node surrounded by trolleys on the four outer nodes. These outer nodes are constrained to move transversely in the Z-direction so that the blade is allowed to twist within its attachment on the rotor as the torque of the aerodynamic force loosens the roots fit. Other forces such as pressure and thermal gradients are neglected. This blade is under a centrifugal load due to a rotational speed of 37,000 rpm according to Milton L. Littlefield of Pratt and Witney, "Mission conditions that include shaft speeds of 37,000 rpm, temperature extremes ranging from minus 265 to 2,300 °F and pressures over 8,000 psi place high stresses on the hardware"[22].

The finite element model of the SSME turbopump blade consists of 55 nodes and 40 four-noded isoparametric elements. Since this is a relatively thin blade, the elements are shell elements. These elements consist of 4 nodes and their corresponding nodal thicknesses composed of 5 layers.

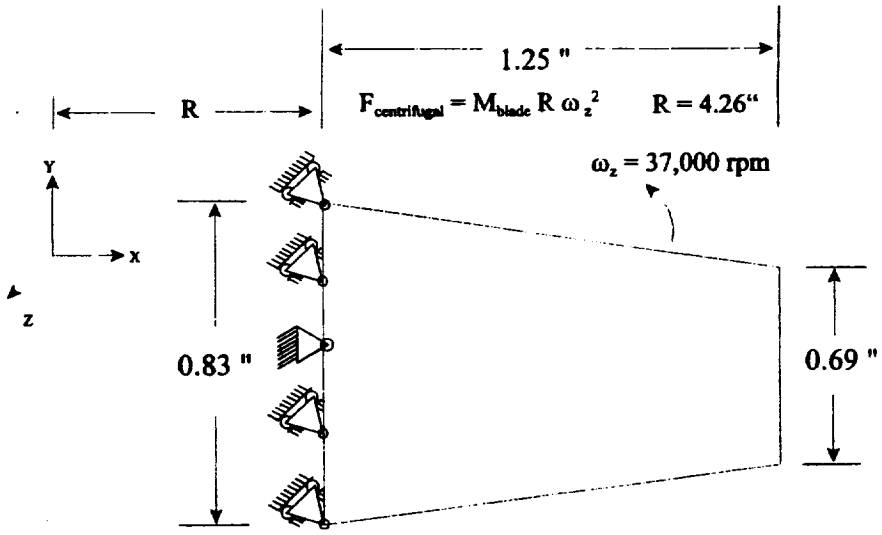


Figure 1.4.2 Drawing of the Blades Constraints and Forces

Random Variable Inputs for Stress

Table 1.4.1 lists the Inconel 718 random variable inputs for the stress calculations. Inconel 718 is a precipitation-hardenable nickel-chromium alloy containing significant amounts of iron, niobium and molybdenum along with lesser amounts of aluminum and titanium. Inconel 718 has excellent creep-rupture strength with properties of high strength, corrosion-resistant material suitable for temperatures from -423 to 1300 °F [23].

These random variables include the modulus of elasticity [24], Poisson's ratio, mass density and centrifugal loading . The random variables above have defined means and standard deviations. The coefficients of variation are initially assumed to be 5% as shown by the equation 1.4.1. Initially, the distribution type for every random variable was assumed to be normal.

$$COV = \frac{Std.dev.}{mean} = \frac{1.240E03}{2.480E04} \qquad (1.4.1)$$

Table 1.4.1 Random Inputs for Stress

FINITE ELEMENT RANDOM VARIABLES				
RANDOM VARIABLE	NAME	MEAN	STANDARD DEVIATION	DISTRIBUTION TYPE
MODULUS OF ELASTICITY	EMOD	2.48E04 (ksi)	1.24E03 (ksi)	NORMAL
POISSON'S RATIO	PMOD	0.271	0.01355	NORMAL
MASS DENSITY	DMOD	0.296 (lbm)/in^3	0.0148 (lbm)/in^3	NORMAL
CENTRIFUGAL LOADING	DLOAD	37,000 (rpm)	1850 (rpm)	NORMAL
BLADE THICKNESS	THICK	0.24" - 0.097"	0.012" - 0.0005"	NORMAL

Correlated Random Fields

The nodal blade thicknesses were input as a random field. Initially this was done initially to compare to the previously run problem [21]. Two different random field analysis were conducted: a fully correlated random field and a partially correlated (95% uncertainty retained). The partially correlated random fields are those where the variance-covariance matrix will be densely populated but diagonally dominant. The correlation coefficient is defined by the following exponential decay equation:

$$\rho_{ij} = e^{-\frac{|x_i - x_j|}{l}} , \qquad (1.4.2)$$

where ρ_{ij} is the correlation coefficient, l is the characteristic length, $\mathbf{X}_i$ and $\mathbf{X}_j$ are the coordinates of point i and j respectively. The characteristic length is estimated measured or related to other physical (measurable) characteristics. This makes for the following variance-covariance matrix:

$$C_{x_i x_j} = \rho_{ij}\sigma_{x_i}\sigma_{x_j} , \qquad (1.4.3)$$

where ρ_{ij} is the correlation coefficient, σ_{Xi} and σ_{Xj} are the standard deviations of the field variable X at points i and j respectively. One item to note is that the transformed random variables are the eigenvectors of the variance-covariance matrix. The associated eigenvalues may be interpreted as the square of the standard deviation of the transformed variables.

For this model, the characteristic length is 1 inch. Since the length of the blade is 1.25 inches and a mesh size is 0.1 inch by 0.2 inch, the characteristic length of 1 inch is plausible. The uncertainty retention measure determines how many quantities need to be retained to capture the randomness of the structure and to shorten the computational time. This means that for small standard deviations, these uncertainties may be neglected to substantially decrease the number of random variables. For certain strongly correlated random fields it is not uncommon that only a few of the significant random variables account for the majority of the uncertainties in the random field. Inside of NESSUS this retained uncertainty is an input to NESSUS/PRE.

The fully correlated random fields are those where the variance-covariance matrix is singular and fully populated. The correlation coefficient ρ_{ij} is equal to 1, thus having the entries of the variance-covariance matrix equal to the equation:

$$C_{x_i x_j} = \sigma_{x_i}\sigma_{x_j} , \qquad (1.4.4)$$

where σ_{Xi} and σ_{Xj} are the standard deviations of the field variable X at points i and j respectively [25].

Random Variable Inputs for Strength

The random variable inputs for strength are listed in Table 1.4.2. Note that these random variables consist of three different types: High-Cycle Fatigue (HCF), High Temperature and Strength. As stated previously, the random variables for HCF include ultimate number of cycles, designated number of cycles, reference number of cycles and the empirical material constant. Likewise, variables for the effect of high temperature include the ultimate temperature, current temperature, reference temperature and empirical material constant for temperature. The last random variable is the initial strength. Note that like the random variables for stress, the standard deviation is 5% of the mean and the distribution type was initially assumed to be normal.

A sample input file for NESSUS is given in the Table 1.4.3. It starts with a keyword called *PFEM which stands for Probabilistic Finite Element Method. The next major keyword is the *ZDEFINE which defines the definition of the performance function. *EXPLICITMODEL defines the input of random variables for the MSD model. The keyword *ZFUNCT 3 0 defines which reliability model to use, with 3 corresponding to the MSD model. Below this is the *MSDM input, which is for the Material Strength Degradation model. The particular effects and their input are placed here. The linear or log type is also designated in the MSDM section. The keyword *COMPUTATIONALMETHOD designates the number of random variables on the stress side. They are given a random variable number and name designation below the *RVDEFINE keyword. The COOR is the thickness change that is applied to the coordinates. The first number is an integer defining the nodal number. Following that is the x, y, z and thickness coordinates. Note that the x, y, and z coordinates are zero. This means that the only change applied to the coordinates is a change in thickness.

Table 1.4.2 Random Inputs for Strength

PROBABILISTIC RANDOM VARIABLES					
TYPE	RANDOM VARIABLE	SYMBOL	MEAN	STANDARD DEVIATION	DISTRIBUTION TYPE
HCF	ULTIMATE NUMBER OF CYCLES	NU	1.0E10	5.0E08	NORMAL
HCF	DESIGNATED NUMBER OF CYCLES	N	2.5E05	1.25E04	NORMAL
HCF	REFERENCE NUMBER OF CYCLES	NO	0.25	0.0125	NORMAL
HCF	EMPIRICAL MATERIAL CONSTANT	W	0.141	0.00705	NORMAL
High Temperature	ULTIMATE TEMPERATURE VALUE	TU	2369 °F	118.45	NORMAL
High Temperature	CURRENT TEMPERATURE	T	1000 °F	50.0	NORMAL
High Temperature	REFERENCE TEMPERATURE	TO	75 °F	3.75	NORMAL
High Temperature	EMPIRICAL MATERIAL CONSTANT	QQ	0.2422	0.01211	NORMAL
Strength	INITIAL STRENGTH	SO (psi)	1.480E5	7.40E03	NORMAL

Table 1.4.3 Sample NESSUS Input File

```
C ssmehcf718nrv1a.dat     The input file for NESSUS
*PFEM
C
C   Z-FUNCTION
C
*ZFDEFINE
*EXPLICITMODEL 9
6, 7, 8, 9, 10, 11, 12, 13, 14
*ZFUNCT 3 0
*MSDM   SO
C Definitions of input for the Random
     TEMP LINEAR  TU T TO QQ    C  Variables of the Material Strength
     HCF LOG NU N NO W          C  Degradation model.
     END
*COMPUTATIONALMETHOD 1 5        C  Random Variable memory allocation for the
  1 2 3 4 5                     C  stress side.
*END
C  RANDOM  VARIABLE  DEFINITIONS   C  Defines the random variables.
*REDEFINE
*DEFINE    1        C  Defines the first random variable, a random field.
                    C  The random field is run through the NESSUS
                    C preprocessor, NESSUS/PRE.
C  While this is in the form of a coordinate input deck, it has zeros in
C  the x, y and z coordinates.  The only nonzero entry is the thickness.
C  This is the change that is applied to the coordinates in the blade.
  THICK1
  1.3650E-01  6.8249E-03 NORMAL
 COOR
    1          0.0000E+00  0.0000E+00  0.0000E+00  1.7583E+00
    2          0.0000E+00  0.0000E+00  0.0000E+00  1.7583E+00
    3          0.0000E+00  0.0000E+00  0.0000E+00  1.7583E+00
    4          0.0000E+00  0.0000E+00  0.0000E+00  1.7583E+00
    5          0.0000E+00  0.0000E+00  0.0000E+00  1.7583E+00
    6          0.0000E+00  0.0000E+00  0.0000E+00  8.0001E-01
    7          0.0000E+00  0.0000E+00  0.0000E+00  1.4446E+00
    8          0.0000E+00  0.0000E+00  0.0000E+00  1.6685E+00
    9          0.0000E+00  0.0000E+00  0.0000E+00  1.7490E+00
*DEFINE  2      C  The second random variable.  2 is its random number.
DMOD
  2.48E07  1.24E06  NORMAL
 PROP  75
  1  40  0  1  0  0  0
*DEFINE  3
  DMOD
  0.271  0.01355  NORMAL
 PROP  75
  1  40  0  0  1  0  0
*DEFINE  4
  DMOD
```

Table 1.4.4 contains an excerpt from the .mov output file. This file includes a summary of the results from the probabilistic analysis of the blade. The first line in Table 1.4.4 shows probability of failure as 0.00022074 corresponding to the limit state of Z=0 at -3.5140 standard deviations from the mean. Below this line is a list of the random variable names, their values at the MPP, their corresponding deviations from their means and their sensitivity factors. Finally, the bottom line is a reprint from the top line with additional decimal places showing.

Table 1.4.4 Sample NESSUS Output File

```
C    Filename:   ssmehcf718nrv1a.mov A Sample output file from NESSUS.
Response/Probability level:     1
 Level       Z-value       u(std. normal)       Probability
    1     0.000000E+00       -3.51401          0.000220740

                Most probable point (MPP) or design point

 Level  1: (Z-value = 0.00000E+00, u =  -3.5140, Probability =
0.000220740)

R.V. name          X-value          Std. Dev. from Mean    Sensitivity factor
     THICK1      0.1309896E+00          -0.807400             -0.229766
     EMOD        0.2479084E+08          -0.007384             -0.002101
     PMOD        0.2706960E+00          -0.022434             -0.006384
     DMOD        0.8082256E-03           1.101191              0.313371
     DLOAD       0.4402004E+04           2.722211              0.774673
     NU          0.9994149E+10          -0.011701             -0.003330
     N           0.2502581E+06           0.020652              0.005877
     NO          0.2498878E+00          -0.008976             -0.002554
     W           0.1422799E+00           0.181542              0.051662
     SO          0.1355315E+06          -1.684931             -0.479489
     TU          0.2335924E+04          -0.279243             -0.079465
     T           0.1014301E+04           0.286011              0.081392
     TO          0.7495304E+02          -0.012522             -0.003564
     QQ          0.2446292E+00           0.200592              0.057084

                    CDF RESULTS
        Z                  U              PROBABILITY          ITER. NO.
  0.00000000E+00  -0.35140116E+01   0.22074004E-03              8
```

The mov output from NESSUS contains several important results. There is a title line followed by a description of what kind of output. The Level term is the level as defined by the user in the FPI input or is a predefined number of levels that NESSUS automatically chooses for a full CDF analysis. The Z-value is the performance level, followed by its location in standard normal coordinates and finally the probability of having that performance level. Following that is the MPP and another line containing the Z-value, the standard normal value and the probability. Next there is a line defining the random variable name, the x-value or the value of that particular random variable in normal space as given in the input file, the standard deviation of that x-value from it mean and finally its sensitivity factor. Finally, the last line below all the random variables is the same as the top of the input file except for the inclusion of more decimal places.

1.5 RELIABILITY RESULTS

AMV+ and Monte Carlo Simulation Results

Table 1.5.1 compares the reliability results from the AMV+ technique with the well known Monte Carlo Simulation method. Percent differences between the two methods were calculated. The number of samples for the Monte Carlo Simulation were increased from 50,000 and 200,000 sample points. The run times varied from one day of CPU time for 50,000 sample points, to six days for 200,000 sample points.

Case 1 was for a fully correlated random field and 50,000 sample points. The probability of failure calculated for Monte Carlo was 2.60E-04 while the probability of failure from the AMV+ method was 2.207E-04. The percent difference was calculated to be 15.1 %. Increasing the number of samples to 200,000 as shown in Case 3 reduced the difference to 7.7%. This is in agreement with the reduction in percent error given by the Shooman equation from approximately 60% to 30% error, roughly one half.

The additional number of samples increased the Monte Carlo run time from one day to six days. The AMV+ solution ran in 3 to 4 minutes, thus giving a substantial savings in processor time. With almost instant feedback from the AMV+ and accuracy comparable to that of Monte Carlo, the AMV+ method offers the ability to examine more variables in a given amount of time.

Case 2 was for the blade thickness modeled as a partially correlated random field and 50,000 sample points. Monte Carlo resulted in a probability of failure of 3.40E-04, while AMV+ yielded a probability of failure of 2.207E-04. The percent difference between these two values was 33.2.%. As before, this difference was decreased by increasing the number of sample points used in the Monte Carlo Simulation from 50,000 to 200,000 sample points as seen in Case 4. The percent difference decreased from 33.2% to 14.7%. Thus, the AMV+ method yielded comparable results with much greater efficiencies than the Monte Carlo method.

Table 1.5.1 Comparison of Probabilities of Failure and Reliability

Case Number	Blade thickness uncertainty	Number of Samples for Monte Carlo	Probability of Failure (Monte Carlo)	Reliability Based on MC	Probability of Failure (AMV+)	Reliability Based on AMV+	%Error (Shooman)	Comparison %Difference AMV+ vs. MC
1	1 fully correlated random field	50,000	2.60E-04	0.99974	2.207E-04	0.99978	60.19	15.1%
2	95% uncertainty retained,partially correlated	50,000	3.40E-04	0.99966	4.530E-04	0.99955	42.01	33.2%
3	1 fully correlated random field	**200,000**	2.05E-04	0.99980	2.207E-04	0.99978	30.10	**7.7%**
4	95% uncertainty retained,partially correlated	**200,000**	3.95E-04	0.99961	0.00045	0.99955	22.31	**14.7%**

Reliability Results Overlap

Figure 1.5.1 is a plot of the probability density functions (PDF's) for both the resulting strength and stress distributions. First only the MSD model was run and then only the stress side of the SSME fuel turbopump turbopump blade was run. Next, the numerical derivatives of the MSD side were calculated and plotted. Finally the numerical derivatives of the stress side were calculated and plotted. The derivatives are given by equations 1.5.1 and 1.5.2, where the p's are the cumulative probabilities, the S's are the strengths and the σ's are the stresses.

$$\frac{dp}{dS} = \frac{p_1 - p_o}{S_1 - S_o}, \qquad (1.5.1)$$

$$\frac{dp}{d\sigma} = \frac{p_1 - p_o}{\sigma_1 - \sigma_o}, \qquad (1.5.2)$$

The overlap of these two PDF's in Figure 1.5.1 is the region where the probability of failure exists.

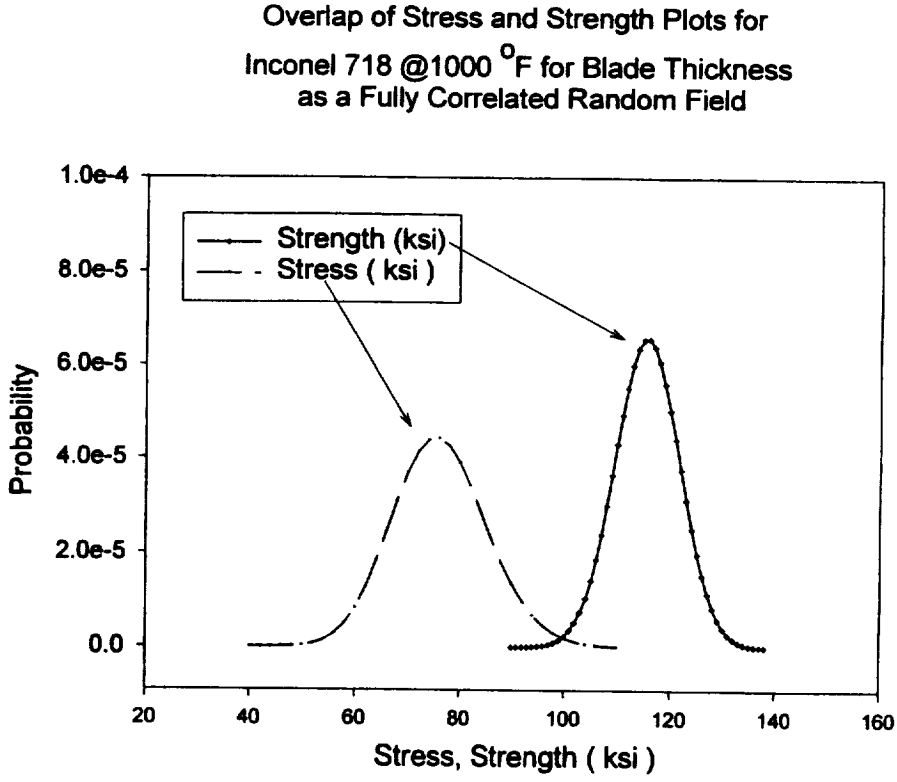


Figure 1.5.1 Overlap of the Strength and Stress Plots

Reliability results for Inconel 718 at a temperature of 1000 °F are shown in Figure 1.5.2. It shows the cumulative distribution functions CDF's for the cases of fully correlated and partially correlated (95% uncertainty retained) random fields. This overlay on normal probability paper shows that there is very little difference between the probability results obtained for a fully correlated random field and those for a partially correlated random field. In the region where the blade fails, i.e. where (strength - stress) = 0, the shift is very minor. The probabilities for the fully correlated and the partially correlated (95% uncertainty retained) fields are essentially right on top of each other.

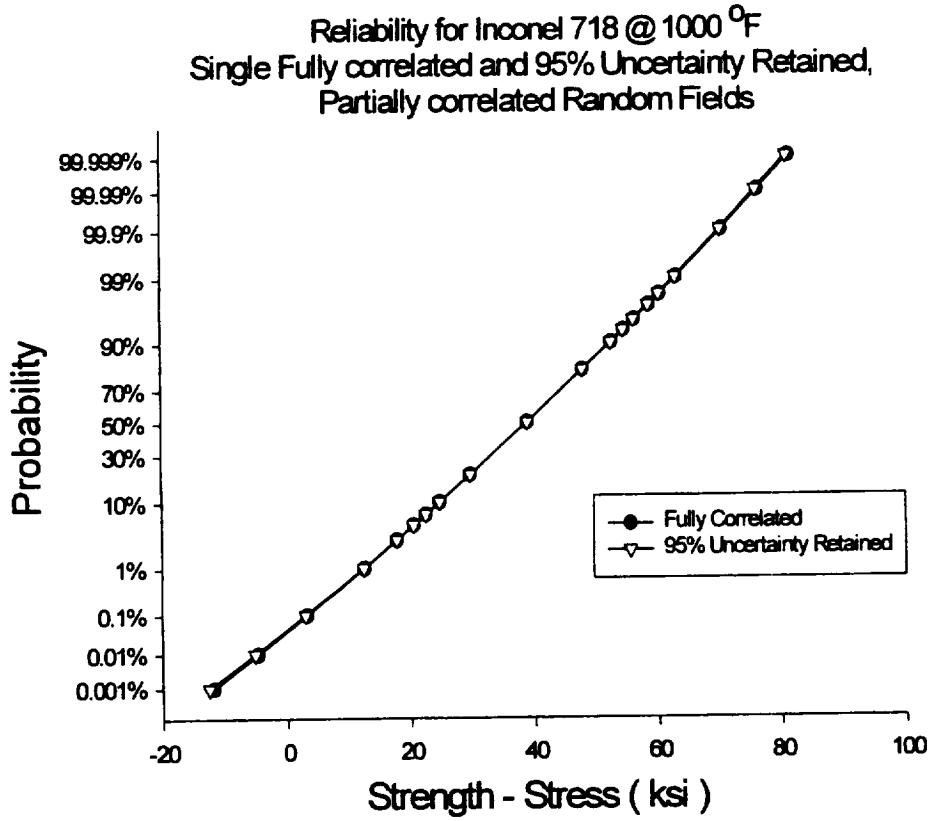


Figure 1.5.2 Reliability Plots on Normal Probability Paper

1.6 SENSITIVITY FACTOR RESULTS

Table 1.6.1 states the sensitivity factors at failure for the SSME fuelpump turbopump blade with the thickness modeled as both a fully correlated random field and a partially correlated random field with 95% of the uncertainty retained.

Note that the order ranking is for the fully correlated random field. For both fully and partially correlated random fields the centrifugal loading (DLOAD) has the highest sensitivity factor, followed by the initial strength (SO). Mass density (DMOD) and thickness (THICK) are third and fourth depending on correlation. The next four random variables, current temperature (T), the ultimate temperature (TU), the temperature empirical material constant (QQ) and the HCF empirical material constant (W), have sensitivity factors that are an order of magnitude smaller and are considered insignificant in comparison with other variables. The last six random variables are smaller by two orders of magnitude and are clearly insignificant in influencing the output.

Table 1.6.1 Ordered Sensitivity Factors

Random Variables	Name	Sensitivity Factor, α Fully Correlated	Partially Correlated 95% Uncertainity Retained	Partially Correlated 80% Uncertainity Retained
centrifugal loading	DLOAD	0.7747	0.7366	0.7435
inital strength	SO	0.4795	0.4452	0.4513
mass density	DMOD	0.3134	0.2938	0.2968
thickness	THICK	0.2298	0.3889	0.3722
current temperature	T	0.0814	0.0760	0.0770
ulimate temperature	TU	0.0795	0.0740	0.0749
empirical constant	QQ	0.0571	0.0534	0.0540
empirical constant	W	0.0517	0.0860	0.0491
Poisson's ratio	PMOD	0.0064	0.0040	0.0041
current number of cycles	N	0.0059	0.0056	0.0056
reference temperature	TO	0.0036	0.0033	0.0034
ultimate number of cycles	NU	0.0033	0.0032	0.0032
reference number of cycles	NO	0.0026	0.0049	0.0024
modulus of elasticity	EMOD	0.0021	0.0019	0.0041

Figure 1.6.1 below, is a graphical representation of the sensitivity factors results. What is important to note is that the four random variables with the highest sensitivity factors are the same for both the fully correlated and the partially correlated random fields. Therefore, the assumption of a fully correlated blade thickness is justified for future analysis.

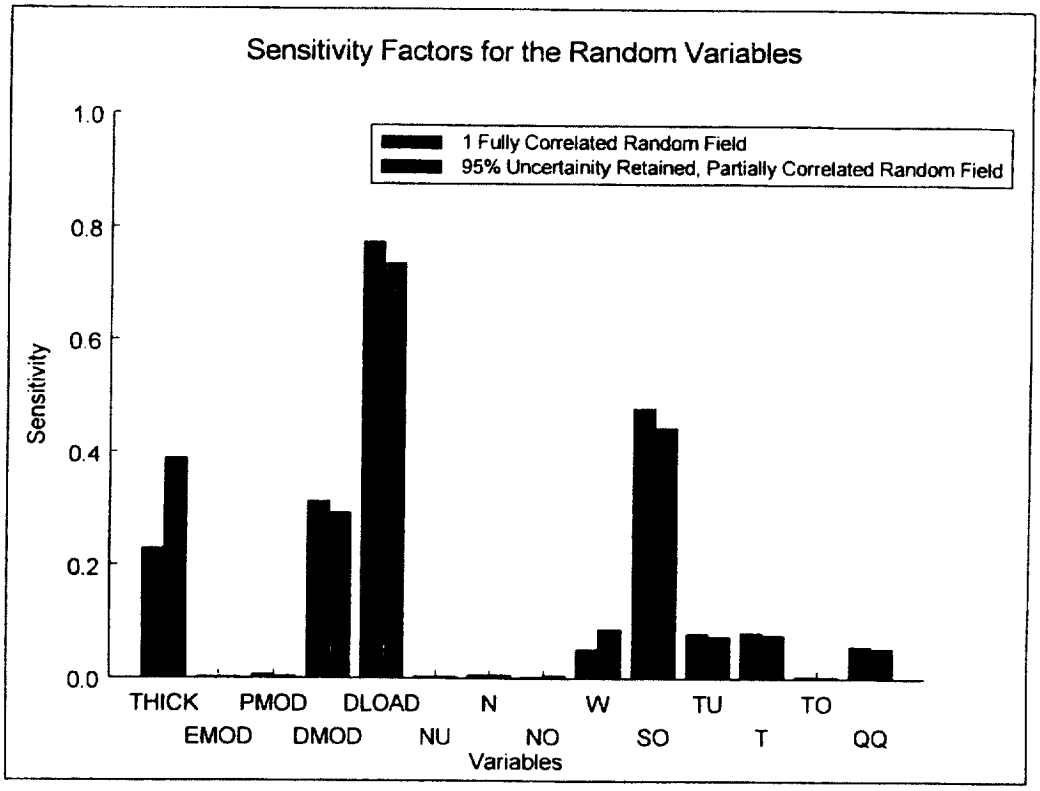


Figure 1.6.1 Sensitivity Factors for the Random Variables

1.7 DISTRIBUTION TYPE ANALYSIS

The type of distribution for each random variable is based on experimental data, which is frequently lacking. There is some uncertainty in choosing the type of distribution to most accurately represent the data. Decisions are often made on the basis of tradition or experience. Choices are often controversial. However, given the mean and standard deviation, the following guidelines exist[16].

- Normal: Useful if COV is "small", say (less than. 10%)
  - Tolerances
  - Modulus of elasticity
  - Poisson's ratio
  - Various material properties

- Lognormal: Good "default" distribution. Can be used for any variable. Plays important role in probabilistic design.
  - Cycles to failure in fatigue
  - Material strengths
  - Loading variables

- Weibull: Very popular distribution, but probably overused.
  - Fatigue
  - Material strength
  - Time to failure in reliability analysis
  - Long-term distribution of stress ranges in fatigue

To see the effect of distribution type on the output, several analyses were conducted. Initially, the distribution types for all random variables were assumed to be normal. Figure 1.7.1 illustrates the effect distribution type had on the probability.

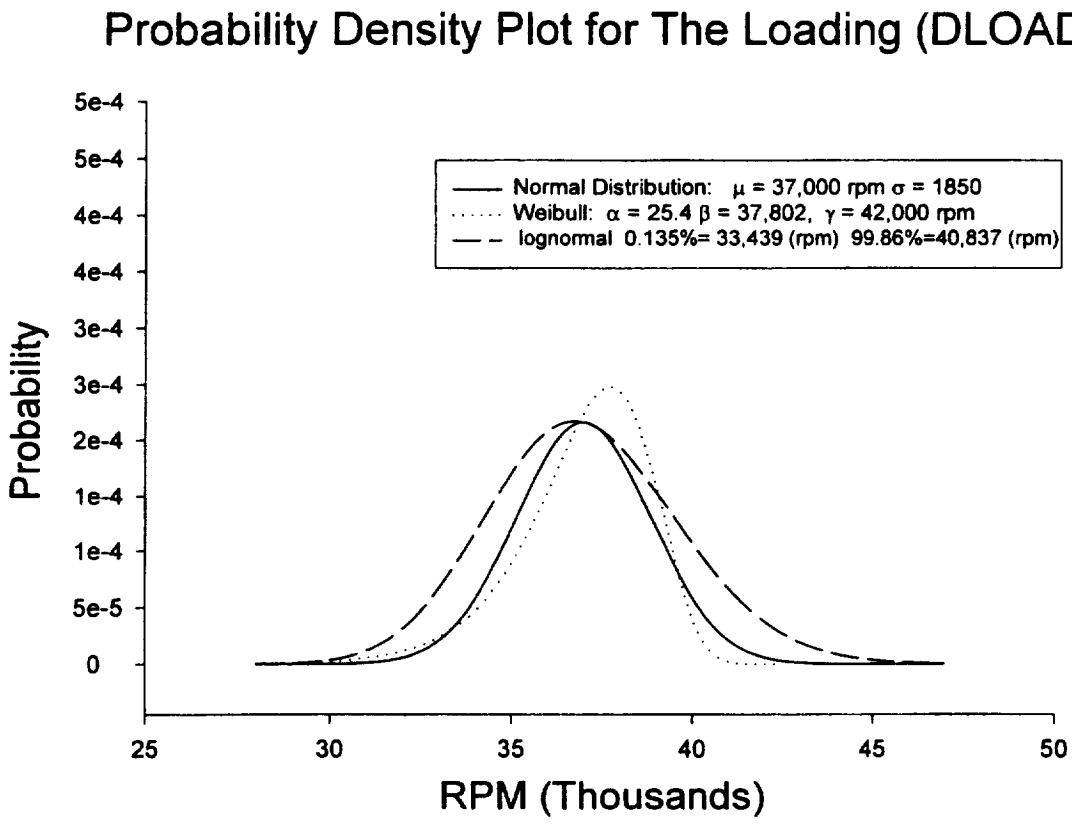


Figure 1.7.1 Probability Density Plot for the Centrifugal Loading (DLOAD)

Effect of Distribution Type on Probability Results

Table 1.7.1 summarizes the probability results for changes in distribution types for both fully and partially correlated random fields. Note that the reliability did not change significantly for a change in distribution type except for the change in distribution to Weibull for the centrifugal load. It has a reliability of 0.9999 or the so-called 4-9's of reliability.

Table 1.7.1 Effect of Distribution on Probabilities of Failure

Blade thickness uncertainty	Random Variable Changed	Distribution for Random Variable Changed	Probability of Failure (AMV+)	Reliability Based on AMV+
1 fully correlated random field	none	no change	2.207E-04	0.999779
1 fully correlated random field	Load	lognormal	3.590E-04	0.999641
1 fully correlated random field	Load	Weibull	1.386E-05	0.999986
1 fully correlated random field	Strength	lognormal	1.979E-04	0.999802
1 fully correlated random field	Strength	Weibull	5.678E-04	0.999432
1 fully correlated random field	Density	lognormal	2.286E-04	0.999771
1 fully correlated random field	Density	Weibull	2.203E-04	0.999780
1 fully correlated random field	Thickness	lognormal	2.191E-04	0.999781
1 fully correlated random field	Thickness	Weibull	2.384E-04	0.999762

Effect of Distribution Type on Sensitivity Factors

Initially, all analysis were performed with the 13 random variables and the thickness random field assumed to have normal or Gaussian distributions. Then the distribution type for one variable at a time was changed from the initial normal to a lognormal and then to a Weibull distribution.

1) Centrifugal Loading (DLOAD)

Figure 1.7.2 illustrates the effect of distribution type on the centrifugal loading (DLOAD) random variable. Changing the distribution type to the lognormal distribution changed the sensitivity factors only nominally. The order of the highest to lowest of the four "significant" sensitivity factors did not change.

However, a change in distribution type to Weibull resulted in a change in both the magnitude and the order of the "significant" sensitivity factors. The order of the first two factors, strength (SO) and centrifugal loading (DLOAD), changed. The magnitude of the "significant" sensitivity factors increased from 31.5% to 43.6 % with the exception of the loading variable (DLOAD) which decreased from 0.7968 to 0.5396, a 32.3% decrease. This was the result of the shift in the Weibull distribution to the right and as was noted before, Weibull tends to be a better distribution for material strength.

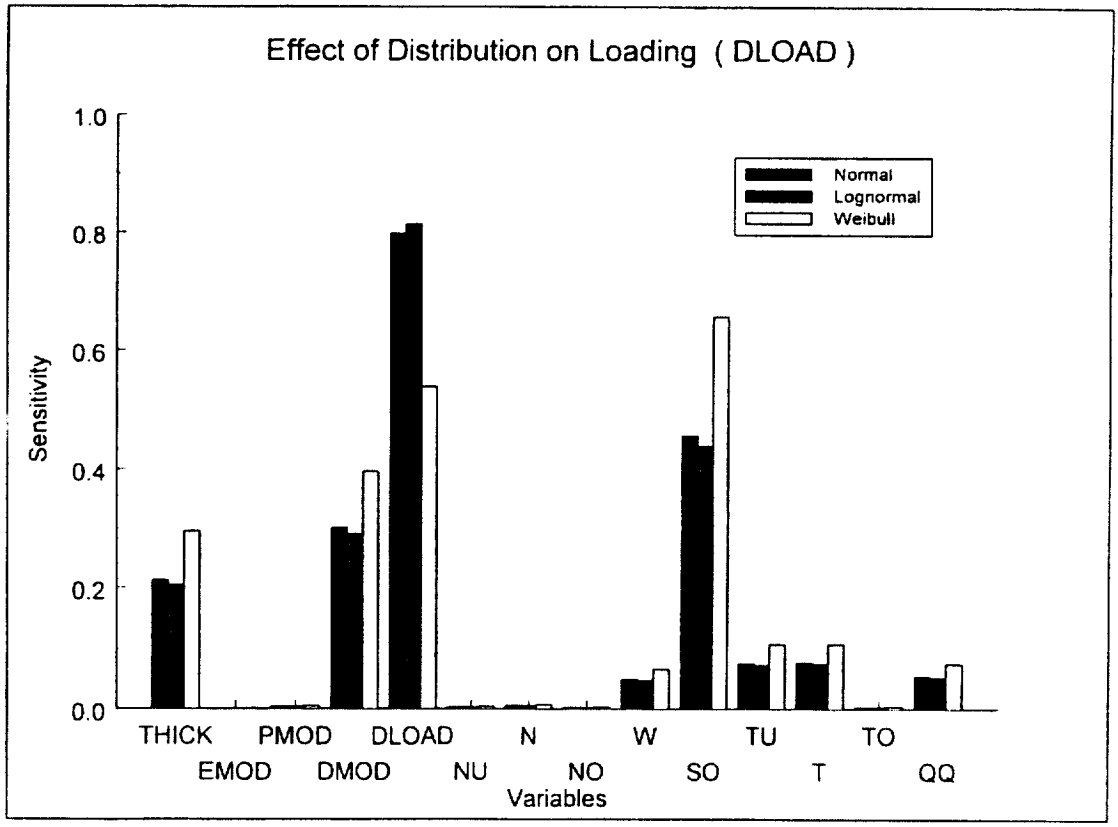


Figure 1.7.2 Effect of Distribution on Loading (DLOAD)

2) Strength (SO)

Figure 1.7.3 illustrates the effect of distribution type on the strength (SO) random variable. Changing the distribution type to the lognormal changed the sensitivity factors only nominally. The order of the highest to the lowest of the four "significant" sensitivity factors did not change. However, a change in distribution type to Weibull resulted in a change in both the magnitude and the order of the "significant" sensitivity factors. The order of the first two factors, strength (SO) and centrifugal loading (DLOAD), changed. The magnitude of the "significant" sensitivity factors decreased from 20.2% to 24.3%. With exception of the initial strength variable (SO) which increased from 0.4566 to 0.73443, a substantial 60.8 % increase.

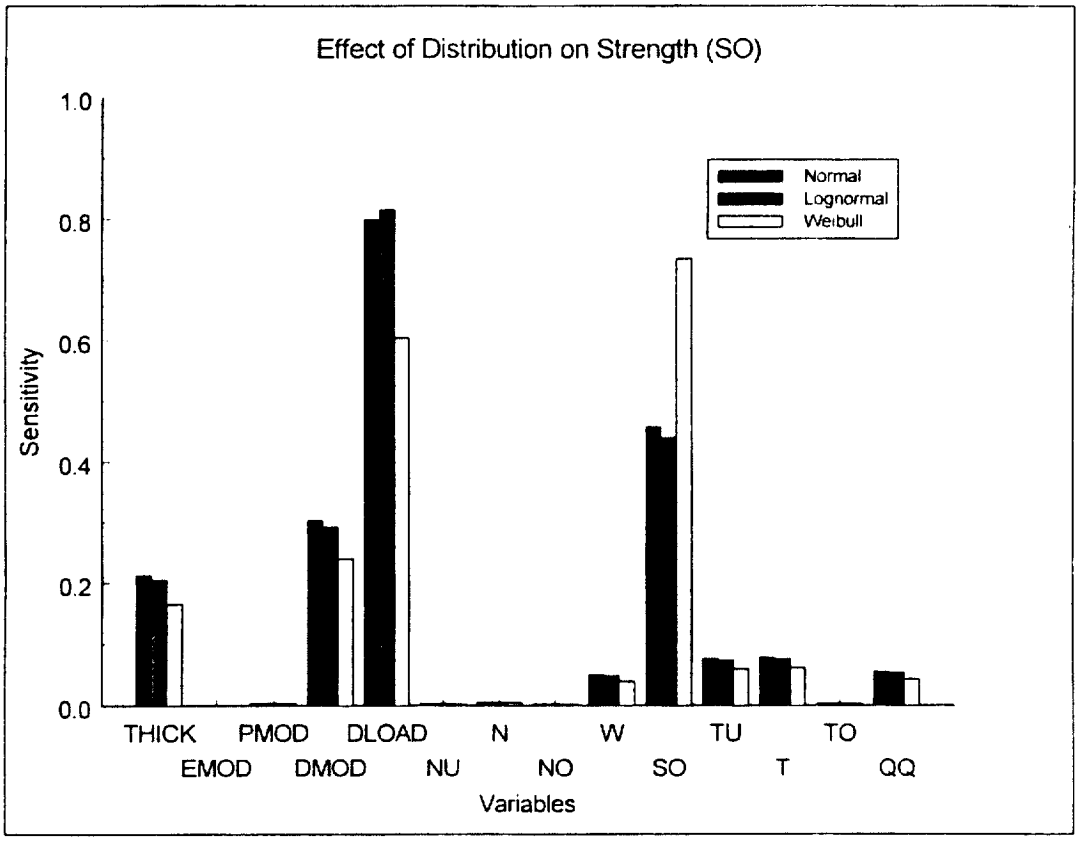


Figure 1.7.3 Effect of Distribution on Strength (SO)

3) Density (DMOD)

Figure 1.7.4 illustrates the effect of distribution type on the mass density (DMOD) random variable. Changing the distribution type to the lognormal distribution changed the sensitivity factors only nominally. The order of the highest to the lowest of the four "significant" sensitivity factors did not change. Changing the distribution type to Weibull resulted in a nominal change in the sensitivity factors. Most of the "significant" sensitivity factors increased slightly from 3.9% to 5.2%. Only the centrifugal loading decreased by 2.8%.

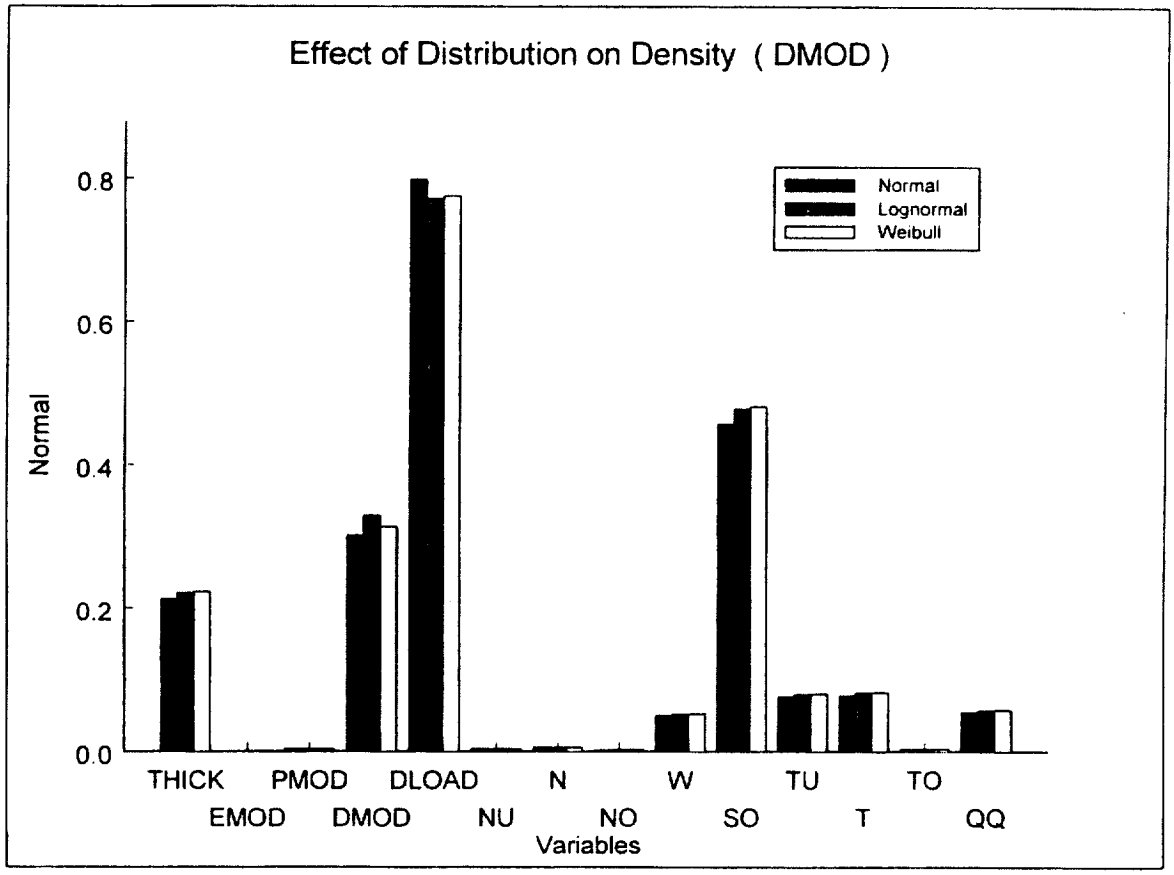


Figure 1.7.4 Effect of Distribution on Density (DMOD)

4) Thickness (THICK)

The final variable tested for distribution type sensitivity was the blade thickness random field. Figure 1.7.5 illustrates the effect of distribution type on the blade thickness. Changing the distribution type to the lognormal distribution changed the sensitivity factors only nominally. The order of the highest to lowest of the four "significant" sensitivity factors did not change. A change in distribution type to Weibull, however resulted in changes in the "significant" sensitivity factors varied from a 4.3% decrease to a 3.4% increase. Only for the blade thickness (THICK) did the magnitude increase from 0.2128 to 0.2812, a 32.5% increase.

The selection of distribution type does affect the sensitivity factors of the centrifugal loading and initial strength. The choice of Weibull for these two random variables increases the initial strength. This result was supported by the guidelines given in the beginning of this section.

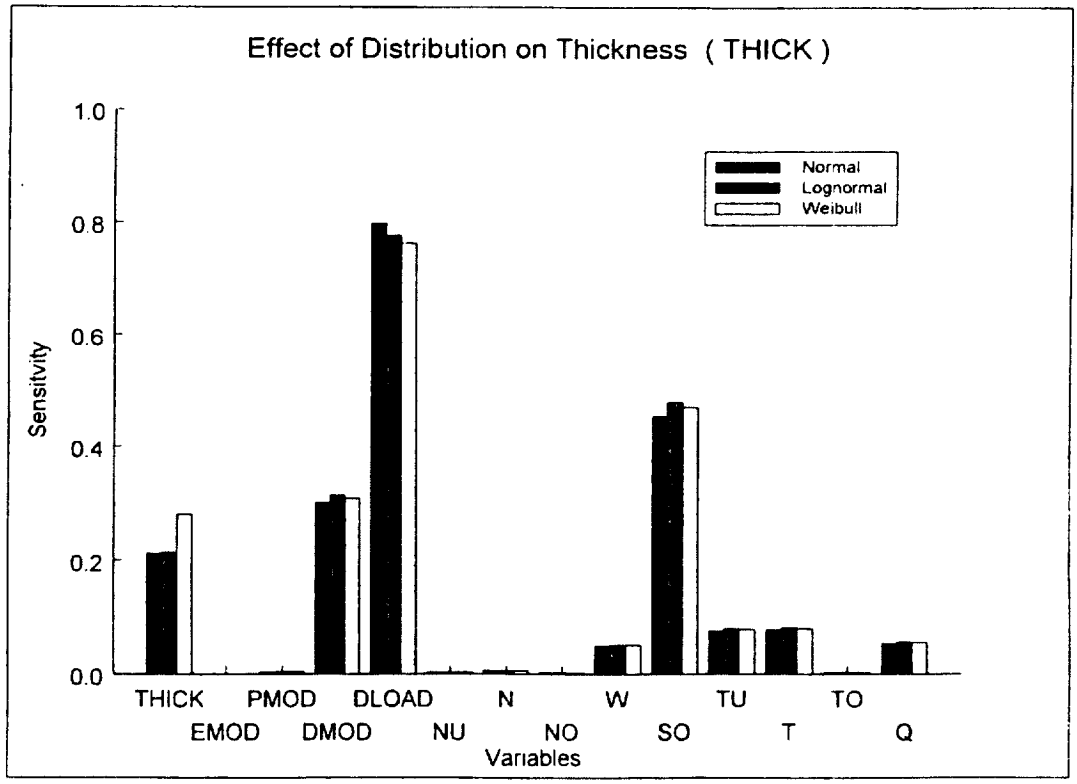


Figure 1.7.5 Effect of Distribution on Thickness (THICK)

1.8 CONCLUSIONS

In this paper, a probabilistic structural analysis of an SSME turbopump blade utilizing the program NESSUS is reported. First, probabilistic analysis yielded a statistical distribution for the critical von Mises stresses at the blade root due to uncertainty in the following variables: Blade thickness, Young's modulus, Poisson's ratio and mass density. Then NESSUS, with the newly implemented MSD model calibrated for Inconel 718 yielded a distribution of the material strength for the combination of high temperature (1000 °F) and high-cycle fatigue effects. With both stress and strength variabilities quantified, the structural reliability of the turbopump blade was determined using both the AMV+ and Monte Carlo Simulation methods.

A comparison of the probability results obtained using the AMV + method to the well known and accepted Monte Carlo Simulation method yielded a percent difference of 14.7% for a partially correlated random field thickness and a percent difference of 7.7% for a fully correlated random field thickness. However, the corresponding 200,000 sample points used for the Monte Carlo Simulation method required six days of computational time versus three to four minutes for the AMV+ computation. Thus, the AMV+ method yielded accurate results with much greater efficiency.

An important advantage of the reliability approach over the factor of safety approach is the ability to assess which random variables contribute most to the variability of the overall system. Sensitivity factors provided this insight which can be used for design optimization. Sensitivity factor results showed centrifugal loading and initial strength to be the most significant random variables for both a fully correlated and a partially correlated random field thickness. Mass density and thickness were third and fourth depending on correlation. The remaining ten random variables were one to two orders of magnitude less and therefore assumed insignificant in influencing the response.

Reliability results and sensitivity factor results varied only slightly for a difference in random field thickness correlation. Hence, only a few of the random variables comprising the random field thickness are significant and account for the majority of the uncertainties in the random field. Thus, the assumption of a fully correlated blade thickness will not decrease the accuracy of results and is justified for future analysis.

The effects of distribution type on both reliability and sensitivity factor results were studied. In both cases, a change in distribution from Gaussian to Lognormal resulted in only nominal changes. However, the change in distribution type from Gaussian to Weibull resulted in an increase in reliability for the centrifugal load variable from 0.99779 to 0.999986 or the so-called 4-9's of reliability. Also, changing distributions to Weibull resulted in a change in both the magnitude and the order of the 'significant" sensitivity factors. Changing the loading

and strength variables' distributions to Weibull swapped the order of the first two sensitivity factors. A Weibull distribution for strength (SO) increased the magnitude of its strength sensitivity factor from 0.4566 to 0.73443, a substantial 60.8% increase.

2.0 EDUCATION

2.1 INTEGRATION OF RESEARCH AND EDUCATION OBJECTIVES

It is well understood that when research is carried out in an academic setting that additional education benefits may occur beyond simply completing the research and delivering the results to the funding agency. These benefits do not automatically occur, but have a higher probability of occurring if the project Principal Investigator incorporates education objectives into the project and designs a carefully thought-out plan to achieve them. NASA and other agencies recognize this potentially effective strategy and have recently begun to request that proposals integrate within a single grant both research and education objectives. This two year NASA/UTSA Partnership Award is an example of such a project.

A short-term education objective carried out during this Partnership Award was to expose undergraduate students to a NASA project in the hopes of encouraging them to obtain an advanced degree. To this end, undergraduate and graduate students were supported in faculty supervised research. Mr. Cody Godines was identified as a good and promising undergraduate student in mechanical engineering. He was recruited to join the first year Partnership Award project and was subsequently hired as an Undergraduate Research Assistant. As a result of working on the project he expressed an interest in continuing his education at the graduate level. He graduated in December 1998 with a BS in Mechanical Engineering and enrolled as a graduate engineering student during the second year of this grant.

2.2 1998 AND 1999 SUMMER COURSES

One long-term education objective of this project was to introduce undergraduate engineering students to probabilistic structural analysis and reliability via NESSUS. ME 4953 Special Studies in Mechanical Engineering: Finite Element Applications in Solid Mechanics and Design, a FEM structural applications course with an introduction to NESSUS was conducted during the 1998 and 1999 summer semesters. These courses attracted over 65 mechanical engineering students. Approximately one third of the 65 students who completed these courses were minority students.

A unique aspect of the course is that it was team taught. The instructor of record and lead laboratory instructor for the 1998 summer course was Ms. Callie C. Bast. Dr. Lola Boyce was the course lecturer and Mr. Mark T. Jurena was the assistant laboratory instructor. The laboratory instructors were budgeted from grant funds. Without the Partnership Award funds,

Ms. Bast would have had no assistance with the course and the quality of the course would have suffered.

The instructor of record for the 1999 summer course was Dr. Randall D. Manteufel. Ms. Callie C. Bast and Mr. Cody Godines were the laboratory instructors. All three instructors for this summer course were supported by grant funds, and the course would not have been offered if not for this Partnership Award. In addition, this grant funded one engineer from SwRI, Mr. David Riha, to present guest lectures and assist with the computer laboratory portions of the summer courses.

Both the 1998 and the 1999 summer courses consisted of a significant laboratory component utilizing student-centered learning activities. Student-centered learning includes laboratory-type assignments and projects on UNIX workstations wherein the students must directly and actively participate. This is in contrast to the lecture-type format wherein the learning is professor-centered and students participate via passive listening. This type of experiment in student-centered learning is receiving wide attention in Schools and Colleges of Engineering in the United States. Syllabi for both summer courses are provided in Appendix I.

2.3 NESSUS STUDENT USER'S MANUAL

A NESSUS Students User's Manual was initiated during the first year of this Partnership Award and completed during the second year. It includes a brief overview of the program, explanations of the minimum number of NESSUS keywords necessary to work laboratory example problems, explanation of output files and a set of example problems/assignments drawn from structural analysis and reliability applications. This manual was used in both summer courses and is planned to be used in the follow-on courses scheduled for Spring 2000 and Summer 2000. This student manual is provided in Appendix II.

3.0 ACCOMPLISHMENTS

The goal of this NASA Partnership Award was to advance innovative research and education objectives in theoretical and computational probabilistic structural analysis, reliability, and life prediction methods for improved aerospace and aircraft propulsion system components. This grant resulted in significant accomplishments in research and education, and the enhancement of UTSA's engineering research environment. It allowed four UTSA Mechanical Engineering students; Mr. Mark T. Jurena , Mr. Cody Godines, Mr. Henock Perez and Mr. Ricardo Ramirez to work directly with the principal investigator, Ms. Callie C. Bast, providing them with a unique research experience that otherwise would not have been possible without this grant.

3.1 ACCOMPLISHMENTS: RESEARCH

Probabilistic structural analysis and reliability methods support the specific needs within the Aeronautics and Space Transportation Technology Enterprise by contributing to the development of a next-generation design tool that promises to improve the safety and reliability of both civil aviation and reusable space launch vehicles. For example, an enhanced NESSUS code is now available to assist in the design of the reusable Space Shuttle Main Engine (SSME) through the calculation of the reliability of turbopump blades. Thus, it is now possible to consider future engine designs based upon target reliabilities through a practical next-generation design tool.

NESSUS Enhancement, Verification and Evaluation

In order to provide NESSUS with the capability of determining the reliability of a structural component utilizing its material strength variability, the MSD model (supported by PROMISS, a probabilistic material strength degradation program developed by NASA Lewis Research Center with UTSA) was implemented in NESSUS in year 1 by SwRI, whom is responsible for maintaining the code. Thus, they assured that the new capabilities of NESSUS were fully integrated into the code and that they were compatible with previous capabilities. Initial verification of the enhanced NESSUS code (version 6.2), conducted in year 1, included two MSD model effects: high cycle mechanical fatigue and high temperature. The cumulative distribution functions (c.d.f.s) of lifetime strength were calculated using both PROMISS and NESSUS. Agreement of results was good in the lower tail but differed in the upper tail. Discrepancies were postulated to possibly be due to the difference in random number generators used in the two codes. It was determined that this phenomenon would be investigated in the proposed second-year continuation of this Partnership Award. Upon further

investigation in year 2, a sampling bias in the PROMISS code was found. The same starting seed was set for sampling each random variable. This bias was easily corrected in the PROMISS code. Verification of the enhanced NESSUS code was then completed.

During year 2, this enhanced version of NESSUS was exercised and evaluated through a reliability analysis of an SSME turbopump blade (see section 1 of this report). This effort resulted in a thesis for one of the students supported on this grant

Also in year 2, convergence criteria were improved for the most probable point based methods (MPP) in NESSUS, resulting in a new enhanced NESSUS code, version 6.3 (see Appendix III, SwRI Final Report). Southwest Research Institute also provided UTSA researchers and students with technical assistance in using the NESSUS code. Mr. David Riha, provided guest lectures and assisted with the computer laboratory for both the 1998 and 1999 summer courses. The complete second year NESSUS Enhancement and Technology Support Final Report is provided in Appendix III of this report.

3.2 ACCOMPLISHMENTS: EDUCATION

The introduction of undergraduate students to probabilistic finite element analysis methods was achieved through a UTSA summer course, ME 4953 Special Studies in Mechanical Engineering: Finite Element Applications in Solid Mechanics and Design. This FEM structural applications course with an introduction to NESSUS was conducted during the 1998 and 1999 summers. Over 65 mechanical engineering students enrolled for this summer course. Students successfully completing it received three semester-hours of credit for a senior-level technical elective. A large number of the students who completed the course were minority students.

A NESSUS Student User's Manual was initiated in Year 1 and completed in Year 2. This manual will provide guidance in using NESSUS for future courses and help insure the continuation of probabilistic finite element analysis courses at UTSA.

3.3 STUDENT ACHIEVEMENTS

A graduate student, Mr. Mark Jurena, was recruited in the second-year continuation of this Partnership Award to complete his Master of Science in Mechanical Engineering degree. Supported by this Partnership Award, his thesis topic directly related to the research objectives of this grant. He presented his thesis "work in progress" at the AIAA/ASME/ASCE/AHS/ASC Structures, Structural Dynamics, and Materials (SDM) Conference last April in St. Louis, Missouri. Having concluded his research, he presented his research results in his thesis entitled "Structural Reliabilty Using Finite Element Analysis And A Probabilistic Material Strength Degradation Model", and successfully completed his MSME degree in August, 1999.

An undergraduate student, Mr. Cody Godines, was recruited in Year 1 of this Partnership Award as an Undergraduate Research Assistant. He earned his Bachelor of Science in Mechanical Engineering last December. While supported by this grant, Mr. Godines worked on a probabilistic finite element analysis of a beam and presented his NESSUS project at a NASA GRC-sponsored HBCU/HSU (Hispanic-Serving University) Research Conference in April, 1999. His conference paper is included in Appendix IV of this report. During this time, he became interested in going to graduate school. He enrolled as a graduate student in Spring 1999. Mr. Godines plans to complete his MSME degree in 2001 under the guidance of Dr. Randall Manteufel and the support of a 1999 Partnership Award for Innovative and Unique Education and Research Projects.

5.0 REFERENCES

1. Chamis, C.C.; Hopkins, D.A., Probabilistic Structural Analysis Methods of Hot Engine Structures, ASME 0402-1215, GT12, Jun 4-8 1989.

2. Southwest Research Institute, NESSUS Documentation vol. I sect. Overview, 1995

3. Dias, J., Nagtegaal, J., and Nakazawa, S., "Iterative Perturbation Algorithms in Probabilistic Finite Element Analysis," Computational Mechanics of Reliability Analysis, W.K. Liu and T. Belytschko (eds.), Elmepress International, Ch. 9, 1989.

4. Southwest Research Institute, NESSUS Documentation, vol. II, sect. PRE, 1995, pp. 1.3- 1.5.

5 Wirshing, P.H. and Wu, Y.T., "Advanced Reliability Methods for Sturctural Behavior," Advances in Aerospace Structural Analysis, 1st ed. American Society of Mechanical Engineers, New York, Nov. 1985, p.75.

6. Thacker, B.H., Millwater, H. R., and Harren, S.V., "Computational Methods for Structural Load and Resistance Modeling", AIAA 32nd Structures, Structural Dynamics, and Materials Conference, AIAA-9100918-CP p. 1229.

7. Bast, C. C. and Boyce, L., Probabilistic Material Strength Degradation Model for Inconel 718 Components Subjected to High Temperature, High-Cycle and Low-Cycle Mechanical Fatigue, Creep and Thermal Fatigue Effects, NASA CR-198426.

8. Bast, C. C., "Probabilistic Material Strength Degradation Model for Inconel 718 Components to High Temperature, Mechanical Fatigue, Creep and Thermal Effects", Thesis University of Texas at San Antonio, 1993.

9. Riha, David S., NESSUS Technology Support and Material Model Implementation, Subcontractor Final Report, SwRI Project no. 06-1301, NAG 3 2060

10. Shigley, J. E. and Mischke, C. R. Mechanical Engineering Design, 5th Ed. , McGraw-Hill, N.Y., 1989, p. 245.

11. Shigley, J. E. and Mischke, C. R. Mechanical Engineering Design, 5th Ed. , McGraw-Hill, N.Y., 1989, p.30.

12. Ugural, A.C. and Fenster, S. K., Advanced Strength and Applied Elasticity, 3rd Ed. , Prentice-Hall, 1995, p. 155.

13. Shigley, J. E. and Mischke, C. R. Mechanical Engineering Design, 5th Ed. , McGraw-Hill, N.Y., 1989, p.299

14. Popov, E.P. Engineering Mechanics of Solids, 1990, pp. 38-45.

15. Rosenblatt, Murray; "Remarks on a Multivariate Transformation", Annals of Mathematical Statistics, Vol 23, No. 3. (Sep., 1952), pp. 470-472.

16. Southwest Research Institute, Short Course on Probabilistic Analysis and Design, Sept. 1998.

17. Elishakoff, I., Probabilistic Methods in the Theory of Structures, John Wiley and Sons New York, 1983, p. 89.

18. Wu., Y.-T., Gureghian, Sager, B., and Codell R. B., "Sensitivity and Uncertainty Analysis Applied to One-Dimensional Transport in a Layered Fractured Rock. Part II: Probabilistic Methods Based on the Limit-State Approach", Nuclear Technology Journal, vol. 104, no. 2, Nov. 1993, pp. 297-308.

19. Wu., Y.-T., Millwater, H.R., and Cruse, T.A., "An Advanced Probabilistic Structural Analysis Method for Implicit Performance Functions," AIAA Journal, vol. 28, no. 9, 1990, pp. 1663-1669.

20. Shooman, M. L., 1968, Probabilistic Reliability: An Engineering Approach, McGraw-Hill, N.Y.

21. Boyce, L., "Probabilistic Structural Analysis Methods for Improving Space Shuttle Engine Reliability", AIAA Journal of Propulsion and Power, vol. 5, no. 4, 1989, pp. 426-430.

22. Littlefield, Milton L. "FMEA/CIL Implementation for the Space Shuttle New Turbopumps" Proceedings of the 1996 Annual Reliability and Maintainability Symposium by IEEE, 1996 p. 48-52.

23. Bast, C. C., "Probabilistic Material Strength Degradation Model for Inconel 718 Components to High Temperature,Mechanical Fatigue, Creep and Thermal Effects", Thesis University of Texas at San Antonio, 1993, p. 15.

24. INCONEL Alloy 718, Inco Alloys International, Inc., Hunting, WV, 1985 pp. 1-6.

25. Southwest Research Institute, NESSUS Documentation, vol. II, sect. PRE, 1995, pp. 1.3-1.5.

APPENDIX I

The University of Texas at San Antonio

Syllabus
ME 4953 Special Studies in Mechanical Engineering:
Finite Element Applications in Solid Mechanics and Design
Summer, 1998

INSTRUCTORS:

Course Instructor of Record and Lead Laboratory Instructor:
Callie Bast, MSME;
Office: 1.04.06 EB; 458-5588; Office Hours: TR, 2:15 - 2:45 pm and 4:45 - 5:30 pm.

Course Lecturer:
Lola Boyce, Ph. D., P.E.,
Office: 3.04.42 EB; 458-5512; Office Hours: By appt.

Assistant Laboratory Instructor:
Mark Jurena, BS

LECTURE/LAB:

Lecture: TR 2:45 pm to 3:40 pm
Lab: TR 3:40 pm to 4:35 pm

PREREQUISITES:

Permission of Instructor.

TEXTBOOK:

No required text. Course given from instructor's notes, handouts, and recommended reading from various texts.

COMPUTER USAGE:

ABAQUS, PATRAN, and NESSUS are available for assistance with projects, reports, and exams.

COURSE OUTLINE:

A review of the necessary mathematical tools for the finite element method (FEM). Approximate numerical solutions to selected solid mechanics examples posed as FEM problems. Introduction to probabilistic methods in solid mechanics and mechanical design posed as FEM problems.

COURSE OBJECTIVE:

To provide an understanding of analysis, design, and applications in solid mechanics and mechanical design using the finite element method (FEM) and appropriate FEM software tools.

GRADING:

A final grade will be assigned based on the following percentages:

Midterm Exam	25%
Final Exam	30%
Homework/Labs	25%
Project	20%

EXAMINATION SCHEDULE:

Midterm Exam: Thursday, June 25, 1998
Final Exam: 3:15 - 5:45 pm; Tuesday, August 4, 1998

ATTENDANCE:

Mandatory. Attendance will be taken randomly.

Note: Homework is assigned weekly and is good preparation for examinations. Questions regarding homework and other assignments are considered during office hours. No late assignments are accepted. Make-up exams are given only for extenuating circumstances discussed in advance and are generally more difficult than the regularly scheduled exam.

ME 4953 Special Studies: Finite Element Applications in Design

Summer 1999
Lecture: T-Th 2:45-4:35 EB 2.04.06
Laboratory: T-Th 1:00-2:30 Session 001
Laboratory: T-Th 5:00-6:30 Session 002

Instructor: Randall D. Manteufel, Ph.D., P.E.
Office: EB 3.04.54
Phone: 458-5522
Office Hours: T-Th 1:30-2:30

Lab Instructor: Callie Bast, MSME
Office: EB 1.04.06
Phone: 458-5588

Lab Assistants: Mark Jurena, BSME
Cody Godines, BSME
Office: EB 1.04.06
Phone: 458-5586

Text: The Finite Element Method in Mechanical Design. C.E. Knight. PWS-Kent, 1993.

Pro/MECHANICA Structure Tutorial, 2nd ed. Roger Toogood, SDC Publications. [http:// www.amazon.com /, ships in 24 hours] price $49.95.

Description: A review of the mathematical foundations of the finite element method (FEM) for problems in continuum mechanics. Design case studies and finite element applications in mechanical design. Introduction to probabilistic FEM design. This class will emphasize the application of the FEM using commercial software.

Course Goals: To give students the opportunity to learn and be able to:
1) understand and explain the mathematical foundations of finite element analysis
2) understand and explain numerical algorithms used in the finite element method
3) understand and explain probabilistic methods used in mechanical design and reliability analyses
4) perform mechanical analysis of components using finite elements
5) use commercial software for finite element analysis in mechanical design

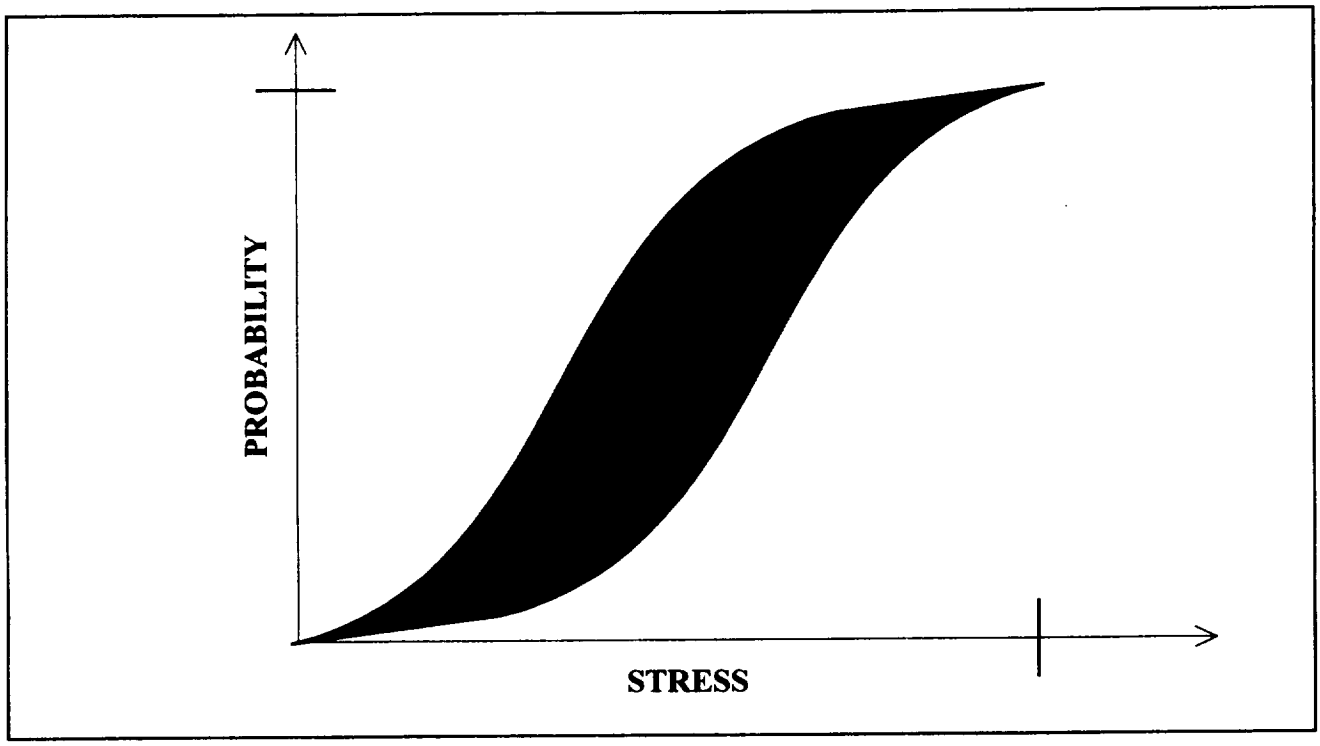
Prerequisites: ME 3813 Solid Mechanics
ME 3423 Applied Engineering Analysis

Grading: Homework/Laboratory Assignments 50%
Individual Design Project 50%

APPENDIX II

The University of Texas at San Antonio

STUDENT MANUAL FOR THE PROBABILISTIC FINITE ELEMENT CODE, NESSUS
(Numerical Evaluation of Stochastic Structures Under Stress)



NASA GLENN RESEARCH CENTER
PARTNERSHIP AWARD
NAG # 3-2060

NESSUS

Introduction

Historically, NESSUS has provided probabilistic structural analysis for the response of engineered structures. It integrates both probabilistic analysis and finite element methods to produce a useful tool for both design and analysis of critical structural components. NESSUS allows for both random and deterministic descriptions of input and output quantities. For example, input parameters for material properties such as Young's modulus, Poisson's ratio, and mass density can be modeled as random variables wherein the user provides the appropriate statistics, namely mean, standard deviation and distribution type [2]. In addition, random input can include random fields, as well as random variables. Distributions such as Gaussian, Weibull, or lognormal may be selected. Other input parameters, such as loading type, geometry, boundary conditions and initial conditions can also be considered random. Then, probabilistic analysis yields the cumulative distribution functions (CDF's) of the output random variables, e.g., stresses, strains, displacements, etc.

Code Organization

NESSUS is divided into ten parts. The preprocessor, NESSUS/PRE, provides for the representation of random fields. NESSUS/PRE computes a set of independent random variables from the random fields using an eigenvalue decomposition [3]. PFEM is the module for coordinating the operations between the finite element code and FPI. Next, a deterministic finite-element module, NESSUS/FEM, generates the deterministic responses of the finite-element structural model to a number of prescribed perturbations of the input variables. NESSUS/FEM contains a mixed iterative procedure to obtain the response of a structure. A Newton-Raphson iterative procedure based on a mixed variational principle can be used in NESSUS/FEM. Besides FEM, BEM, the boundary element module is used for structural analysis. These deterministic solutions provide the data from which a first or second-order Taylor series of the response is fit that defines the explicit functional relationship between the input random variables and the response of interest. The postprocessor, NESSUS/FPI (Fast Probability Integration), performs the probability calculations. The postprocessor also includes a choice of probabilistic analysis methods other than FPI, including for example, Adaptive Importance Sampling (AIS) and Monte Carlo simulation [4,5]. SIMFEM however, contains the driving module for the Monte Carlo as well as the Latin Hypercube sampling of the structure. There are also other packages for specialized analysis such as the RISK, SYSTEM

and SYSRSK modules. The RISK module computes the risk with respect to cost or a user defined criteria. The SYSTEM module is an alternate system reliability method for probabilistic fault tree analysis. The SYSRSK module computes the system risk by combining the cost of failure, in terms of replacement, inspection, repair or other criteria of individual components of the system with their probability of failure. The current version of NESSUS provides these ten component parts in an integrated package. These modules can be used in various combinations as the user desires.

Input and Output Files

NESSUS utilizes many different files. Filenames are based upon a logical naming convention. Depending upon input quantities within certain *PRINT or *PRINTOPTION statements, various output files will be created. The primary files are as follows:

myfile.dat	This is the name of the input file. It contains information pertaining to finite element input, probabilistic input and Fast Probability Integration input.
myfile.out	This file contains the majority of the output. It is the output most used for determining if the input data was correct. Explainations of errors are detailed within this file.
myfile.pdb	This is the perturbation database. It is used by NESSUS to extract data for probabilistic analysis and is in a binary format.
myfile.fem	This is the deterministic input analyzed by the NESSUS/FEM module.
myfile.mov	This is the primary results from the probabilistic analysis. It contains information in a concise format for quick evaluation.
myfile.zal	A probabilistic results file suitable for input into a spreadsheet such as Microsoft Excel and subsequent graphical output.
myfile.fpi	An intermediate output from NESSUS containing only the FPI input values. The following files are occasionally seen with various print statements.
myfile.fpo	An intermediate output from NESSUS containing the probabilistic output.
myfile.rvd	An intermediate output file form NESSUS. It is usually seen as the output from the NESSUS/PRE module.
myfile.feo	The deterministic output from the NESSUS/FEM module.

NESSUS Keywords

*PFEM The Probabilistic Finite Element Analysis Method
This is the section that defines what random variables are input into NESSUS and what kind of analysis is performed on them.

*ZFDEFINE The beginning of the z-function or performance function definition. This defines what kind of response function is what adding variables that resist the analysis input.

*ZFUNCTION {Resistance model #} {# of coefficients} Selects the response function.

{zcoef} Listing of real coefficients to be made available to the response function.

C { Resistance model #} = 1 Structural design factor model.
This predefined resistance model defines (strength – stress).

= 2 Structural design factor model.
This predefined resistance model defines (stress - strength).

= 3 Material Strength Degradation (MSD) model.
This predefined resistance model is explained in detail in a later section of this manual.

*MSDM Only required when using Resistance model #3. (See MSD model section of this manual)

*COMPUTATIONAL METHOD {method #} {number of random variables}

C ➢*comments* ➢ {method #} selects the type of analysis.
C 1 corresponds to the Finite Element Analysis method
C {number of random variables} : the number of computational random variables.

{integer list of random variables} A list of the random variable numbers (1 2 3, etc.)

*END Signifies the end of the input for the ZFDEFINE section.

*RVDEFINE This is the start of random variable definitions.

*DEFINE {random variable #} Designation # of random variable.

{random variable name} The name of the random variable. This is useful for the user to keep track of the random variables; give them meaningful names.

{mean#} {standard deviation #} {distribution type}

C {mean#} The mean of the distribution.

C {standard deviation #} The standard deviation of the distribution.

C {distribution type} The types of distributions in NESSUS:
C NORMAL -Normal or Gaussian Distribution
C WEIBULL
C EXTREMEVALUE
C LOGNORMAL
C CHISQUARE
C MAXENTROPY
C NESSUS
C FRECHET
C TWEIBULL Truncated Weibull Distribution
C TNORMAL Truncated Normal Distribution

{type} Defines the type of finite element data this random variable corresponds to. Includes the following types:

C	ACCELERATION	ORIENTATION
C	BEAMSECTION	PRESSURE
C	COEFFICIENTS	PROPERTIES
C	COORDINATES	PSD
C	DAMPING	SPRINGS
C	DISPLACEMENT	TEMPERATURE
C	DISTRIBUTED LOAD	UPERT
C	FORCES	VELOCITY
HARMONIC		YIELDFUNCTION

{databock} Defines a block of additional data as required by an input. See expanded explanation in the *DEFINE {type} section.

*PERTURB {perturbation #} Defines an individual perturbation
{random variable #} {standard deviation shift}

C	{random variable #}	The random variable that is to be perturbed.
C	{standard deviation shift}	The number of standard deviations that an individual random variable will be perturbed or shifted.

C *MEAN VALUE PROBABILISTIC ANALYSIS*

*MVDEFINE This signals the start of the section where the keywords and random variables will be analyzed using the mean value first or second order methods. States type of data to be analyzed and which nodes or components are to be analyzed.

*PERT {# of perturbations}	Selects the total # of perturbations to be used in the probabilistic analysis.
{list of perturbations}	an integer list of perturbations to be perturbed
*RANVAR {# of random variables}	Selects the total number of random variables to be analyzed.
{random variable # list}	an integer list of random variable numbers to be perturbed
*DATATYPE {type of data #}	Specifies the type of data on which to perform the probabilistic analysis.
C {type of data #}	= 0 specifies Incremental
C	= 1 specifies Eigenvalue
C	= 2 specifies Harmonic/spectral

*RESPTYPE {response type #} The type of response variable to extract from the perturbation database.

C {response type #}

C	1= TOTAL DISPLACEMENT	36 = THE FREQUENCY IN CYCLES PER TIME
C	2 = TOTAL STRAIN	51 = REAL DISPLACEMENT
C	3 = TOTAL STRESS	52 = REAL STRAIN
C	11 =PLASTIC STRAIN	53 = REAL STRESS
C	12 = BACKSTRESS	61 = IMAGINARY DISPLACEMENT
C	13 = CREEP STRAIN	62 = IMAGINARY STRAIN
C	14 = THERMAL STRAIN	63 = IMAGINARY STRESS
C	17 = GENERALIZED STRAIN	71 = THE AMPLITUDE OF THE DISPLACEMENT
C	18 = GENERALIZED STRESS	72 = THE AMPLITUDE OF THE STRAIN
C	21 = MATERIAL STATE	73 = THE AMPLITUDE OF THE STRESS
C	VARIABLES	
C	25 = VELOCITIES	81 = THE PHASE OF THE DISPLACEMENT
C	26 = ACCELERATIONS	82 = THE PHASE OF TIIE STRAIN
C	30 = THE EIGENVALUE FOR	83 = TIIE PIIASE OF THE STRESS
C	THE MODE	
C	31 = MODAL DISPLACEMENT	91 = MEAN SQUARE DISPLACEMENT
C	(EIGENVECTOR)	
C	32 = MODAL STRAIN	92 = MEAN SQUARE STRAIN
C	33 = MODAL STRESS	93 = MEAN SQUARE STRESS
C	35 = THE FREQUENCY IN	96 = STRESS VELOCITY
C	RADIAN PER TIME	

*CONDITION {beginning condition #} {ending condition #} Selects the beginning and ending condition numbers for the mean value analysis.

C Select condition type with previous DATATYPE keyword. The condition refers to
C here refers to either the increment number, the mode number or the
C harmonic/spectral case number respectively.

*NODE {beginning node #} {ending node #} Selects the beginning and ending node numbers for the mean value analysis. If there is only one node, then only one number is needed.

*COMPONENT {beginning component #} {ending component #} Selects the beginning and ending component numbers for the mean value analysis.

C Component numbers:

C *1 = translation in the x direction*
C *2 = translation in the y direction*
C *3 = translation in the z direction*
C *4 = rotation with respect to the positive x direction*
C *5 = rotation with respect to the positive y direction.*
C *6 = rotation with respect to the positive z direction*

*PRINT {print control} Controls the amount of printed output that will be generated during a PFEM analysis.

C {print control}: = SHORT All finite element and fast probability output sent to the .feo and .fpo files, respectively.
C = MEDIUM All finite element and fast probability output sent to the .feo and .fpo files, respectively
C = LONG All output is sent to the .out file.

*END Signifies the end of the MVDEFINE section.

C *ADVANCED MEAN VALUE PROBABILISTIC ANALYSIS*
*AMVDEFINE Signifies the start of the advance mean value analysis definition.

*ITERATION Defines the convergence criteria for the AMV+ z-level and p-level iteration procedures.
{maximum # of iterations} {error tolerance}

C {maximum # of iterations}: The maximum number number of iterations the procedure is allowed to perform before exiting
C {error tolerance}: The relative error between successive iterations.
C Using the Zlevel Algorithm, convergence is defined to be
C $= |\beta_i - \beta_{i-1}|/\beta_{i-1} = \varepsilon$ when using the relative change in beta and
C $= | Z_I - Z_{i-1}|/ Z_{i-1} = 0.2$ when using the relative change in the Z
C and the angle between the MPP's from the last two iterations, θ, is less
C than the allowable maximum of 30°.
C Theta is defined as $\cos\theta = \alpha_i \cdot \alpha_{i-1}$, where α_i are the direction cosines to
C the MPP from integration i .
C Using the Plevel Algorithm, convergence is defined as
C $= | Z_I - Z_{i-1}|/ Z_{i-1} = \varepsilon$ and
C the angle between the MPP's from the last two iterations, θ, is less than the
C allowable maximum of 30°.
C Theta is defined as $\cos\theta = \alpha_i \cdot \alpha_{i-1}$, where α_i are the direction cosines to
C the MPP from integration i

*CONDITION {beginning condition #} {ending condition #} Selects the beginning and ending condition numbers for the Advanced Mean Value analysis.

*NODE {beginning node #} {ending node #} Selects the beginning and ending node numbers for the Advanced Mean Value analysis.

*COMPONENT {beginning component #} {ending component #} Selects the beginning and ending component numbers for the Advanced Mean Value analysis.

*END Signifies the end of the AMVDEFINE section.

*END End of PFEM input.

*FEM Signals the start of the deterministic Finite Element section.

*CONS {constitutive model #} Selects the constitutive material model.

C {constitutive model #} = 0 for linear elastic model.
C = 1 selects the simplified plasticity
C = 2 selects classical von Mises J2-flow plasticity
C = 3 selects Walker's creep-plasticity model.

*ELEMENTS {# of elements} Allocates memory for a maximum number of elements.
{element type #} The element type used for analysis.
C {element type #} The following element type #'s are valid:
C 3 = bilinear, isoparametric plane stress element.
C 7 = trilinear isoparametric, solid element.
C 10 = bilinear, isoparametric, axisymmetric element.
C 11 = bilinear isoparametric plane strain element.
C 75 = bilinear, isoparametric, variable-thickness shell element.
C 98 = linear, isoparametric, tapered beam element.
C 151 = bilinear, isoparametric, plane stress element.
C 152 = bilinear, isoparametric, plane strain element.
C 153 = bilinear, isoparametric, axissymmetric element.
C 154 = trilinear, isoparametric, solid element

*NODES {# of nodes} Allocates memory for the number of nodes on the mesh.

*BOUNDARY {# of boundary conditions} Allocates memory for the boundary conditions.

*FORCES {# of forces} Allocates memory for the applied forces.

*PRINT {# quantities printed} This controls the amount of data printed to the output file.
C {# quantities printed} The maximum number of quantities printed to the output
C file. The default is 10.

*MONITOR {# of monitored values} Monitors a small number of values when the code is run interactively. This shows what is happening to a certain quantity.

*END The end of the memory allocation.

*ITER {begining' perturbation #} {ending perturbation #}
{maximum # of perturbations} {relative error} {absolute error} {displacement error} {energy error}

C This sets the convergence tolerances for the iterative solution algorithms.

*MONITOR To monitors certain values at the end of an iteration.
{Monitored quantity} {Location} {Component #} This selects a small number of values that will be reported at the end of each iteration. Used primarily when running the code interactively.

C {Monitored quantity} The string denoting the quantity to be monitored. The following
C quantities are valid:
C CREEPSTRAIN STRAIN
C EQUIVALENTPLASTICSTRAIN STRESS
C FORCE TEMPERATURE
C INCREMENTALDISPLACEMENT THERMALSTRAIN
C PLASTICSTRAIN TOTALDISPLACEMENT
C REACTION/RESIDUAL

C {Location} The component or location to be monitored, i.e., NODE #
C {Component #} The string specifying a particular component or location. The valid componets are:
COMPONENT #
NODE #

*COORDINATES Used to specify nodal point coordinates for the finite element mesh used in the analysis.
{node #} {1st-coordinate #} {2nd-coordinate #} {3rd-coordinate #}...

C For the element type 3, 11 151 and 152, the two coordinates required are:
C {coordinate #}= 1 is the x global coordinate.
C 2 is the y global coordinate.

C For the elements of type 10 or 153, the two coordinates are:
C {coordinate #}= 1 is the (z) axial coordinate.
C 2 is the (r) radial coordinate.

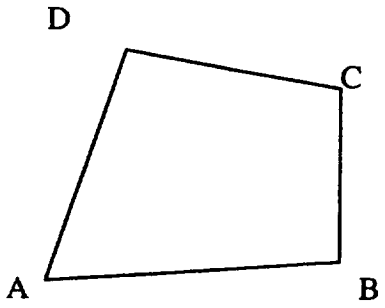
C For the elements of type 7 or 154, the three coordinates are:
C {coordinate #}= 1 is the x global coordinate.
C 2 is the y global coordinate.
C 3 is the z global coordinate.

C For the three-dimensional shell element type 75, the four coordinates are:
C {coordinate #}= 1 is the x global coordinate.
C 2 is the y global coordinate.
C 3 is the z global coordinate.
C 4 is the thickness of the shell.
This defaults to the last nonzero thickness entered.
C For the three-dimensional meshes using element type 98, the six coordinates are
{coordinate #}= 1 is the x global coordinate.
2 is the y global coordinate.
3 is the z global coordinate
4 is the x-component of the beam normal
5 is the y-component of the beam normal
6 is the z-component of the beam normal.

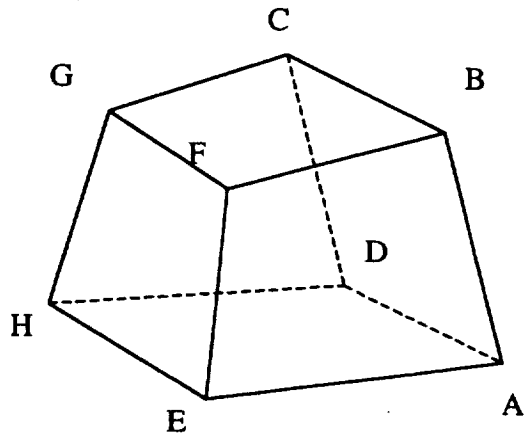
```
*ELEMENTS {element type #}
{element  #} {node # a} {node # b} {node # c} {node # d}

C       These lines express element  connectivity .
C       {element type #}        The element type used for analysis.
                                (See *ELEMENTS in *FEM section for valid #'s.)
```

The total number of elements n must be less than or equal to the maximum specified in parameter data using the keyword option *ELEMENTS. The exact number m of nodes used to define the connectivity list for a given element will depend on the element type used for the analysis. It is important that the element connectivity list be entered in the correct sequence. For a two-dimensional, four-noded element, this means that the nodes must be entered in counterclockwise order, as shown in Figure 1. The node numbering convention for a three- dimensional, eight-noded element is also shown. The correct node order is as indicated by the alphabetic sequence A, B, C ... Z. If the node sequence for an element is found to be incorrect, the code will attempt to fix it by reordering the nodes. A warning message will be printed to the output file, listing the modified node order. When this happens, the user should always check the modified node sequence to see whether it still agrees with the desired mesh topology.



Plane stress, plane strain, or axisymmetric



3D Solid element

Node numbering for continuum-type elements.

*BOUNDARY To specify displacement boundary conditions.
{node #} { component #} {prescribed displacement}

C {node #} The node number.
C {component #} The components of the boundary conditions.
C *1 = translation in the x direction*
C *2 = translation in the y direction*
C *3 = translation in the z direction*
C *4 = rotation with respect to the positive x direction*
C *5 = rotation with respect to the positive y direction.*
C *6 = rotation with respect to the positive z direction*
C {prescribed displacement} The displacement prescribed for that particular direction at
C that particular node.

*PROPERTIES {element type #} This defines the material properties for a particular set of nodes.
{beginning node #} {ending node #} {prop #1} {prop #2} {prop #3} {prop #4} {prop # 5} {prop # 6}

C {beginning node #} Specifies the first node number in a series.
C {ending node #} Specifies the last node number in a series.
C {prop #1} Specifes the element thickness for a plane stress analysis.
C A dummy paramenter otherwise.
C {prop #2} Specifies the elastic modulus in units of force/unit length..
C {prop #3} Specifies Posssion's ratio a dimensionless quantity.
C {prop #4} Specifies the thermal expansion coefficient in units of Length/temperature. Also called alpha.
C {prop #5} Specifies the mass density in unit of mass/length ^3
C {prop #6} Specifies the shear modulus for a plane stress element and Axisymmetric problems and three dimensional solid analysis, in units of force/length^2. Unused otherwise.

*FORCES To specify applied forces.
{node #} {component #} {force} Specifies the location, component and force applied to a node.

C {node #} Specifies the node number
C {component #} Specifies the direction of the force (see *BOUNDARY)
C {force} Specifies the magnitude of the load applied .

*PRINT
{quantity type} {beginning #} {ending #} {location parameter} {beginning #} {ending #}
C Controls the amount of data printed to the output file.
C The beginning and ending #'s are optional, otherwise all
C components will be printed.
C {quantity type} Specifies particular quantity to be printed.
C The possible quantity types are:
C CREEPSTRAIN
C EQUIVALENTPLASTICSTRAIN
C FORCE
C INCREMENTALDISPLACEMENT
C PLASTICSTRAIN
C REACTION/RESIDUAL
C STRAIN
C STRESS
C TEMPERATURE
C THERMALSTRAIN
C TOTALDISPLACEMENT
C {location parameter}
C The possible location parameters are:
C ELEMENTS
C INTEGRATIONPOINTS
C LAYERS
C NODES

*END Specifies the end of all model data input.

*FPI Specifies the start of the Fast Probability analysis input setion.

*RVNUM {random variable #} The number of random variables to be analyzed by Fast Probability Integration.

*GFUNCTION {function type #} Defines the g-function approximation.

C {function type #} The type of function desired by the user.
C = 1 for a linear g-function approximation.
C N+1 datasets are required for linear, where N is the number
C of random variables or pertubations.
C = 2 for a quadratic g-function approximation.
C 2*N+1 data sets are required for the quadratic
C approximation.
C = 5 for a g-function of the form (strength-stress). Used for
C reliability analysis with the strength-stress form, i.e. R-S.
C Only the probability of failure, i.e. P[g(x)<0], will be
C determined.
C = 6,7,8 for a user defined response function.
C g-function must be programmed in routine RESPON or
C USERES, or defined in the input deck provided that the
C g-function has a continuous first derivative.

*DATASETNM {# of data sets} Designates the number of data sets for a particular problem. (See *GFUNCTION for the number required.)

*METHOD {method type #} Defines the solution type used in FPI analysis.

C {method type #}

= 0 First order reliability method (FORM).

C = 1 Advanced first order reliability method (FPI).
C Computes both first order reliability method and
C advanced first order reliability method solutions.
C Parameter = 1 is recommended.

C = 2 Fast convolution in the regular-space (CONVX).
C FORM solution computed first.

C = 3 Fast convolution in the standard normal-space
C (CONVU).
FORM solution computed first.

C = 4 Second order reliability method (SORM).
C FORM solution computed first.

C = 5 Importance sampling method with radius reduction
C factor (ISAMF). *MONTE keyword and data are
C expected in the Model section of FPI.
C Monte Carlo can only be used for user-defined
C response levels (ZLEVELS), *ANALTYP=1.

C = 6 Conventional Monte Carlo method (MONTE).
C *MONTE keyword and data are expected in Model
C section. Monte Carlo can only be used for
*ANALTYP = 0 or 1.

C = 7 Same as parameter = 5 except that the radius is user-
C supplied (ISAMR).Limited to *ANALTYP = 1.
C = 8 Adaptive importance sampling (linear
C surface)(AIS1). *ITOL keyword and data are
C expected in Model section.
C Limited to *ANALTYP = 1.

```
C                                   = 9     Adaptive importance sampling (quadratic surface)
C                                           (AIS2). *ITOL keyword and data are expected in
C                                           Model section.
C                                           Limited to *ANALTYP = 1.

C                                   =10     Mean value method (MV).

C                                   =11     Advanced mean value method (AMV).

C                                   =12     Advanced mean value method plus (AMV+).
C                                           *ITER keyword and data are expected in Model
C                                           section.

*PRINTOPT   {printout type #}

C           {printout type #}       Defines the amount of data to be printed out from FPI.
C                                   = 0 for the short print out.
C                                   = 0 for long print out.

*ANALYTYPE {analysis type #}
C       {analysis type #}           Specifies the analysis type.
C                                   The types used are:
C                                   = 0     FPI defined probability levels are used. These are
C                                           automatic and are typically from –4.5 to 4.5 standard
C                                           deviations from the mean of the response.
C                                   = 1     User defined response levels(Z levels). The *ZLEVELS
C                                           keyword and the Zlevels are required in the FPI model
C                                           section. This is the most efficient method.
C                                   = 2     User defined probability levles. The PLEVELS keyword
C                                           and the probability levels are required in the FPI model
C                                           section.

*END                        Signifies the end of the parameter data. What follows this first *END is
                            the FPI model data section.

*ZLEVELS  {# of levels}     Defines the number of response levels; maximum =20

*PLEVELS  {# of levels}     Defines the number of probability levels.

*MONTE
 {# of samples} {seed #} {beta factor}
C                           Specifies the data  necessary for running Monte Carlo Simulations. This
C                           line is required when Method=5, 6 or 7 in the FPI parameter section.

C     {# of samples}        The number of random samples for each response level using *METHODs
C                           5 and 7.
                            It is the total number of random sampels for METHOD 6.
      {seed #} The random number generator seed, however, it must be an integer.
      {beta factor}   = 5   This defines the reduction factor for the sampling radius based on
C                           the minimum distance.
C                     = 6   This value is zero .
C                     = 7   This value is a user-supplied radius.

*ITOL
*ITER
*CONFINTVL
*END                        End of input file.
```

Material Strength Degradation (MSD) Model

The MSD model in the form of a postulated randomized multi-factor equation provides for quantification of uncertainty in the lifetime strength of components subjected to a number of diverse random effects. The mathematical expression for this MSD model is:

$$\frac{S}{S_O} = \Pi\left[\frac{A_{iU} - A_i}{A_{iU} - A_{iO}}\right]^{a_i} \qquad (1)$$

where, A_i, A_{iU} and A_{iO} are the current, ultimate and reference values, respectively, of a particular effect; a_i is the value of the calibrated empirical material constant for the i^{th} effect terms of the variables in the model; and S and S_O are the current and reference values of material strength. Each term has the property that if the current value equals the ultimate value, the lifetime strength will be zero. Also, if the current value equals the reference value, the term equals one and strength is not affected by that value. The product form of equation (1) assumes independence between individual effects. This equation may be viewed as a solution to a separable partial differential equation in the variables with the further limitation or approximation that a single set of separation constants, a_i, can adequately model the material properties.

The model is currently set up for five fixed effects and 12 user defined effects that typically reduce lifetime strength. These effects are listed below:

- High temperature
- High-cycle mechanical fatigue
- Low-cycle mechanical fatigue
- Creep
- Thermal fatigue
- Up to 12 user defined (General) effects

When expanded for all effects, the equation is as follows:

$$S = S_O\left[\frac{T_u - T}{T_u - T_o}\right]^q\left[\frac{N_u - N}{N_u - N_o}\right]^w\left[\frac{N'_u - N'}{N'_u - N'_o}\right]^r\left[\frac{t_u - t}{t_u - t_o}\right]^v\left[\frac{N''_u - N''}{N''_u - N''_o}\right]^u\left[\frac{A_u - A}{A_u - Ao}\right]^a, \qquad (2)$$

Temperature HCF LCF Creep Thermal Fatigue General

where T is temperature, N is cycles, t is time, and A is a user-defined effect. The lower case exponents are the empirical material constants for each effect. The subscript, u, refers to an ultimate value, the subscript, o, is the reference value, and the non-subscripted term is the current value for the effect.

To increase model sensitivity for certain effects, a logarithmic base ten transformation is introduced resulting in the following form.

$$S = S_o\left[\frac{LOG(A_{iU}) - LOG(A_i)}{LOG(A_{iU}) - LOG(A_{iO})}\right]^a \tag{3}$$

The nature of the material data will dictate the use of the log transformation. The effects to be used and the model type (log transformation) are defined in the Z-function definition section of the PFEM input file. Any combination of effects can be selected and any of the terms can be considered random if desired. The form of the g-function used by NESSUS is

$$zg = S_O\prod_i\left[\frac{A_{iU} - A_i}{A_{iU} - A_{iO}}\right]^{a_i} - \sigma \quad , \tag{4}$$

where

S_O is the reference value of material strength

A_{iU} is the ultimate value of the particular effect

A_{iO} is the reference value of the particular effect

A_i is the current value of the particular effect

a_i is the empirical material constant for the particular effect

σ is the structural response as calculated by NESSUS/FEM, i.e. stress.

As an example, the equation is expanded for the two effects of high temperature and high-cycle mechanical fatigue as shown in equation (5) below:

$$\frac{S}{S_O} = \left[\frac{T_U - T}{T_U - T_O}\right]^q \left[\frac{\text{LOG } (N_U) - \text{LOG } (N)}{\text{LOG } (N_U) - \text{LOG } (N_O)}\right]^w - \sigma, \quad (5)$$

The MSD model was calibrated for INCONEL 718 by appropriate curve-fitted least squares linear regression of experimental data. Linear regression of the data for each effect resulted in estimates for the empirical material constants, as given by the slope of the linear fit. These estimates, together with ultimate and reference values, were used to calibrate the model specifically for Inconel 718. Lifetime material strength results, in the form of cumulative distribution functions (CDF's), illustrate the sensitivity of lifetime strength to any one, or a combination of, the effects.

The formulation defined in NESSUS is

$$Z = S_O\left[\frac{T_U - T}{T_U - T_O}\right]^q \left[\frac{\text{LOG } (N_U) - \text{LOG } (N)}{\text{LOG } (N_U) - \text{LOG } (N_O)}\right]^w - \sigma$$

By defining S to be 1.0 and not including a computational model to compute stress (σ = 0.0), then NESSUS is solving the problem for S/S_O. The random variables are defined in Table 1.

Table 1. Random Variable Definitions

Effect	Symbol	Distribution	Mean	Standard Deviation
High Cycle Mechanical Fatigue (at 75 °F)	N_U	Normal	1.0×10^{10} cycles	1.0×10^{9} cycles
	N	Normal	2.5×10^{5} cycles	2.5×10^{4} cycles
	N_O	Normal	0.25 cycles	0.025 cycles
	W	Normal	0.3785	0.0114
High Temperature (at 1000 °F)	T_U	Normal	2369.0°	236.90°
	T	Normal	1000.0°	100.0°
	T_O	Normal	75.0°	7.5°
	Q	Normal	0.2422	0.0088

The relevant NESSUS input for this problem is shown in Figure 1. Note that to consider a term in an effect random, the alphanumeric name must match the name in the RVDEFINE input. An example of this is the highlighted NU variable shown in both the ZFDEFINE section and the RVDEFINE section in Figure 1.

```
*ZFDEFINE
*EXPLICITMODEL  8
1,2,3,4,5,6,7,8
*ZFUNCT       3   0
 *MSDM  1.0  (S0)
     TEMP  LINEAR  TU  T  TO  QQ
     HCF  LOG  NU  N  NO  W
     END
*END
*RVDEFINE
*DEFINE 1
NU
1.0E10 1.0E9    NORMAL
*DEFINE 2
N
2.5E5  2.5E4    NORMAL
*DEFINE 3
NO
0.25  0.025     NORMAL
*DEFINE 4
W
0.3785  0.0114 NORMAL
*DEFINE 5
TU
2369.0  236.9  NORMAL
*DEFINE 6
T
1000.0  100.0  NORMAL
*DEFINE 7
TO
75.0  7.50      NORMAL
*DEFINE 8
QQ
0.2422  0.0088 NORMAL
```

Figure 1. NESSUS Input for Example Problem

***DEFINE {type}**

ACCELERATION
nodel dacc1 1 dacc21 daccml
node2 dacc1 2 dacc22 daccm2
noden dacc1 n dacc2n ... daccmn

where the values dacc denote relative perturbations to the m components of the initial accelerations at each node. This means that, when the associated random variable is perturbed by one full standard deviation, a total change of dstdev times dacc2n should be observed in the second component of the initial acceleration for node n. The same general rule also holds for other components

COORDINATES
nodel dcoor1 1 dcoor21 ... dcoorml
node2 dcoor1 2 dcoor22 ... dcoorm2
noden dcoor1 n dcoor2n ... dcoormn

where the values dcoor denote relative perturbations to the m components of the nodal coordinates at each mesh point. The input format for DataBlock is identical to the one used to specify *COORDINATES as discussed elsewhere in this section.

The input format used for defining a perturbation variable associated with the Rayleigh damping coefficients is
DAMPING 1
dalpha dbeta

where jdamp is set to 1, for Rayleigh damping, and dalpha and dbeta are the relative perturbations to the two Rayleigh damping parameters

DAMPING 2
imodel jmodel dratio1
imode2 jmode2 dratio2
imoden jmoden dration

where jdamp is set to 2, for modal viscous damping, and the values of dratio denote the relative perturbations to the modal damping ratios.

DAMPING 3
imodel jmodel dratio1
imode2 jmode2 dratio2
imoden jmoden dration

where jdamp is set to 3, for structural damping, and the values of dratio are again used to denote the relative perturbations to the modal damping ratios. In all three cases, the formats are identical to the ones used to prescribe a given damping model using the *DAMPING keyword option.

DISPLACEMENT
nodel ddisl 1 ddis2l ... ddisml
node2 ddis12 ddis22 ... ddism2
noden ddisl n ddis2n ... ddismn

where the values ddis are relative perturbations to the m components of the initial displacements at each node.

DISTRIBUTEDLOAD jetyp
ieleml jelem1 indexl ddistl 1 ddist2l ... ddistml
ielem2 jelem2 index2 ddist12 ddist22 ... ddistm2
ielemn jelemn index3 ddistl n ddist2n ... ddistmn

where the values ddist are relative perturbations to the m distributed loads for each element between ielem and jelem. Notice the flag jetyp, which is used to indicate the element type used for the analysis.
FORCES
nodel ndof 1 dforcel
node2 ndof2 dforce2
noden ndofn dforcen

where dforce are the relative perturbations to the force (or moment) acting at degree- of-free dom ndof of node node. It is assumed that a set of unperturbed loads has been defined at these nodes and degrees-of-freedom (even though these unperturbed loads may have zero magnitude).

The three different perturbation variables associated with harmonic excitation parameters are discussed next.
HARMONIC jharm
dfreq
FORCES
nodel ndof 1 damplil dphasel
node2 ndof2 dampQ dphase2
noden ndofn damplin dphasen

where dampli and dphase are relative perturbations to the amplitude and phase of the harmonic loads acting at degree-of-freedom ndof of node node, and df req - is the perturbation to the excitation frequency. It is assumed that unperturbed harmonic force excitations have been previously specified at these nodes and degrees-of-freedom for harmonic case jharm.

To define a perturbation variable associated with harmonic base acceleration parameters, the input format is
HARMONIC jharm
dfreq
ACCELERATION
nodel ndof 1 damplil dphasel
node2 ndof2 dampli2 dphase2
noden ndofn damplin dphasen

where dampli and dphase are the relative perturbations to the amplitude and phase of the harmonic base accelerations for degree-of-freedom ndof of node node, and dfreq is the perturbation to the excitation frequency. It is assumed that unperturbed base accelerations have been specified previously at these nodes and degrees-of-freedom for harmonic case jharm.

Finally, the input format used for defining a perturbation variable associated with the harmonic pressure loading parameters is
HARMONIC jharm
df req
PRESSURE
inodel jnodel damplil dphasel
inode2 jnode2 damplQ dphase2
.
inoden jnoden damplin dphasen

where dampli and dphase are the relative perturbations to the amplitude and phase of the harmonic pressure loading defined at nodes inode through jnode, and dfreq is the perturbation to the excitation frequency.

ORIENTATION
inodel jnodel dalphal dbetal dgammal
inode2 jnode2 dalpha2 dbeta2 dgamma2
.
inoden jnoden dalphan dbetan dgamman

where dalpha, dbeta, and dgamma denote relative perturbations to the three direction angles defining the material orientation in three dimensions. For two-dimensional analysis, only the first angle needs to be specified.

PRESSURE
inodel jnodel dpressl
inode2 jnode2 dpress2
.
inoden jnoden dpressn

where the values of dpress are relative perturbations to the nodal pressures acting at nodes inode through jnode.

PROPERTIES jetyp
inodel jnodel dpropl 1 dprop2l ... dpropm1
inode2 jnode2 dprop12 dprop22 ... dpropm2
.
inoden jnoden dpropln dprop2n ... dpropmn

where the values of dprop are used to denote relative perturbations to the m material properties assigned to nodes inode through jnode. Notice the flag jetyp, which is used to indicate the element type used for the analysis.

The three different types of perturbation variables associated with power spectrum excitations are discussed next. The input format used for defining a perturbation variable involving power spectra for nodal forces is:

PSD jpsd
df req 1 dpsdl
df req2 dpsd2
dfreqm dpsdm
FORCES
nodel ndof 1 damplil
node2 ndof2 dampV
noden ndofn damplin

where dfreq and dpsd define changes to the profile of the power spectrum excitation curve, and dampli is the relative change in amplitude of the power spectrum excitation for degree-of-freedom ndof at node node. It is assumed that unperturbed power spectrum forces have been previously specified at these nodes and degrees-of-freedom for the jpsd power spectrum case.

The input format used for defining a perturbation variable associated with the power spectrum excitation parameters for base acceleration is
PSD jpsd
df req 1 dpsdl
dfreq2 dpsd2
.
dfreqm dpsdm
ACCELERATION
nodel ndof 1 damplil
node2 ndof2 dampdi2
.
noden ndofn damplin

where dfreq and dpsd define changes to the profile of the power spectrum excitation curve, and dampli is the relative change in amplitude of the power spectrum excitation for degree-of-freedom ndof at node node. Again, it is assumed that unperturbed power spectrum accelerations have been specified at these nodes and degrees-of-freedom for the jpsd power spectrum case.

To define a perturbation variable involving the power spectrum excitation parameters for nodal pressures, the input format is

PSD jpsd
df req 1 dpsdl
df req2 dpsd2
.
dfreqm dpsdm
PRESSURE
inodel jnodel damplil
inode2 jnode2 dampi2
.
inoden jnoden damplin

where dfreq and dpsd define changes to the profile of the power spectrum excitation curve, and dampli denotes the relative change in the amplitude of the random pressure loading acting at nodes inode through jnode.

In all cases, the number of lines defining the profile of the power spectrum excitation curve is limited by the parameter npsdp, and the number of data lines following FORCES, ACCELERATION, or PRESSURE is limited by the parameter npsep, both defined by the *PSD option in the parameter data block for the problem..

Perturbation variables involving ground spring stiffnesses may be defined using the following input format
*DEFINE jpvar
dmean dstdev
SPRINGS
nodel ndofl dstiff 1
node2 ndof2 dstiff2
.
noden ndof n dstiffn

where dstiff is used to denote the relative perturbation to the ground spring stiffness at degree-of-freedom ndof of node node. It is assumed that a set of unperturbed ground springs has been defined at these nodes and degrees-offreedom.
The input format used for defining a perturbation variable associated with the nodal temperatures is

TEMPERATURE
inodel jnodel dtempl 1 dtemp2l ... dtempml
inode2 jnode2 dtemp12 dtemp22 ... dtempm2

inoden jnoden dtempln dtemp2n dtempmn

where the values dtemp denote relative perturbations to the m temperatures at each mesh point. The input for most elements requires only one temperature value at each mesh point. . However, elements with multiple layers, such as the bilinear shell element (type 75), will need to have temperatures specified for each one of the m layers at a node.

The NESSUS finite element code also provides a facility for defining general loading time-histories that are a function of one or more random variables. These random variables are not necessarily, associated with any particular loading type, and may even represent quantities that are not explicitly defined in the finite element code, such as engine power level, flow rate, and inlet temperatures in a duct, etc. The functional dependence of the loading on these random variables may be coded as a general analytical (or algorithmic) expression in subroutine UPERT.
The input format for defining a random variable to be used as an input to the UPERT user routine is
UPERT
Notice that a DataBlock is not included, since this information will be defined in the coding for the UPERT subroutine. Although the statistics for the random variables may not (at present) be taken to be a function of time, the functional dependence of the loading on these random variables may be expressed as a function of time.

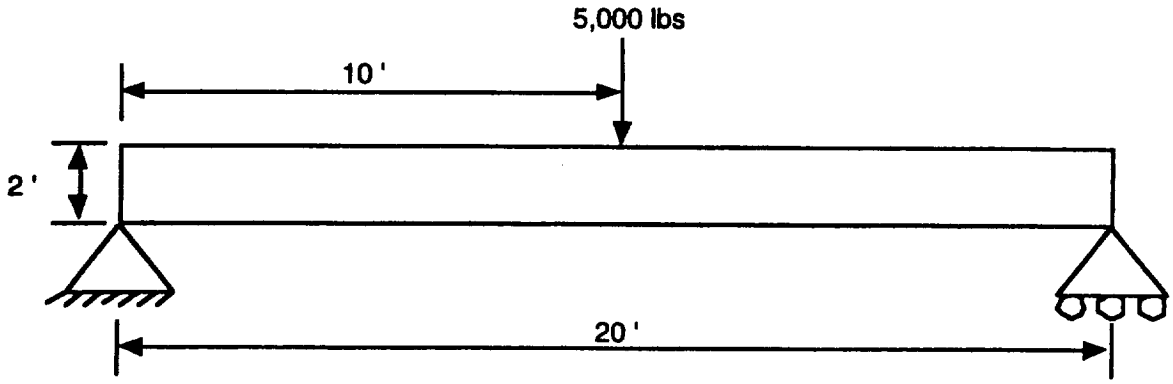
The input format for defining a perturbation variable associated with the initial velocity for a dynamic problem is
VELOCITY
nodel dvel 11 dve121 ... dvelml
node2 dvel 12 dve122 ... dvelm2
noden dvel1n dvel2n ... dvelmn

where the values dvel are relative perturbations to the m components of the initial velocity at each node..

A slightly more cumbersome format is used to define perturbation variables associated with the yield stress and work-hardening curves for elastoplastic materials. However, this somewhat complicated format also provides a great deal of flexibility in the way elastoplastic behavior is defined paramaterically at different mesh nodes. The input format for defining perturbation variables involving the work-hardening curves is
YIELDFUNCTION
inodel jnodel
dsigmal depspI 1 domegl
dsigma2 depsp12 domeg2
.
dsigmak depsplk domegk
inode2 jnode2
dsigmak+1 depsplk+1 domegk+1
dsigmak+2 depsplk+2 domegk+2
.
dsigma2k depspl2k domeg2k

where dsigma, depspl, and domeg denote the relative perturbations to the yield stress, equivalent plastic strain, and backstress for the work-hardening curves from inode through jnode. These values should be arranged as a set of 3 x k tables, where k=- nhard as defined by the *HARDENING option in the parameter data block. One or more node lists, each one with the associated work-hardening table, may be input in a single *DEFINE option, provided that all the tables contain exactly 3 x k entries. This concludes the discussion of the many different types of Level 2 perturbation variables currently available in the NESSUS finite element code. One or more of theses variables may be changed in a given perturbation, as discussed under the keyword *PERTURB.

Example problem : Simply Supported Beam

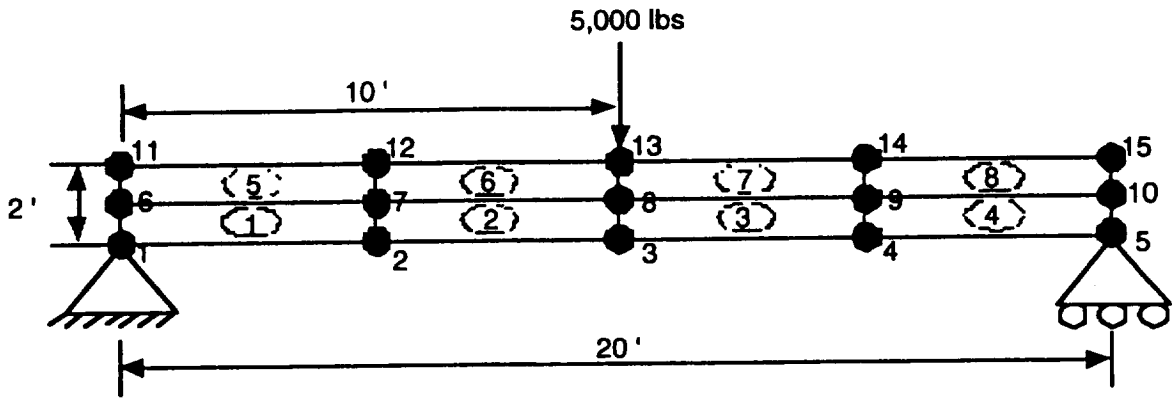


Problem Definition: Random Variables in NESSUS input file

Variable	Description	Type	Mean	Standard Deviation (10%)	Distribution
PMAX	Point Load	loading	5,000 lbs	500	Normal
L	Beam Length	Geometry	20 ft.	2.0	Normal
H	Beam Height	Geometry	2 ft.	.2	Normal

Using the probabilistic finite element analysis program,NESSUS, determine the mean maximum bending stress, σ_x. Compare to the expected Mechanics of Solids deterministic solution using the flexure formula, σ=-My/I.

Divide your beam into 8 elements (15 nodes) with the following numbering scheme. Then further divide your beam to increase the accuracy of your results.



```
*PFEM
C THREE POINT BEND PROBLEM
C
C*************************************************************************
C
C   Computational Methods for Probabilistic Engineering Analysis
C
C*************************************************************************
C
C NESSUS Advanced Mean Value First Order Iteration CDF analysis (AMV+)
C
C The material is STEEL.
C
C Random variables include:
C
C    1    PMAX   point load acting at the center of the beam
C    2    L      length of the beam
C    3    H      height of the beam
C
C.........................................................................
C
C Z-FUNCTION DEFINITION
C
C 3 RANDOM VARIABLES (3-COMPUTATIONAL)
C
*ZFDEFINE          The beginning of the z-function definition
*COMPUTATIONALMETHOD 1 3      This invokes the NESSUS/FEM section with 3 random
                               variables.
 1 2 3                        This is a list of the random variable numbers.
C
*END        This is used to indicate the end of the ZFDEFINE section.
C
C
C RANDOM VARIABLES
C
C
*RVDEFINE   This is the start of the definition of the random variables.
*DEFINE 1   The random variable numbered as 1.
 PMAX       The random variable name .
 -5000   500  NORMAL     The mean, standard deviation an distribution type.
C
C
 FORCES     This denotes the type of random variable.
 13  2  1.0
*DEFINE 2   This random variable is numbered 2.
 L          The name of the random variable.
 20.0  2.0  NORMAL       The mean, standard deviation and distribution type.
 COORDINATES             The type of data block.
  1   0.00   0.0         The start of the data block. 1 is the node number 0.00
C                        is the perturbation amount in the x direction, 0.0 is
C                        the perturbation in the y direction.
  2   0.25   0.0
  3   0.50   0.0
  4   0.75   0.0
  5   1.00   0.0
  6   0.00   0.0
  7   0.25   0.0
  8   0.50   0.0
```

```
  9   0.75    0.0
 10   1.00    0.0
 11   0.00    0.0
 12   0.25    0.0
 13   0.50    0.0
 14   0.75    0.0
 15   1.00    0.0
*DEFINE 3          This random variable is numbered 3.
 H                 The random variable name.
 2.0  0.2 NORMAL   The mean, standard deviation and distribution type.
 COORDINATES       The type of data block.
  1   0.0   0.0   The start of the data block. 1 is the node number 0.00
C                       is the perturbation amount in the x direction, 0.0 is
C                       the perturbation in the y direction.
  2   0.0   0.0
  3   0.0   0.0
  4   0.0   0.0
  5   0.0   0.0
  6   0.0   0.5
  7   0.0   0.5
  8   0.0   0.5
  9   0.0   0.5
 10   0.0   0.5
 11   0.0   1.0
 12   0.0   1.0
 13   0.0   1.0
 14   0.0   1.0
 15   0.0   1.0
*PERT    1         The first perturbation for random variable number one.
    1         0.1 The perturbation for the first random variable and 0.1 is the
C                   amount of that random variable's standard deviation that is to
C                   be perturbed.
*PERT    2         The second perturbation for random variable two.
    2         0.1 The perturbation for the second random variable and the amount
C                   of standard deviation that is to be perturbed.
*PERT    3         The third perturbation for random variable number three.
    3         0.1 The perturbation for the third random variable and the amount
C                   of standard deviation that is to be perturbed.
*END  The end of the random variable parameter input.
C
C
C MEAN VALUE PROBABILISTIC ANALYSIS
C
*MVDEFINE   Signals the start of the mean value analysis section.
*PERT 3     The number of perturbations to be probabilistically analyzed.
1 2 3       The order of perturbations to be perturbed.
*RANVAR 3   The number of random variables to be used in the perturbations.
1 2 3       The order of random variables to be perturbed.
*DATATYPE 0 The incremental(0) type of data on which to perform the
C           probabilistic analysis.
*RESPTYPE 3 The stress type(3) of response variable to extract from the
C            perturbation database.
*CONDITION 0      The beginning and ending datatypes.
*NODE 3           The beginning and ending node numbers to probabilistically
C                  analyze.  Here it is the same node.
*COMPONENT 1      The beginnning and ending component numbers to be
C                 probabilistically analyze. Here it is the x direction.
*PRINT LONG       The keyword to signify a long printout.
```

```
*END                The end of the MVDEFINE section
C
C
C ADVANCED MEAN VALUE PROBABILISTIC ANALYSIS
C
*AMVDEFINE          Signals the start of the Advanced Mean Value anlysis section.
*ITERATION          The convergence criteria for the AMV+ anlaysis.
 10 0.05            The maximum number of iterations(10) and the relative error
C                   (0.05)between consecutive runs.
*CONDITION 0        The beginning and ending nodes for the AMV analysis.
*NODE 3             The beginning and ending node numbers for the AMV analysis.
*COMPONENT 1        The beginnning and ending component numbers for the AMV
C                    analysis. Here it is the x direction.
*END                The end of the AMVDEFINE section.
C
C END PFEM INPUT
C
*END                The end of the Probabilistic Finite Element Analysis input.
C
*FEM                The start of the input for the deterministic finite element
C                    program
*CONS 0             This invokes the linear elastic constitutive model used for
C                    analysis
*ELEMENTS 8         This line reserves memory for 8 elements.
 151                 This line indicates the element type is a plane stress
 C                   element.
*NODES 15           This line reserves memory for 15 nodes.
*BOUNDARY 3         This line reserves memory for 3 boundary conditions.
*FORCES 1           This line reserves memory for 1 applied force.
*PRINT              This line prints out 10 output quantities to the ouput file.
*MONITOR 2          This line prints out 2 monitored values reported at the end of
C                   each iteration.
*END                The end of the memory allocation or parameter input.
*ITER 0 3           The iteration tolerance for the iterative solution for 3
C                    iterations.
 50 0.001           The maximum number of iterations and the relative error
C                    between successive iterations.
*MONITOR            To monitor certain values at the end of an iteration.
 TOTALDISPLACEMENT NODE 3 COMPONENT 2     Monitor the total displacement for
C                                         node 3 in the y direction.
 STRESS             NODE 3 COMPONENT 1    Monitor the stress for node 3 in the x
C                                         direction.
*COORDINATES        Nodal coordinate locations
  1   0.0   0.0          Node 1 is located at x = 0.0, y = 0.0.
  2   5.0   0.0          Node 2 is located at x = 5.0, y = 0.0
  3   10.0   0.0
  4   15.0   0.0
  5   20.0   0.0
  6   0.0   1.0
  7   5.0   1.0
  8   10.0   1.0
  9   15.0   1.0
 10   20.0   1.0
 11   0.0   2.0
 12   5.0   2.0
 13   10.0   2.0
 14   15.0   2.0
 15   20.0   2.0
```

```
*ELEMENTS  151     The element connectivity for the plane stress element 151.
 1 1  2  7  6      Element number 1, nodal counter-clock-wise direction for A, B,
C                  C and D.
 2 2  3  8  7
 3 3  4  9  8
 4 4  5 10  9
 5 6  7 12 11
 6 7  8 13 12
 7 8  9 14 13
 8 9 10 15 14
*BOUNDARY          Boundary conditions
 1 2 0.0           Boundary at node 1 is constrained not to move in the y
C                  direction
 1 1 0.0
 5 2 0.0
*PROPERTY          The physical properties of the elements prescribed at the
C                  nodes.
 1 15 1.0 4.320E9 0.3 1.0 1.0       The first node, last node, dummy variable,
C                                   modulus of elasticity, Poission's ratio,
C                                   thermal expansion coefficient and mass
C                                   density.
*FORCES            The force applied.
 13 2 -5000        Its applied at node 13 in the y direction of -5000 units.
*PRINT             What quantities to print to the output file.
TOTAL NODE         Print the total displacement at all of the nodes.
STRESS NODE        Print the stress at all of the nodes.
*END               The end of the model data input.
C
C FPI ANALYSIS CONTROL CARDS
C
*FPI        Signifies the start of the Fast Probability Input section.
C
*RVNUM 3           This defines the number of random variables/perturbations.
*GFUNCTION 1       This defines the the Linear (1) type of g-function
C                   approximation.
*DATASETNM 4       This defines the 4 datasets in the problem. This is necessary
C                  as RVNUM + 1 datasets are output.
*METHOD 1          This defines the Advanced first order method(1) solution
C                  technique.
*PRINTOPT 0        This denotes the short printout(0) option.
*ANALTYPE 0        This defines the full CDF analysis output (0) with 10 levels.
*END               This signifies the end of the FPI section.
*END               This signifies the end of the input file.
```

NESSUS Example problem

The system to be analyzed is the cantilevered beam shown in Fig. 2. The beam is composed of steel (ASTM-A36). The system has two concentrated loads acting on it. Determine the maximum average normal stress and its location using NESSUS.

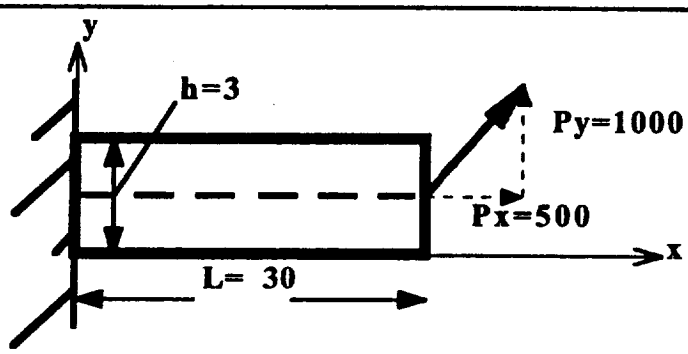


Figure 2. Cantilevered beam. All dimensions are in inches and forces are in pounds. *The beam has a unit depth.*

```
?FEM
?FDEFINE
?OMPUTATIONALMETHOD 1 4
 2 3 4
END


?VDEFINE

DEFINE 1
X
00 0.6666666 LOGNORMAL
ORCES
 1 1.0

DEFINE 2
Y
000 0.8 LOGNORMAL
ORCES
 2 1.0

DEFINE 3

.0 0.2 NORMAL
'OORDINATES
 0.0 0.0
 0.0 0.0
 0.0 0.0
 0.0 0.5
 0.0 0.5
 0.0 0.5
 0.0 1.0
 0.0 1.0
 0.0 1.0
*DEFINE 4
30 0.8 NORMAL
COORDINATES
1 0.0 0.0
2 0.5 0.0
3 1.0 0.0
4 0.0 0.0
5 0.5 0.0
6 1.0 0.0
7 0.0 0.0
8 0.5 0.0
9 1.0 0.0
*PERT 1
 1 0.1
*PERT 2
 2 0.1
*PERT 3
 3 0.1
*PERT 4
 4 0.1
*END
C
C
*MVDEFINE
```

```
*PERT 4
1 2 3 4
*RANVAR 4
1 2 3 4
*DATATYPE 0
*RESTYPE 3
*CONDITION 0
*NODE 1
*COMPONENT 1
*PRINT LONG
*END
C
C
C
*ANYDEFINE
*ITERATION
10 0.05
*CONDITION 0
*NODE 1
*COMPONENT 1
*END
C
C
C
C END PFEM INPUT
*END
C
C
*FEM
*CONS 0
C....MIXED METHOD
*ELEMENTS 4
151
*NODES 9
*BOUNDARY 6
*FORCES 2
*PRINT
*MONITOR 2
*END
*ITER 0 4
50 0.001
*MONITOR
STRESS              NODE 1 COMPONENT 1
*COORDINATES
1 0.0 0.0
2 15.0 0.0
3 30.0 0.0
4 0.0 1.5
5 15.0 1.5
6 30.0 1.5
7 0.0 3.0
8 15.0 3.0
9 30.0 3.0
*ELEMENTS 151
1 1 2 5 4
2 2 3 6 5
3 4 5 8 7
4 5 6 9 8
*BOUNDARY
1 1 0.0
```

```
1 2 0.0
4 1 0.0
4 2 0.0
7 1 0.0
7 2 0.0
*PPOPERTY
1 9 1.0 30.0E6 0.3 1.0 1.0
*FORCES
6 1 500
6 2 1000
*PRINT
TOTAL NODE
STRESS NODE
*END
C
C
*FPI
C pfemd4
*RVIUM 4
*GFUNCTION 1
*DATASETNM 5
*METHOD 1
*PRINTOPT 0
*ANALTYPE 2
*END
*PLEVELS 11
 0.0001
 0.001
 0.01
 0.1
 0.2
 0.5
 0.8
 0.9
 0.99
 0.999
 0.9999
C
*END
```

APPENDIX III

NESSUS ENHANCEMENTS AND TECHNOLOGY SUPPORT

FINAL REPORT

SwRI Project No. 18-1301
Grant #NAG 3 2060

prepared by

David S. Riha

prepared for

The University of Texas ★ San Antonio
San Antonio, TX 78249-0620

September 1999

Southwest Research Institute
6220 Culebra Road • Post Office Drawer 28510
San Antonio, TX 78228-0510

NESSUS ENHANCEMENTS AND TECHNOLOGY SUPPORT

FINAL REPORT

SwRI Project No. 18-1301
Grant #NAG 3 2060

prepared by

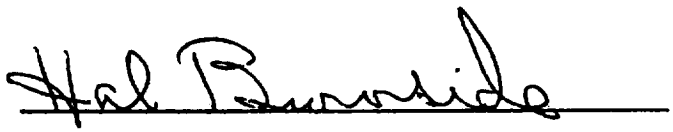
David S. Riha

prepared for

The University of Texas ★ San Antonio
San Antonio, TX 78249-0620

September 1999

APPROVED:



Hal Burnside, Ph.D., P.E., Director
Structural Engineering Department

Table of Contents

Page

EXECUTIVE SUMMARY 99

1. INTRODUCTION 101

2. OBJECTIVES AND ACCOMPLISHMENTS 102

3. MATERIAL MODEL IMPLEMENTATION IN NESSUS 103

4. CONVERGENCE CHECKS IMPLEMENTATION IN NESSUS 107

5. PROMISS CODE UPDATE 110

6. SUPPORT OF NESSUS ACTIVITIES AT UTSA 110

7. SUPPORT OF EDUCATIONAL ACTIVITIES AT UTSA 110

8. CONCLUSIONS 110

9. REFERENCES 111

List of Figures

Figure — Page

1 NESSUS Capabilities 102

2 NESSUS Input for Example Problem 106

3 CDF for Example Problem 107

List of Tables

Table — Page

1 Random Variable Definitions 105

Executive Summary

This report describes the work performed on the project entitled "NESSUS Enhancements and Technology Support." This project was in support of the NASA grant entitled "Research and Education in Probabilistic Structural Analysis and Reliability" awarded to the University of Texas at San Antonio (UTSA). The project included NESSUS software enhancements and technology support for staff and students at UTSA.

The NESSUS probabilistic structural analysis computer program combines state-of-the-art probabilistic algorithms with general-purpose structural analysis methods to compute the probabilistic response and the reliability of engineering structures. Uncertainty in loading, material properties, geometry, boundary conditions and initial conditions can be simulated. The structural analysis methods include nonlinear finite element methods, boundary element methods, and user-written subroutines. Several probabilistic algorithms are available such as the advanced mean value method and the adaptive importance sampling method.

The previous version of NESSUS (version 6.2) was able to perform a reliability analysis of a structure when the failure mode is strength exceeding a stress. However, it required the user to develop a model for the strength portion of the limit-state function using a user subroutine. Another option was to define the strength (i.e., yield stress) as a single random variable. A material strength degradation (MSD) model has been implemented in NESSUS to provide for an alternative material strength capability.

The implementation of the material strength degradation model in NESSUS was compared to previously published results using the PROMISS code. The PROMISS computer program determines the random strength of an aerospace propulsion material due to a number of random effects such as high and low cycle fatigue, temperature, creep, and thermal fatigue. However, the NESSUS results did not match the solution using PROMISS. Upon further investigation of NESSUS and PROMISS, it was found that the sampling scheme in PROMISS was incorrect. This was corrected in the updated version of PROMISS and test cases were developed and exercised for normal, lognormal, Weibull, and nominal variables. After this correction, NESSUS and PROMISS provided the same solution.

The convergence criteria have been improved for the most probable point based methods (MPP) in NESSUS. Specifically for the advanced mean value method (AMV+) and the first order reliability method (FORM). In addition, two new keywords have been added to allow the user more control over the tolerances used to determine convergence.

SwRI supported UTSA in the use and understanding of the NESSUS program. In particular, many questions were answered about the NESSUS input and output in support of Mark Jurena's master's thesis research. Also, questions were answered and assistance provided in developing a suitable problem for an undergraduate course. In addition, David Riha provided two lectures for the UTSA course ME 4653 "Finite Element Applications in Solid Mechanics and Design" describing the NESSUS computer program capabilities and several example problems (Summer 1998 and 1999). SwRI also assisted with computer laboratories associated with these classes

where the students used NESSUS to compute the probabilistic distribution of stress of a simply supported beam.

Southwest Research Institute met the objectives of the grant within budget by enhancing the NESSUS computer program and supporting UTSA in advancing probabilistic mechanics in its curriculum. The NESSUS version 6.3 computer program and updated documentation were delivered at the completion of the project.

1. Introduction

This report describes the work performed on the project entitled "NESSUS Enhancements and Technology Support." This project was in support of the NASA grant entitled "Research and Education in Probabilistic Structural Analysis and Reliability" awarded to the University of Texas at San Antonio (UTSA). The scope of the project included NESSUS software enhancements and technology support for staff and students at UTSA. This report describes the accomplishments of this project

NESSUS

The NESSUS probabilistic structural analysis computer program combines state-of-the-art probabilistic algorithms with general-purpose structural analysis methods to compute the probabilistic response and the reliability of engineering structures. Uncertainty in loading, material properties, geometry, boundary conditions and initial conditions can be simulated. The structural analysis methods include nonlinear finite element methods, boundary element methods, and user-written subroutines. Several probabilistic algorithms are available such as the advanced mean value method and the adaptive importance sampling method.

The application of the code includes probabilistic structural response, component and system reliability and risk analysis of structures considering cost of failure. Figure 1 summarizes the overall capabilities of NESSUS. As seen in the figure, NESSUS contains an integration of probabilistic methods with nonlinear finite element and boundary element methods. A general interface for defining random variables is included. A variety of probabilistic results can be obtained from the analysis of a user-defined structural model.

Combined Stress and Strength Models

The previous version of NESSUS (version 6.2) was able to perform a reliability analysis of a structure when the failure mode is strength exceeding a stress. However, it required the user to develop a model for the strength portion of the g-function using a user subroutine. Another option was to define the strength (i.e., yield stress) as a single random variable. A material strength degradation (MSD) model has been implemented in NESSUS to provide for an alternative material strength capability. All input for the MSD capability is included in the NESSUS/PFEM input file. All previous capabilities in NESSUS for defining the response function are still available.

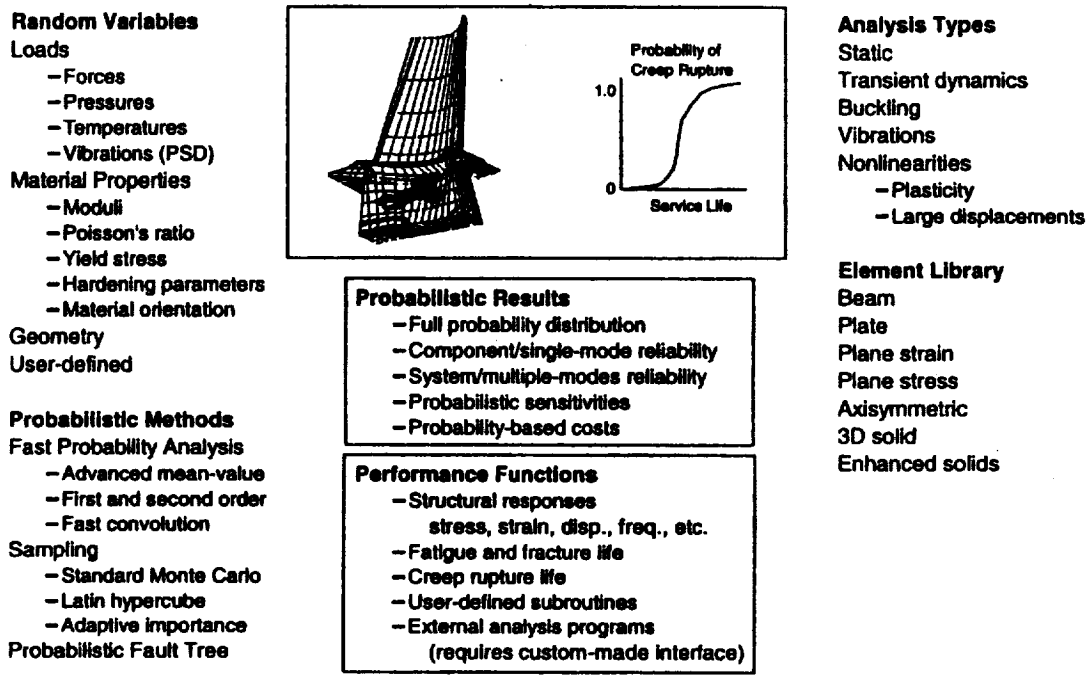


Figure 1. NESSUS Capabilities

2. Objectives and Accomplishments

This report describes the work performed on the project entitled "NESSUS Enhancements and Technology Support." This project is in support of the NASA grant entitled "Research and Education in Probabilistic Structural Analysis and Reliability" awarded to the University of Texas at San Antonio. Southwest Research Institute's (SwRI) tasks under this project were:

1. Provide consulting support for NESSUS-related activities,
2. Ensure that research and educational results can be integrated into NESSUS and that the new capabilities are compatible with previous ones,
3. Implement an identified suitable material model in NESSUS,
4. Implement convergence checks into NESSUS for most probable point (MPP) based methods, and
5. Correct the sampling bias in the PROMISS computer software.

Under this contract, SwRI has successfully implemented the material strength degradation model and convergence checks in NESSUS and the associated documentation has been updated for the new capabilities. The PROMISS computer code was modified to correct a sampling bias. Consulting support for NESSUS-related activities was provided to UTSA researchers and SwRI assisted UTSA in instructing two undergraduate courses dealing with NESSUS. These tasks

were completed within the allocated funding. The following sections describe the completed tasks.

3. Material Model Implementation in NESSUS

3.1 Material Strength Degradation Model

The multi-factor equation for material strength degradation (MSD) has been implemented in NESSUS using the NZFUNC subroutine that was initially developed for predefined resistance models. All input for the MSD model is in the NESSUS/PFEM input deck using a keyword interface consistent with previous versions of NESSUS. The required input is fully described in an updated version of the NESSUS/PFEM User's manual. In addition, all previous capabilities for defining the response function in NESSUS are still available.

This MSD model is based on the multi-factor equation defined in Reference 2. This is an empirical equation and the coefficients are defined using test data and regression. Reference 2 provides values for Inconel 718. The model is currently set up for five fixed effects and 12 user defined effects. These effects are

- Temperature
- High cycle mechanical fatigue
- Low cycle mechanical fatigue
- Creep
- Thermal fatigue
- Up to 12 user defined effects

The form of the equation is

$$S = S_o \underbrace{\left[\frac{T_U - T}{T_U - T_O}\right]^q}_{\text{Temperature}} \underbrace{\left[\frac{N_U - N}{N_U - N_o}\right]^w}_{\text{HCF}} \underbrace{\left[\frac{N'_U - N'}{N'_U - N'_o}\right]^r}_{\text{LCF}} \underbrace{\left[\frac{t_U - t}{t_U - t_o}\right]^v}_{\text{Creep}} \underbrace{\left[\frac{N''_U - N''}{N''_U - N''_o}\right]^u}_{\text{Thermal Fatigue}} \underbrace{\left[\frac{A_U - A}{A_U - A_o}\right]^a}_{\text{User}}$$

Where T is temperature, N is cycles, t is time, and A is used for user defined generic quantities. The lower case exponents are the empirical material constants for each effect. The U subscript refers to an ultimate value, the O subscript is the reference value, and the unscripted term is the current value for the effect.

To increase model sensitivity for any effect as discussed in Reference 2, a log transformation can be introduced. For Inconel 718, all effects except temperature use the log transformation and have the form:

$$S = S_O \left[\frac{\mathrm{LOG}(A_{iU}) - \mathrm{LOG}(A_i)}{\mathrm{LOG}(A_{iU}) - \mathrm{LOG}(A_{iO})} \right]^a$$

For other materials, the nature of the data will dictate the use of the log transformation. The effects to be used and the model type (log transformation) are defined in the Z-function definition section of the PFEM input file. Any combination of effects can be selected and any of the terms can be considered random if desired.

The random variables used in MSD model can also be used in the computational model. For example, if temperature is a random variable, it can be a temperature loading on the finite element model (contributing uncertainty to the stress) and a term in the material strength model (contributing uncertainty to the strength).

The form of the *Z*-function used by NESSUS is

$$z = S_O \, \Pi \left[\frac{A_{iU} - A_i}{A_{iU} - A_{iO}} \right]^{a_i} - \sigma$$

where

S_O	is the reference value of material strength
A_{iU}	is the ultimate value of the particular effect
A_{iO}	is the reference value of the particular effect
A_i	is the current value of the particular effect
a_i	is the empirical material constant for the particular effect
σ	is the structural response, i.e., stress

3.2 Material Strength Degradation Model Input

The material strength degradation model input is described in the NESSUS/PFEM user's manual. The section on predefined resistance models describes the MSD model and all keywords used are defined in the keyword section of the manual. An example problem is presented in the next section to assist with using this new capability.

3.3 Example Problem

The example problem is to compute S/S_O for two effects, high cycle mechanical fatigue and high temperature. The equation for these two effects is

$$\frac{S}{S_O} = \left[\frac{T_U - T}{T_U - T_O} \right]^q \left[\frac{\mathrm{LOG}\ (N_U) - \mathrm{LOG}\ (N)}{\mathrm{LOG}\ (N_U) - \mathrm{LOG}\ (N_O)} \right]^w$$

The formulation defined in NESSUS is

$$Z = S_O \left[\frac{T_U - T}{T_U - T_O}\right]^q \left[\frac{\text{LOG } (N_U) - \text{LOG } (N)}{\text{LOG } (N_U) - \text{LOG } (N_O)}\right]^w - \sigma$$

By defining S to be 1.0 and not including a computational model to compute stress ($\sigma = 0.0$), then NESSUS is solving the problem for S/S_O. The random variables are defined in Table 1

Table 1. Random Variable Definitions

Effect	Symbol	Distribution	Mean	Standard Deviation
High Cycle Mechanical Fatigue (at 75 °F)	N_U	Normal	1.0×10^{10} cycles	1.0×10^{9} cycles
	N	Normal	2.5×10^{5} cycles	2.5×10^{4} cycles
	N_O	Normal	0.25 cycles	0.025 cycles
	W	Normal	0.3785	0.0114
High Temperature (at 1000 °F)	T_U	Normal	2369.0°	236.90°
	T	Normal	1000.0°	100.0°
	T_O	Normal	75.0°	7.5°
	Q	Normal	0.2422	0.0088

The relevant NESSUS input for this problem is shown in Figure 2. Note that to consider a term in an effect random, the alphanumeric name must match the name in the RVDEFINE input. An example of this is the highlighted NU variable shown in both the ZFDEFINE section and the RVDEFINE section in Figure 2.

```
*ZFDEFINE
*EXPLICITMODEL  8
1,2,3,4,5,6,7,8
*ZFUNCT       3    0
 *MSDM  1.0  (So)
     TEMP  LINEAR  TU  T  TO  QQ
     HCF  LOG  NU  N  NO  S
     END
*END
*RVDEFINE
*DEFINE 1
NU
1.0E10 1.0E9    NORMAL
*DEFINE 2
N
2.5E5  2.5E4    NORMAL
*DEFINE 3
NO
0.25  0.025     NORMAL
*DEFINE 4
S
0.3785  0.0114 NORMAL
*DEFINE 5
TU
2369.0  236.9  NORMAL
*DEFINE 6
T
1000.0  100.0  NORMAL
*DEFINE 7
TO
75.0  7.50      NORMAL
*DEFINE 8
QQ
0.2422  0.0088 NORMAL
```

Figure 2. NESSUS Input for Example Problem

The cumulative distribution function is shown in Figure 3.

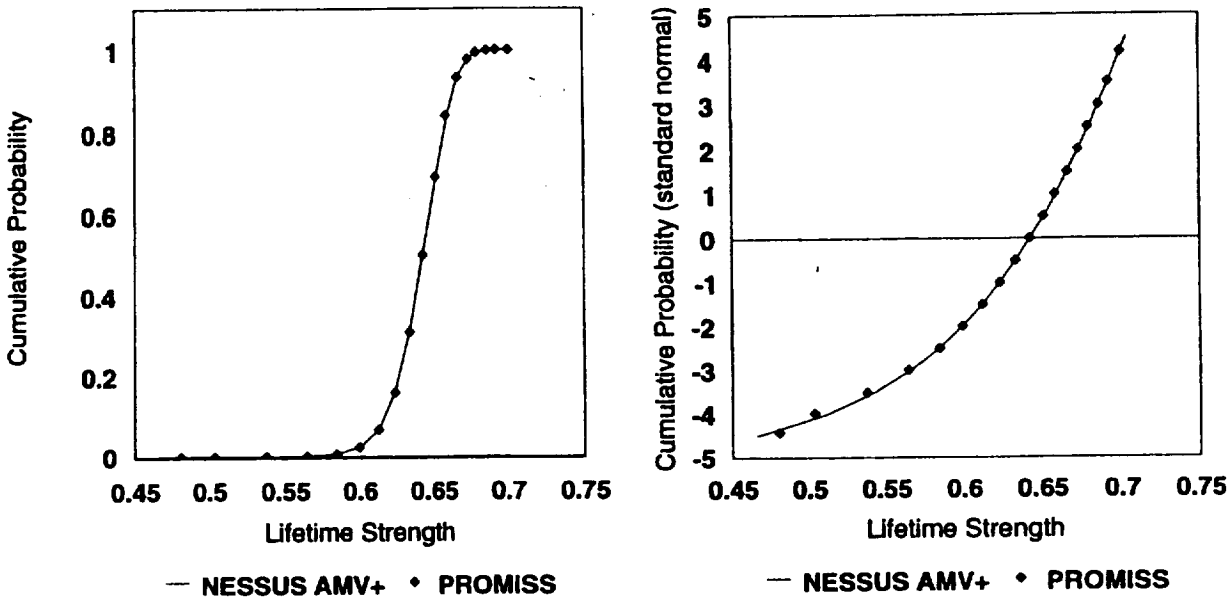


Figure 3. CDF for Example Problem

4. Convergence Checks Implementation in NESSUS

The convergence criteria have been improved for the most probable point based methods (MPP) in NESSUS, specifically for the advanced mean value method (AMV+) and the first order reliability method (FORM). In addition, two new keywords have been added to allow the user more control over the tolerances used to determine convergence. Default values for all tolerances are still available but there are times when these may need to be adjusted. The first order reliability method (FORM) in NESSUS is the cornerstone of several other methods. The following methods use the most probable point (MPP) as a starting point for the probability calculation:

second order reliability method (FORM)
fast probability integration (FPI)
linear based adaptive importance sampling (AIS1)
curvature based adaptive importance sampling (AIS2)
Harbitz importance sampling (ISAMF)

The FORM or FPI method is also used in the AMV+ procedure to compute the probability based on the approximate function.

The FORM uses the Rackitz-Feissler optimization algorithm to locate the MPP. While this is an efficient method and works well for most well behaved problems, it is not guaranteed to converge. There have been several instances where the FORM solution has not calculated the correct results. In many cases this is because of an unobtainable performance value. The previous version of NESSUS did not check the Z value to insure that the located MPP was on the limit-state function. The p-level algorithm using FORM as implemented in NESSUS uses a

quadratic fit of the CDF to determine the Z value for the input probability value. New convergence checks and additional control over the convergence checks have been implemented.

Similar convergence criteria have been implemented in NESSUS for the AMV+ and FORM algorithms. The convergence criteria is different when using the *p*-level (user inputs a probability level and NESSUS computes the performance value) or *z*-level (user inputs a performance value and NESSUS computes the probability value) algorithms. Further details about the convergence criteria and new keyword options are contained in the updated NESSUS documentation. The following convergence criteria are implemented in NESSUS for the AMV+ and FORM algorithms.

FORM Convergence Criteria

For the *z*-level algorithm convergence is defined as

a) the relative change in β is less than a default (0.0001) or user specified tolerance, beta_tol,

$$\frac{|\beta_i - \beta_{i-1}|}{\beta_{i-1}} \leq \text{beta_tol}$$

(note that beta_tol is used for $\beta<4.0$ and 10* beta_tol for $\beta>4.0$)

AND

b) the difference in the computed value of Z and the input value of Z* is less than a maximum allowable tolerance, ztol, times the approximate standard deviation, σ_{app} (the default is 0.001)

$$|Z - Z^*| < \text{ztol} \cdot \sigma_{app}$$

AND

c) the measure of the angle between the MPP's from the last two iterations, θ, is less than a maximum allowable (default of 30° or user defined). θ is defined as $\cos\theta = \alpha_i \bullet \alpha_{i-1}$ where α_i are the direction cosines to the MPP from iteration *i*.

For the *p*-level algorithm convergence is defined as

a) the relative change in *z* is less than a default (.001) or user specified tolerance, ztol, times the approximate standard deviation , σ_{app} ,

$$\Delta Z < \text{ztol} \cdot \sigma_{app}$$

AND

b) the measure of the angle between the MPP's from the last two iterations, θ, is less than a maximum allowable (default of 30° or user defined). θ is defined as $\cos\theta = \alpha_i \bullet \alpha_{i-1}$ where α_i are the direction cosines to the MPP from iteration *i*.

AMV+ Convergence Criteria

For the *z*-level algorithm convergence is defined as

a) the relative change in β is less than a user specified tolerance, beta_tol (default is 0.01)

$$\frac{|\beta_i - \beta_{i-1}|}{\beta_{i-1}} \leq \text{beta_tol}$$

AND

b) the relative change in the computed value of Z compared to the input value of Z* is less than a maximum allowable, ztol (default is 0.01),

$$\frac{|Z - Z^*|}{Z} \leq \text{z_tol}$$

AND

c) the measure of the angle between the MPP's from the last two iterations, θ, is less than a maximum allowable (default of 30° or user defined). θ is defined as $\cos\theta = \alpha_i \bullet \alpha_{i-1}$ where α_i are the direction cosines to the MPP from iteration *i*.

For the *p*-level algorithm convergence is defined as

a) the relative change in *z* is less than a default (0.01) or user specified tolerance, z_tol,

$$\frac{|Z_i - Z_{i-1}|}{Z_{i-1}} \leq \text{z_tol}$$

AND

b) the measure of the angle between the MPP's from the last two iterations, θ, is less than a maximum allowable (default of 30° or user defined). θ is defined as $\cos\theta = \alpha_i \bullet \alpha_{i-1}$ where α_i are the direction cosines to the MPP from iteration *i*.

5. PROMISS Code Update

The PROMISS computer program determines the random strength of an aerospace propulsion material due to a number of random effects such as high and low cycle fatigue, temperature, creep, and thermal fatigue. The implementation of the material strength degradation model in NESSUS was verified using data for Inconel 718 (Reference 2) and compared to the cumulative distribution function. The NESSUS computed CDF did not match the results using PROMISS. Upon further investigation of NESSUS and PROMISS, it was found that the sampling scheme in PROMISS was incorrect. The same starting seed was used for sampling each random variable. This was corrected in the updated version of PROMISS and test cases were developed and exercised for normal, lognormal, Weibull, and nominal variables. In addition for testing purposes, input and output files were given a common file name with appropriate extensions.

6. Support of NESSUS Activities at UTSA

Southwest Research Institute (SwRI) supported UTSA in the use and understanding of the NESSUS program. In particular, many questions were answered about the NESSUS input and output in support of Mark Jurena's master's thesis research. Also, questions were answered and assistance provided in developing a suitable problem for an undergraduate course.

7. Support of Educational Activities at UTSA

Southwest Research Institute (David Riha) provided two lectures for the UTSA course ME 4653 "Finite Element Applications in Solid Mechanics and Design" describing the NESSUS computer program capabilities and several example problems (Summer 1998 and 1999). SwRI also assisted with computer laboratories associated with these classes where the students used NESSUS to compute the probabilistic distribution of stress of a simply supported beam.

8. Conclusions

Previous versions of NESSUS required the user to develop a user subroutine to model the strength portion for a structural reliability analysis or use a single random variable for the strength (i.e., yield stress). The material strength degradation model (MSD) has been successfully implemented and tested in the NESSUS computer program. The MSD model provides a new capability in NESSUS in that there is now a material strength model option for performing reliability analysis with NESSUS that is defined by keywords in the NESSUS input file. All previous capabilities for defining the response function are still available in NESSUS. After correcting a sampling bias in the PROMISS code, NESSUS and PROMISS provide the same results.

The convergence criteria have been improved for the most probable point based methods (MPP) in NESSUS. Specifically for the advanced mean value method (AMV+) and the first order reliability method (FORM). In addition, two new keywords have been added to allow the user more control over the tolerances used to determine convergence. These improved convergence checks will help prevent NESSUS from providing wrong results. This information could be used

to switch to another method to locate the MPP. Future enhancements to NESSUS may include automatically switching to another MPP search method when the solution does not convergence.

Southwest Research Institute also aided the researchers at UTSA with the use of NESSUS in explaining the input and output of the NESSUS program. In addition, SwRI assisted with two undergraduate courses at UTSA by providing lectures about NESSUS and assisting with computer laboratories in which the NESSUS program was used.

9. References

1. Southwest Research Institute and Rocketdyne, "Probabilistic Structural Analysis Methods (PSAM) for Select Space Propulsion System Components," Final Report, NASA Contract NAS3-24389, NASA Lewis Research Center, Cleveland, Ohio, September 1995
2. Bast, C. and Boyce, L., "Probabilistic Material Strength Degradation Model for Inconel 718 Components Subjected to High Temperature, High-Cycle and Low-Cycle Mechanical Fatigue, Creep and Thermal Fatigue Effects," NASA CR 198426, NASA Lewis Research Center, Cleveland, Ohio, November 1995.

Release Notes for NESSUS Version 6.3

prepared by

Southwest Research Institute

NASA Grant NAG 3-2060

prepared for the
National Aeronautics and Space Administration
NASA Glenn Research Center

September 1999

Table of Contents

Page

1 INTRODUCTION 117

2 MATERIAL STRENGTH DEGRADATION MODEL 117

2.1 MATERIAL STRENGTH DEGRADATION MODEL INPUT 119
2.2 EXAMPLE PROBLEM 119

3 MPP (AMV+ AND FORM) CONVERGENCE ENHANCEMENTS 121

3.1 FORM CONVERGENCE CRITERIA 122
3.2 AMV+ CONVERGENCE CRITERIA 123

4 OTHER MODIFICATIONS AND ENHANCEMENTS 124

5 REFERENCES 124

6 APPENDIX 125

List of Tables

Page

TABLE 1. RANDOM VARIABLE DEFINITIONS 119
TABLE 2. MODIFIED NESSUS SUBROUTINES FOR PORT FROM CRAY TO SGI 125
TABLE 3. MODIFIED NESSUS SUBROUTINES FOR THE MATERIAL 125
TABLE 4. MODIFIED NESSUS SUBROUTINES FOR AMV CONVERGENCE ENHANCEMENTS 125
TABLE 5. MODIFIED NESSUS SUBROUTINES FOR FORM CONVERGENCE ENHANCEMENTS. 126
TABLE 6. MODIFIED NESSUS SUBROUTINES FOR OTHER MODIFICATIONS 126
TABLE 7. MODIFIED NESSUS SUBROUTINES FOR CODE CORRECTIONS 127

List of Figures

Page

FIGURE 1. NESSUS INPUT FOR EXAMPLE PROBLEM 120
FIGURE 2. CDF FOR EXAMPLE PROBLEM 121

1 Introduction

These release notes describe the modifications and enhancements of version 6.3 of the NESSUS probabilistic structural analysis code. The relevant sections of the NESSUS documentation have been updated for the new features. The new features in version 6.3 include:

- Material Strength Degradation Model
- MPP (AMV+ and FORM) Convergence Enhancements
- Other Modifications and Enhancements

The following sections describe these enhancements and modifications in more detail. The appendix at the end of this document lists the modified NESSUS subroutines.

2 Material Strength Degradation Model

The previous version of NESSUS (version 6.2) was able to perform a reliability analysis of a structure when the failure mode is strength exceeding a stress. However, it required the user to develop a model for the strength portion of the limit-state function using a user subroutine. Another option was to define the strength (i.e., yield stress) as a single random variable. A material strength degradation (MSD) model has been implemented in NESSUS to provide for an alternative material strength capability.

The multi-factor equation for material strength degradation (MSD) has been implemented in NESSUS using the NZFUNC subroutine that was initially developed for predefined resistance models. All input for the MSD model is in the NESSUS/PFEM input deck using a keyword interface consistent with previous versions of NESSUS. The required input is fully described in an updated version of the NESSUS/PFEM User's manual. In addition, all previous capabilities for defining the response function in NESSUS are still available.

This MSD model is based on the multi-factor equation defined in Reference 1. This is an empirical equation and the coefficients are defined using test data and regression. Reference 1 provides values for Inconel 718. The model is currently set up for five fixed effects and 12 user defined effects. These effects are

- Temperature
- High cycle mechanical fatigue
- Low cycle mechanical fatigue
- Creep
- Thermal fatigue
- Up to 12 user defined effects

The form of the equation is

$$S = S_o\left[\frac{T_U - T}{T_U - T_O}\right]^q \left[\frac{N_U - N}{N_U - N_O}\right]^w \left[\frac{N'_U - N'}{N'_U - N'_O}\right]^r \left[\frac{t_U - t}{t_U - t_O}\right]^v \left[\frac{N''_U - N''}{N''_U - N''_O}\right]^u \left[\frac{A_U - A}{A_U - A_O}\right]^a$$

Temperature HCF LCF Creep Thermal Fatigue User

Where T is temperature, N is cycles, t is time, and A is used for user defined generic quantities. The lower case exponents are the empirical material constants for each effect. The U subscript refers to an ultimate value, the O subscript is the reference value, and the unscripted term is the current value for the effect.

To increase model sensitivity for any effect as discussed in Reference 1, a log transformation can be introduced. For Inconel 718, all effects except temperature use the log transformation and have the form:

$$S = S_O\left[\frac{\mathrm{LOG}(A_{iU}) - \mathrm{LOG}(A_i)}{\mathrm{LOG}(A_{iU}) - \mathrm{LOG}(A_{iO})}\right]^a$$

For other materials, the nature of the data will dictate the use of the log transformation. The effects to be used and the model type (log transformation) are defined in the Z-function definition section of the PFEM input file. Any combination of effects can be selected and any of the terms can be considered random if desired.

The random variables used in the MSD model can also be used in the computational model. For example, if temperature is a random variable, it can be a temperature loading on the finite element model (contributing uncertainty to the stress) and a term in the material strength model (contributing uncertainty to the strength).

The form of the Z-function used by NESSUS is

$$z = S_O \prod\left[\frac{A_{iU} - A_i}{A_{iU} - A_{iO}}\right]^{a_i} - \sigma$$

where

S_O	is the reference value of material strength
A_{iU}	is the ultimate value of the particular effect
A_{iO}	is the reference value of the particular effect
A_i	is the current value of the particular effect
a_i	is the empirical material constant for the particular effect
σ	is the structural response, i.e., stress

2.1 Material Strength Degradation Model Input

The material strength degradation model input is described in the NESSUS/PFEM user's manual. The section on predefined resistance models describes the MSD model and all keywords used are defined in the keyword section of the manual. An example problem is presented in the next section to assist with using this new capability.

2.2 Example Problem

The example problem is to compute S/S_O for two effects, high cycle mechanical fatigue and high temperature. The equation for these two effects is

$$\frac{S}{S_O} = \left[\frac{T_U - T}{T_U - T_O}\right]^q \left[\frac{\text{LOG } (N_U) - \text{LOG } (N)}{\text{LOG } (N_U) - \text{LOG } (N_o)}\right]^w$$

The formulation defined in NESSUS is

$$Z = S_o\left[\frac{T_U - T}{T_U - T_o}\right]^q \left[\frac{\text{LOG } (N_U) - \text{LOG } (N)}{\text{LOG } (N_U) - \text{LOG } (N_o)}\right]^w - \sigma$$

By defining S to be 1.0 and not including a computational model to compute stress (σ = 0.0), then NESSUS is solving the problem for S/S_O. The random variables are defined in Table 1.

Table 1. Random Variable Definitions

Effect	Symbol	Distribution	Mean	Standard Deviation
High Cycle Mechanical Fatigue (at 75 °F)	N_U	Normal	1.0×10^{10} cycles	1.0×10^{9} cycles
	N	Normal	2.5×10^{5} cycles	2.5×10^{4} cycles
	N_O	Normal	0.25 cycles	0.025 cycles
	W	Normal	0.3785	0.0114
High Temperature (at 1000 °F)	T_U	Normal	2369.0°	236.90°
	T	Normal	1000.0°	100.0°
	T_O	Normal	75.0°	7.5°
	Q	Normal	0.2422	0.0088

The relevant NESSUS input for this problem is shown in Figure 1. Note that to consider a term in an effect random, the alphanumeric name must match the name in the RVDEFINE input. An example of this is the highlighted NU variable shown in both the ZFDEFINE section and the RVDEFINE section in Figure 1.

```
*ZFDEFINE
*EXPLICITMODEL  8
1,2,3,4,5,6,7,8
*ZFUNCT       3   0
 *MSDM  1.0  (S0)
     TEMP  LINEAR  TU  T  TO  QQ
     HCF  LOG  NU  N  NO  S
     END
*END
*RVDEFINE
*DEFINE 1
NU
1.0E10 1.0E9    NORMAL
*DEFINE 2
N
2.5E5  2.5E4    NORMAL
*DEFINE 3
NO
0.25  0.025     NORMAL
*DEFINE 4
S
0.3785  0.0114 NORMAL
*DEFINE 5
TU
2369.0  236.9  NORMAL
*DEFINE 6
T
1000.0  100.0  NORMAL
*DEFINE 7
TO
75.0  7.50      NORMAL
*DEFINE 8
QQ
0.2422  0.0088 NORMAL
```

Figure 1. NESSUS Input for Example Problem

The cumulative distribution function is shown in Figure 2.

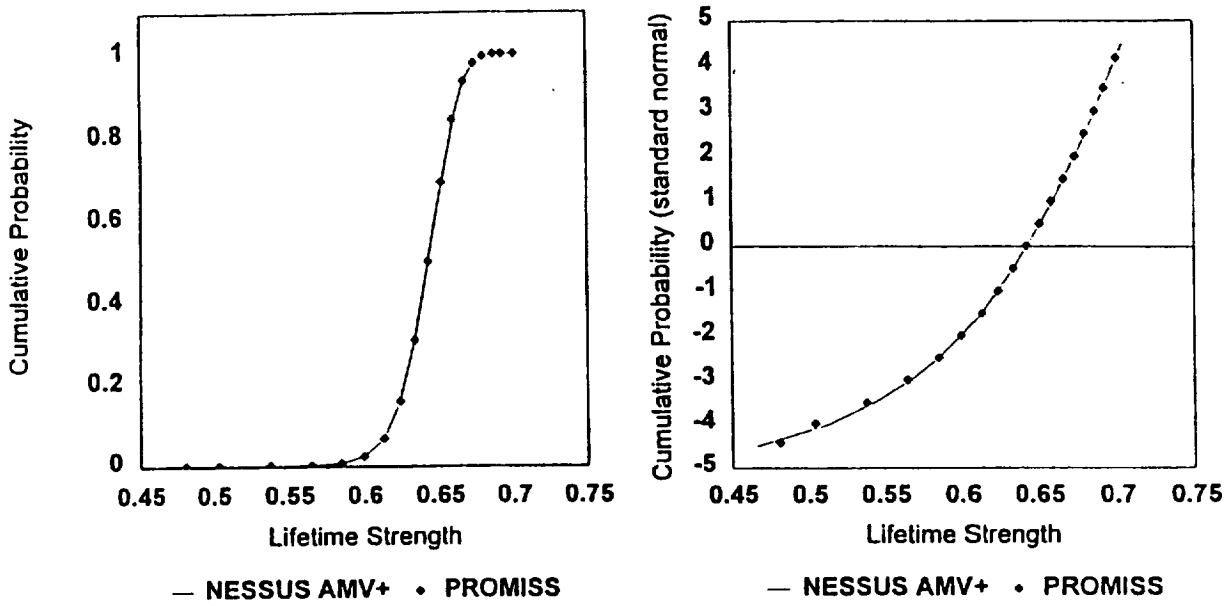


Figure 2. CDF for Example Problem

3 MPP (AMV+ and FORM) Convergence Enhancements

The convergence criteria have been improved for the most probable point based methods (MPP) in NESSUS, specifically for the advanced mean value method (AMV+) and the first order reliability method (FORM). In addition, two new keywords have been added to allow the user more control over the tolerances used to determine convergence. Default values for all tolerances are still available but there are times when these may need to be adjusted. The first order reliability method (FORM) in NESSUS is the cornerstone of several other methods. The following methods use the most probable point (MPP) as a starting point for the probability calculation:

second order reliability method (FORM)
fast probability integration (FPI)
linear based adaptive importance sampling (AIS1)
curvature based adaptive importance sampling (AIS2)
Harbitz importance sampling (ISAMF)

The FORM or FPI method is also used in the AMV+ procedure to compute the probability based on the approximate function.

The FORM uses the Rackitz-Feissler optimization algorithm to locate the MPP. While this is an efficient method and works well for most well behaved problems, it is not guaranteed to converge. There have been several instances where the FORM solution has not calculated the correct results. In many cases this is because of an unobtainable performance value. The previous version of NESSUS did not check the Z value to insure that the located MPP was on the limit-state function. The p-level algorithm using FORM as implemented in NESSUS uses a

quadratic fit of the CDF to determine the Z value for the input probability value. New convergence checks and additional control over the convergence checks have been implemented.

Similar convergence criteria have been implemented in NESSUS for the AMV+ and FORM algorithms. The convergence criteria is different when using the *p*-level (user inputs a probability level and NESSUS computes the performance value) or *z*-level (user inputs a performance value and NESSUS computes the probability value) algorithms. Further details about the convergence criteria and new keyword options are contained in the updated NESSUS documentation. The following convergence criteria are implemented in NESSUS for the AMV+ and FORM algorithms.

3.1 FORM Convergence Criteria

For the *z*-level algorithm convergence is defined as

a) the relative change in β is less than a default (0.0001) or user specified tolerance, beta_tol,

$$\frac{|\beta_i - \beta_{i-1}|}{\beta_{i-1}} \leq \text{beta_tol}$$

(note that beta_tol is used for β<4.0 and 10* beta_tol for β>4.0)

AND

b) the difference in the computed value of Z and the input value of Z* is less than a maximum allowable tolerance, ztol, times the approximate standard deviation, σ_{app} (the default is 0.001)

$$|Z - Z^*| < \text{ztol} \cdot \sigma_{app}$$

AND

c) the measure of the angle between the MPP's from the last two iterations, θ, is less than a maximum allowable (default of 30° or user defined). θ is defined as $\cos\theta = \alpha_i \bullet \alpha_{i-1}$ where α_i are the direction cosines to the MPP from iteration *i*.

For the *p*-level algorithm convergence is defined as

a) the relative change in *z* is less than a default (.001) or user specified tolerance, ztol, times the approximate standard deviation , σ_{app} ,

$$\Delta Z < \text{ztol} \cdot \sigma_{app}$$

AND

b) the measure of the angle between the MPP's from the last two iterations, θ, is less than a maximum allowable (default of 30° or user defined). θ is defined as $\cos\theta = \alpha_i \bullet \alpha_{i-1}$ where α_i are the direction cosines to the MPP from iteration *i*.

3.2 AMV+ Convergence Criteria

For the *z*-level algorithm convergence is defined as

a) the relative change in β is less than a user specified tolerance, beta_tol (default is 0.01)

$$\frac{|\beta_i - \beta_{i-1}|}{\beta_{i-1}} \leq \text{beta_tol}$$

AND

b) the relative change in the computed value of Z compared to the input value of Z* is less than a maximum allowable, ztol (default is 0.01),

$$\frac{|Z - Z^*|}{Z} \leq \text{z_tol}$$

AND

c) the measure of the angle between the MPP's from the last two iterations, θ, is less than a maximum allowable (default of 30° or user defined). θ is defined as $\cos\theta = \alpha_i \bullet \alpha_{i-1}$ where α_i are the direction cosines to the MPP from iteration *i*.

For the *p*-level algorithm convergence is defined as

a) the relative change in *z* is less than a default (0.01) or user specified tolerance, z_tol,

$$\frac{|Z_i - Z_{i-1}|}{Z_{i-1}} \leq \text{z_tol}$$

AND

b) the measure of the angle between the MPP's from the last two iterations, θ, is less than a maximum allowable (default of 30° or user defined). θ is defined as $\cos\theta = \alpha_i \bullet \alpha_{i-1}$ where α_i are the direction cosines to the MPP from iteration *i*.

4 Other Modifications and Enhancements

The following lists identifies several other corrections and enhancements implemented in NESSUS version 6.3:

- corrected error check on Z for AMV+ analysis
- corrected error for implicit sampling using Harbitz method
- changed default tolerance from 0.2 to 0.01 on Z check for AMV+
- tightened tolerance on chi square distribution iteration
- skip integration for special cases of the maximum entropy distribution (e.g. uniform)
- check for valid FPI methods for AMV analyses, correlated variables and implicit sampling
- corrected open statement error in SIMFEM

5 References

1. Bast, C. and Boyce, L., "Probabilistic Material Strength Degradation Model for Inconel 718 Components Subjected to High Temperature, High-Cycle and Low-Cycle Mechanical Fatigue, Creep and Thermal Fatigue Effects," NASA CR 198426, NASA Lewis Research Center, Cleveland, Ohio, November 1995.

6 Appendix

The following tables describe the modified subroutines for NESSUS 6.3.

Table 2. Modified NESSUS Subroutines for Port from Cray to SGI

Description	routines modified
replaced CPU time system call for SGI	quit.f
date and time system call on SGI	dater.f
double precision flag change for 32 bit machine (IDP)	nessus.f
modified arguments as required on SGI for call to GETARG	prompt.f
replaced CPU time system call for SGI	timer.f
initialize ICREAD=5 in nessus main routine	nessus.f
set NDBREC to 80 (file record size)	intint.f

Table 3. Modified NESSUS Subroutines for the Material Strength Degradation Model (MSDM)

Description	routines modified
added predefined equation 3 for material strength degradation model	nzfunct.f
added call to rdmfie to read MSDM input	redpfm.f
new routine to read MSD model input	rdmfie.f
added call to msdump	pfdump.f
new routine to echo MSD model input	msdump.f
added test model	respon.f

Table 4. Modified NESSUS Subroutines for AMV Convergence Enhancements

Description	Routines modified
added input echo for *CONVERGENCE_CONTROL card	pfdump.f
added user control over convergence tolerances	pfemal.f
added user control over convergence tolerances	pfnopt.f
added user control over convergence tolerances	pfyspt.f
added input and checks *CONVERGENCE_CONTROL card	redpfm.f
added user control over convergence tolerances	rfemal.f
added user control over convergence tolerances	uconv.f
added write statement for new convergence tolerances	wrtmov.f

Table 5. Modified NESSUS Subroutines for FORM Convergence Enhancements

Description	routines modified
added z and θ convergence checks and user control over tolerances	fit.f
added input for the *FCONVERGENCE card	redmod.f
added z and θ convergence checks and user control over tolerances	zlevel.f
added write of *FCONVERGENCE card to FPI input deck	fpiter.f

Table 6. Modified NESSUS Subroutines for Other Modifications

Description	routines modified
Changed version number and release date	nessus.f
Corrected format for year 2000	header.f

Table 7. Modified NESSUS Subroutines for Code Corrections

Description	Correction	routines modified
Bus error when using Harbitz method through PFEM. Only affects jobs using ISAMF and IMPLICIT during a PFEM run.	RWORK array not dimensioned in FASTMC. Add RWORK to all calls to FASTMC and other calling subroutines.	cdfglb.f cdfloc.f cintvl.f fastmc.f xfpi.f zlevel.f
Error check on Z incorrect when Z is negative for AMV+ analysis	Take absolute value of ZFUN when making check.	uconv.f
Improved tolerance	change ZERR_TOL form 0.2 to 0.01	uconv.f
Allow small negative eigen values when transforming from correlated variables to independent variables. Can appear for very highly correlated random variables where some independent variables are expected to have variance at or very close to zero. Caused by the numerical algorithm.	Set the eigen value to 10e-10 times the maximum eigen value when negative and if the absolute value is within 1/1000 of the maximum eigen value value.	rottrn.f
Tighten tolerance on chi square distribution	change convergence criteria from 1E-4 to 1E-8 and increase iterations from 10 to 50.	chi.f
Skip integration of maximum entropy distribution if the pdf is constant (uniform distribution).	Add check for constant distribution	cdf6.f
Checks for valid FPI methods for AMV analyses, correlated variables, and implicit sampling.	Added checks after reading input.	redpfm.f
Open too many files on some systems when running SIMFEM	add a close statement for the scratch file	simres.f
Passes single precision number as double precision to XINV (for confidence interval)	set variable P95	fastmc.f
Incorrectly made AD a small number	removed statement	decomp.f

APPENDIX IV

Cody Godines, B.S.M.E.

NASA Grant # NAG 3-2060
Grant Title: Research and Education in Probabilistic Structural Analysis and Reliability

Conference Paper for the 1999 HBCU conference
Sponsored by NASA
Hosted by OAI

Stress Analysis of a Cantilever Beam Using a Deterministic and Probabilistic Finite Element Code (NESSUS).

University of Texas at San Antonio
Spring Semester 1999

Abstract

This paper deals with stress analysis of a cantilever beam. The analysis was performed three different ways. The first analysis of the stresses at different regions within the body were done using simple beam theory. This is an algebraic way of arriving at the stresses without having to do extensive calculations. Stress components were calculated at the location of maximum stress. The maximum stress within the beam was found to occur at the fixed end, it happened to be the normal stress in the longitudinal direction of the beam. Its value was calculated to be 20.2 k.s.i. The second way the stress was calculated was by modeling and analyzing the same beam using NESSUS, a probabilistic finite element code. NESSUS accounts for model uncertainty by allowing the user to input one or more random design variables. Random variables have a range of possible values and associated probabilities of occurring. Three parameters were modeled as being random: the beam's length, its height, the horizontal load, and the vertical load. Thus, the output will also exhibit uncertainty. Three runs were performed using NESSUS. For the first run, the beam was discretized into 4 plane stress elements. The displacement method of analysis was used; hence, NESSUS assumed a displacement field form. The maximum stress occurred at the fixed end and was found to be the normal stress in the x-direction. It's average value was 15 k.s.i, which is a 25.7% difference with respect to simple beam theory. For the second run, the beam was modeled with 40 plane stress elements. The displacement method of analysis was also used for this run. The maximum stress was noted to occur in the same location and was the normal stress in the x-direction. It's average value was 19.5 k.s.i, which is a 3.5% difference with respect to simple beam theory. The third and final way of analyzing the beam in NESSUS was by modeling the beam with 4 plane stress elements, except the mixed method of analysis was used by NESSUS. This means that a stress *and* a displacement field form were assumed by the code. The maximum stress occurred in the same location and was in the same direction. It's average value was 20.3 k.s.i, which is a 0.5% difference with respect to simple beam theory. The final way of calculating the stresses within the beam was done by writing a finite element code, which used the finite element method by way of weighted residuals on the plane stress elasticity equations. The displacement method was used, and the beam was discretized into 40 plane stress elements. The Galerkin-Bubov approach was implemented; hence, the weight functions were chosen from the same shape functions used to bilinearly approximate the displacement field vector. Also, isoparametric mapping was used; thus, because bilinear shape functions were used to approximate the displacement field, the global coordinates were bilinearly mapped to the local coordinates. The maximum stress occurred at the same location and is also the normal stress in the x-direction. It's value was calculated to be 18.8 k.s.i, which is a 3.59% difference with respect to the 40 element, displacement method run performed by NESSUS. A cumulative distribution function was obtained for the 3rd mixed method run. From this probabilistic output, one was able to deduce that there was a 99.99% probability that the maximum normal stress in the x-direction will be less than or equal to 30.4 k.s.i. Therefore, there is a probability smaller than 1/10000 that the beam will fail by yielding.

Introduction

A Cantilevered beam is useful model of reality that engineers use to analyze real structures or parts of real structures. Centrifugal pump impellers and Space Shuttle Main Engine turbopump turbine blades are examples of structures that can be initially modeled as cantilevered beam. Thus, a cantilevered beam is a good, simple model of reality that is useful to acquire a "feel" for the stress magnitudes within a structure.

Many times one would analyze a whole or part of a system to ensure that failure does not occur in a way that hinders the performance of the system. If a system does not perform well when a piece of it breaks, then that is the way it fails. If a system does not perform well when a component permanently deforms or deforms too much, then that is its respective mode of failure. For this paper, we will ensure that a cantilevered beam does not fail by permanently deforming, or yielding. Thus, we analyze to ensure that a system does not fail in a certain way. The system to be analyzed here is a cantilevered beam because it is a good model of things like a turbine blade, which is expensive; and, at their speed of operation, some types of failure can be disastrous.

The System

The system that was analyzed was the cantilevered beam shown in Figure 1. A characteristic of a cantilevered beam is that the horizontal and vertical displacements are zero for all points on the fixed end, this is known as a boundary condition. The beam was composed of steel (ASTM-A36). This material has several associated average

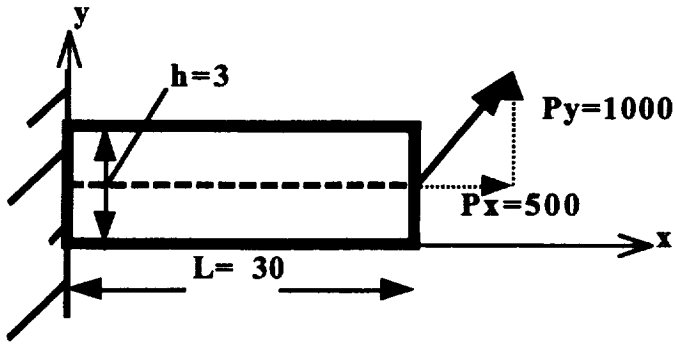


Figure 1. Cantilevered beam. All dimensions are in inches and forces are in pounds. *The beam has a unit depth.*

material properties. For calculations, an average modulus of elasticity and an average Poisson's ratio of 30,000 k.s.i. and 0.3, respectively, were used. The materials average yield strengths in tension and in shear were found to be 36 and 21 k.s.i., respectively.

The system also has certain average geometric properties: its depth is 1.0 inch, the height is 3.0 inches, the length is 30 inches, and its area moment of inertia about the axis normal to the page was calculated from the average dimensions to be 2.25 in^4.

The system has two concentrated loads acting upon it, as shown in Figure 1. These loads cause the system to deform and exhibit internal stresses. A horizontal load and a vertical load, whose average values are 500 lbs. and 1000 lbs., respectively, are applied to the beam's free end, at a point halfway up the height of the beam and uniformly distributed across the thickness. Also, both loads are assumed to be applied quasi-statically so that the dynamic effects of the load application are to be ignored; and, the beam is considered to be in static equilibrium throughout its analysis.

NESSUS

The analysis for this system was performed using NASA Glenn Research Center's Numerical Evaluation of Stochastic Structures Under Stress (NESSUS) software, a probabilistic finite element code. It has the capability of analyzing static and dynamic problems, linear or even nonlinear problems, and it can compute the sensitivity of the wanted output calculations with respect to small variations in the user defined random input variables.

Three different plane stress analyses were accomplished using NESSUS. Therefore, the following assumptions of plane stress must be true:

1. Only σ_{xx}, σ_{yy}, and σ_{xy} are nonzero, the other 6 stress components are zero.
2. Any body force in the z direction is assumed to be zero.
3. As a result of these assumptions and Hooke's Law, which relates stress to strain, we find that strains in the z direction (γ_{xz} and γ_{yz}) are also zero.

4. All variables, stresses, forces, strains, etc. are functions of x and y only, and any loading is assumed to be distributed uniformly across the thickness.
5. Also, from it is known that plane stress prevails in a beam that is thin with respect to its other dimensions [3].

Therefore, since our beam shown in Figure 1 meets all of the assumptions previously stated (as well as those for simple beam theory, which will be discussed later), the plane stress elements in NESSUS can be used to model our beam; and, one should expect results close to those obtained using simple beam theory.

NESSUS uses a finite element method to obtain a solution. It is an approximate method because one cannot generally solve the differential equations that will give us all of the stress or deformation components at every point within the body. Thus, we give up on the hopes of an exact solution and solve the equations only at certain points within the body. These points are known as *nodes*. Based on the values of our solution at these nodes, we can estimate the solution values between the nodes.

The NESSUS code lets one enter certain parameters of our physical model as random variables. Random variables are variables that can be any of a set of values, be this set continuous (infinite in amount), or discrete; and, each value has an associated chance or probability of occurring. These values and their respective chances or probabilities of occurring form a probability distribution function (p.d.f.) for that random variable. Table 1 shows the probabilistic input parameters to be used for all runs in NESSUS.

Table 1. Probabilistic input parameters of the cantilever beam.

Name	**Symbol**	**Distribution Type (mean, std. dev.)**	**Units**
Length	L	Normal (30.0, 0.8)	in.
Height	h	Normal (3.0, 0.2)	in.
Horizontal Load	P_x	Lognormal (500, 0.666)	lb.
Vertical Load	P_y	Lognormal (1000, 0.8)	lb.

Note the distribution types used for geometric and load variables and that these p.d.f.s need only the mean value and the standard deviation to completely describe the respective random variable. Using these random variables and the deterministic or single valued parameters shown in Figure 1, several different analyses were performed using NESSUS. Some typical outputs that NESSUS can compute are the displacements, velocities, accelerations, stresses and strains for each node. For this report, the stress is the output variable and it will be in the form of a random variable. The stress output at each user requested node will have a range of values and each value will have an associated probability of occurring (an output p.d.f. is the result).

1st run.

The first run in NESSUS had a node scheme like that shown in Figure 2. The system was discretized into 4 elements and 9 nodes. The displacement method was used by the software to solve the system of equations, which means that the displacement field took on an assumed form. This analysis required a stress output for each node to ensure that the beam does not fail by permanently deforming. For this first run, the maximum average normal stress on the x face was found to be approximately 15.0 k.s.i., it occurred at node 1. Also, all shear stresses within the beam were less than 1 k.s.i.

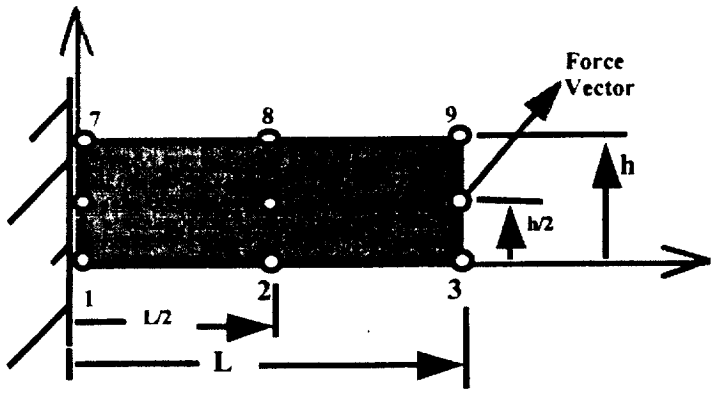


Figure 2. Global node scheme for NESSUS 1st run: 4 element, displacement method.

2nd run.

The second run in NESSUS had the same nodal scheme as the first run. The system model can be seen in Figure 3. This time, the mixed method of analysis was used by the software in solving the system of equations. This means that the software assumes a displacement and stress field form. For this 4-element mixed-method run, the maximum average normal stress on the x face was found to occur at node 1, and was found to be approximately 20.3 k.s.i.. The average shear stresses were all found to be less than 1 k.s.i.

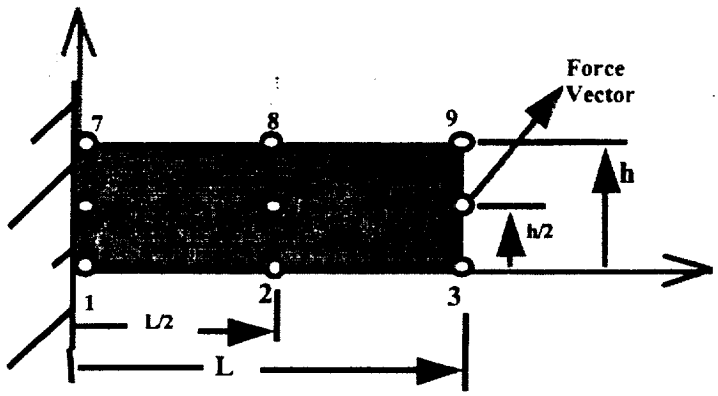


Figure 3. Global node scheme for NESSUS 2nd run: 4 element, mixed method.

3rd run.

The third and final run that was performed in NESSUS had a much finer mesh or node scheme as is shown in Figure 4. Not all elements are shown. The beam was divided into 40 finite elements, the node numbers are shown in ()'s. There are 20 element edges that are equally spaced across the beam's length, and 2 element edges that are equally spaced across the beam's height. The element aspect ratio for this beam is

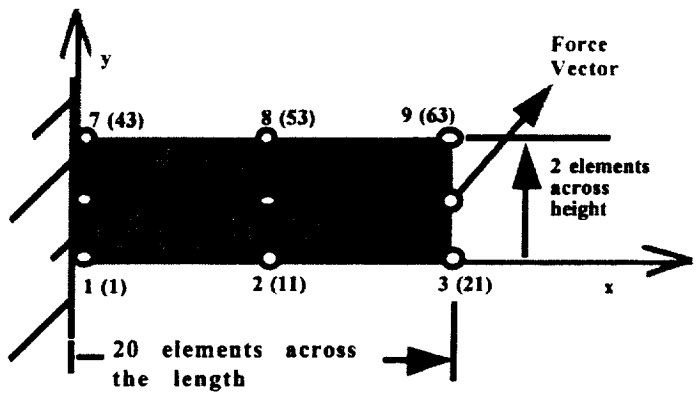


Figure 4. Global node scheme for 3rd NESSUS run: 40 element, displacement method.

1.5:1. This number is the ratio of the element's maximum dimension to its minimum dimension. A conservative approach for any finite element mesh is to try to get this ratio to be as close to 1:1 as possible. This model had a total of 63 nodes that would be reported on in the output file of NESSUS. For this run, NESSUS used the displacement method of analysis to calculate the results. The maximum average normal stress on the x face of all of the 63 nodal points within the body was found to be 19.5 k.s.i. This stress state was found to occur at node 1. Again, all shear stresses on any face at any of the nodal points within the body were found the be less than 1 k.s.i.

How do we know that our values are correct? One way to build confidence in the answers to any black box is to do simple calculations that give an approximate, quick, and cheap answer. The results for the three runs mentioned were checked by using simple beam theory.

Simple Beam Theory

This theory of analysis is also called technical or Euler's beam theory. It is based on certain assumptions that simplify the deformation pattern so that the strain field for a cross section of the member can be determined. The key assumption of this theory is that plane sections before deformation (or loading) must remain plane after deformation (or loading). This is an exact assumption for axially loaded prismatic bars, circular prismatic torsion rods, and for prismatic beams in pure bending. This assumption approaches reality when the shear deformation of the beam is negligible. It has been shown that the bending deflection is about 100 times more than the shear deflection when the length to height ratio of the beam is 10:1; and, as the length to height ratio increases the significance of the bending deflection relative to the shear deflection also increases. Thus, for the beam to be analyzed, simple beam theory is a justifiable method [3].

Also, note that there are two loads whose separate effects on the beam must be superimposed in order to obtain the effects of both loads acting simultaneously. In order to do this, one must have a linear elastic material which remains in the linear elastic range after loading; that is, the stresses within the beam must not exceed their yielding value for

that material. Also, the beam must exhibit small deformations. These deformations are considered small when they produce small strains compared to unity; thus, higher order terms involving theses small strains are also neglected [3].

The first stress calculated was the normal stress in the x direction due to the axial load. This stress was considered constant throughout the beams length and was calculated using the equation

$$\sigma_{xx} = P_x / A \qquad \text{Eq. 1}$$

where σ_{xx} is the stress on the x face in the x direction (hence the subscript), P_x is the axial load shown in Figure 1, and A is the cross sectional area of the beam.

The second stress calculated was the bending stress due to the bending moment within the body. Note from Figure 1 that there are no pure moments applied to the beam, but there does exist a moment at any cross section within the beam, due to the vertical load P_y and the fact that one end is fixed. The bending stress varies with x and y. It can be calculated from the flexure formula:

$$\sigma_{xx} = -\frac{M(x)y'}{I} \qquad \text{Eq. 2}$$

where M(x) is the bending moment within a cross section of the beam at x, I is the area moment of inertia of the beam, and y' is *not* the coordinate used in Figure 1 but one that has its zero at the neutral axis of the beam. Its positive direction must be the same as that of the coordinate y; also, the moment is positive if it produces a positive curvature of the beam (smiley face) with respect to the x coordinate shown in Figure 1 and the y' coordinate just mentioned.

When the moments were summed about an arbitrary centroid of a cross section of the beam, the following equation resulted

$$M(x) = P_y L - P_y x \qquad \text{Eq. 3}$$

where the only undefined term is L, the length of the beam. Note from equation 2 that the maximum stress due to the bending moment occurs when y' is a maximum (at the outer surface), and when the bending moment is a maximum (at the fixed end, x=0; as verified from equation 3). Therefore, since the normal stress due to the axial load is constant

throughout, equations 1, 2, and 3, can be combined to give the following equation that represents the maximum total normal stress on the x face

$$\sigma_{xx} = \frac{P_x}{A} - \frac{P_y(L)(-h/2)}{bh^3/12} \qquad \text{Eq. 4}$$

where h is the height of the beam, and $bh^3/12$ is the area moment of inertia for this beam. Note, this state of stress occurs at x=0, y=0 ($y' = -h/2$). After substituting into equation 4 the numerical values from Figure 1, a value of 20.17 k.s.i. was obtained for the maximum total normal stress in the x direction. Recall that the yield strength in tension for this type of steel is 36 k.s.i; therefore, the beam remained in the linear elastic range after loading. The shear stress was found by using the shear formula

$$\tau_{xy} = \frac{V}{2I}\left(\frac{h^2}{4} - y'^2\right) \qquad \text{Eq.5}$$

where V is the shear force within a cross section of the beam, I is the area moment of inertia of the beam, h is the beam height, and y' is the coordinate system used for the flexure formula [1]. From equation 5, one can see that the shear stress is a maximum at the neutral axis of the beam, where y' is a minimum (zero). When we plug in numerical values into equation 5, the result for the maximum shear stress is 0.5 k.s.i, which is nowhere close to the yield strength in shear, 21 k.s.i. Both the maximum normal (x dir) and the shear stresses were below their respective yield stresses. Therefore, from a deterministic standpoint, this beam does not fail by permanently deforming.

Comparing NESSUS to Simple Beam Theory

The maximum average normal stress within the body was found to be the most significant stress. The magnitude of this stress and its nodal location from all three runs in NESSUS, as well as the results from our simple beam theory calculations are shown in Table 2. This table also shows the percent difference of each NESSUS run with respect to the simple beam theory calculations and the yield strength in tension for ASTM-A36.

Table 2. Maximum average normal stress for NESSUS runs and simple team theory calculations. The percent difference was calculated with respect to the simple bean theory value.

Maximum Average Stress	NESSUS 4 element Displacement Method	NESSUS 4 element Mixed Method	NESSUS 40 element Displacement Method	Simple Beam Theory	Respective yield strengths for ASTM-A36
Node 1, normal	15 k.s.i	20.3 k.s.i.	19.5 k.s.i.	20.2 k.s.i.	36 k.s.i.
% Difference	25.7 %	0.5 %	3.5 %	0 %	N/A

Note from Table 2 that when the amount of elements used to model our beam was increased from 4 to 40 (both using the displacement method of analysis), the normal stress approached the value obtained from simple beam theory. The percent difference was reduced from 25.7 % to 3.5 %. The mixed method of analysis converged to 0.5% of the simple beam theory value using only 4 elements. It took about 12 seconds of computer time, while the displacement method of analysis needed 40 elements and about 19 seconds of computer time to get within range of the simple beam theory stress values. Also note from the table that none of the maximum average stresses for any run exceeded its respective yield strength of the material. Now let us compare NESSUS to a finite element code that I wrote. However, before we do that we shall discuss the theory of the finite element method by way of weighting the residuals.

Finite Element Method by Weighting the Residuals

Using the assumptions mentioned above in the NESSUS portion, the 3D elasticity equations were simplified to the following governing differential equations of plane stress:

$$[L]^T([C][L]\{\delta\}) = \begin{Bmatrix} 0 \\ 0 \end{Bmatrix} \qquad \text{Eq. 8}$$

where L is a differential operator matrix, C is our linear elastic constitutive model for plane stress, and the last term is the displacement vector[2]. Equation 8 can be rewritten to show all elements of each tensor as follows

$$\begin{bmatrix} \frac{\partial}{\partial x} & 0 & \frac{\partial}{\partial y} \\ 0 & \frac{\partial}{\partial y} & \frac{\partial}{\partial x} \end{bmatrix} \left(\frac{E}{1-\nu^2} \begin{bmatrix} 1 & \nu & 0 \\ \nu & 1 & 0 \\ 0 & 0 & \frac{1-\nu}{2} \end{bmatrix} \begin{bmatrix} \frac{\partial}{\partial x} & 0 \\ 0 & \frac{\partial}{\partial y} \\ \frac{\partial}{\partial y} & \frac{\partial}{\partial x} \end{bmatrix} \begin{Bmatrix} u(x,y) \\ v(x,y) \end{Bmatrix} \right) = \begin{Bmatrix} 0 \\ 0 \end{Bmatrix} \qquad \text{Eq. 9}$$

where E is the modulus of elasticity of the steel beam (30,000 ksi), and ν is Poisson's ratio (0.3).

Let us begin the method of residual weighting by premultiplying Equation 9 by a weight function and integrating over the domain of the problem. The result is the following set of equations

$$\int_{\Omega}[W][L]^{T}[C][L]\{\delta\}d\Omega=\int_{\Omega}[W]\begin{Bmatrix}0\\0\end{Bmatrix}d\Omega=\begin{Bmatrix}0\\0\end{Bmatrix} \qquad \text{Eq.10}$$

where W is our weight function matrix. Once equation 10 was integrated by parts and we realize that there are only nodal forces we end up with the following system of equations

$$\int_{\Omega}\left([L][W]^{T}\right)^{T}[C][L]\{\delta\}d\Omega=\{F\} \qquad \text{Eq.11}$$

where F is a vector whose elements are the external forces acting on the system at the nodes in for each direction[2]. For example, if a system has 63 nodes and everything occurs in either the x or y direction (planar), then F would be a vector with 126 rows or entries. After equation 11 is descritized by applying it to each element and summing all of the element equations together, the next step of the finite element method is to approximate our displacement field. For this problem, our displacement fields (u and v) were approximated by bilinear interpolation from the nodal values. This approximation is mathematically realized by the following equation

$$\{\delta\}=\begin{Bmatrix}u(x,y)\\v(x,y)\end{Bmatrix}\cong\left\{\tilde{\delta}^{e}\right\}=[N]\left\{\delta^{e}\right\}=\begin{Bmatrix}\sum_{i=1}^{4}N_i(x,y)u_i\\\sum_{i=1}^{4}N_i(x,y)v_i\end{Bmatrix}$$

$$=\begin{bmatrix}N_1&0&N_2&0&N_3&0&N_4&0\\0&N_1&0&N_2&0&N_3&0&N_4\end{bmatrix}\begin{Bmatrix}u_1\\v_1\\u_2\\v_2\\u_3\\v_3\\u_4\\v_4\end{Bmatrix}=[N]\left\{\delta^{e}\right\} \qquad \text{Eq.12}$$

where u_i and v_i are the nodal displacements of the ith node of the element e in the x and y directions, respectively. The N's are the shape functions for the displacement fields. We

must also make the weight function more specific by setting it equal to the transpose of the shape function matrix

$$[W]=[N]^T \qquad \text{Eq.13}$$

hence, because of this step, we have used the Galerkin approach of the finite element method[2]. When we substitute equations 12 and 13 into equation 11, and if we define an element strain interpolation matrix as

$$[B]=[L][N] \qquad \text{Eq.14}$$

we end up with the following set of equations

$$\left[K^e\right]\left\{\delta^e\right\}=\left[\int_{\Omega^e}[B]^T[C][B]d\Omega^e\right]\left\{\delta^e\right\}=\left\{F^e\right\} \qquad \text{Eq.15}$$

where

$$\left[K^e\right]=\int_{\Omega^e}[B]^T[C][B]d\Omega^e \qquad \text{Eq.16}$$

is defined as the element stiffness matrix and is equal to the term to be integrated (shown in brackets) in equation 15. The stiffness matrix now needs to be calculated. The matrix multiplication, while time consuming, is not difficult. The integration over a two dimensional domain is the difficult part of this step. Gauss quadrature, a typical type of numerical integration, will be used to integrate the 64 terms of each element's 8 by 8 stiffness matrix. In order to do this, we need to change our global coordinate system (x,y), to a local coordinate system (ζ and η). The ζ axis values range from -1 to 1 as does the η axis. Bilinear maping was used to map the x and y coordinates to the ζ and η coordinates. The resulting mapping functions, which are the same shape functions for our field variable and our weight function, are given by the following equations

$$\begin{aligned}
N_1(\zeta,\eta)&=\frac{1}{4}(1-\zeta-\eta+\zeta\eta)\\
N_2(\zeta,\eta)&=\frac{1}{4}(1+\zeta-\eta-\zeta\eta)\\
N_3(\zeta,\eta)&=\frac{1}{4}(1+\zeta+\eta+\zeta\eta)\\
N_4(\zeta,\eta)&=\frac{1}{4}(1-\zeta+\eta-\zeta\eta)
\end{aligned} \qquad \text{Eq.17}$$

Note that in order for the coordinate mapping to be complete, the limits of integration must change from -1 to +1 for both integrals, and our integration variables must change in the following manner

$$d\Omega^e = dx \cdot dy = \left|J^e\right| \cdot d\zeta \cdot d\eta \qquad \text{Eq.18}$$

where J is the Jacobian matrix[2]. The determinant of this matrix is given by the following equation

$$\left|J^e\right| = \frac{\partial x^e}{\partial \zeta}\frac{\partial y^e}{\partial \eta} - \frac{\partial x^e}{\partial \eta}\frac{\partial y^e}{\partial \zeta} \qquad \text{Eq.19}$$

where x and y are the global coordinates of the element whose stiffness matrix is being calculated, given as a function of ζ and η. The resulting equation for the element stiffness matrix comes about by substituting equation 19 into 18, and then 18 into 16.

$$\left[K^e\right] = \int_{-1}^{1}\int_{-1}^{1}[B]^T[C][B]\left(\frac{\partial x^e}{\partial \zeta}\frac{\partial y^e}{\partial \eta} - \frac{\partial x^e}{\partial \eta}\frac{\partial y^e}{\partial \zeta}\right)d\zeta d\eta = \int_{-1}^{1}\int_{-1}^{1} f_{ij}(\zeta,\eta)d\zeta d\eta \qquad \text{Eq.20}$$

where the integrand in equation 20, denoted by $f_{ij}(\zeta,\eta)$, is the function used by Gauss quadrature. The integration operators will be replaced by the sum of the product of the function evaluated at a certain ζ and η value and the weight values for those Gauss points. Therefore, since 2nd order Guass quadrature is sufficient for each coordinate direction [2], equation 20 then becomes

$$\left[K_{ij}^e\right] = \sum_{g=1}^{2}\sum_{h=1}^{2} f_{ij}(\zeta_g,\eta_h)w_g w_h \qquad \text{Eq.21}$$

where $\zeta_1 = \eta_1 = 0.5773502692$, $\zeta_2 = \eta_2 = -0.5773502692$ and the weight functions, w's, are all equal to 1.0. Using equation 21, an element stiffness matrix can be obtained for all isoparametric quadrilateral elements. Remember we are trying to analyze a cantilevered beam and get results comparable to that of NESSUS and simple beam theory. Therefore, our system will be exactly like the 40-element beam modeled in NESSUS, is shown again in Figure 5. Therefore, all 40 element stiffness matrices can be obtained; and, since all of the elements look the same, all the stiffness matrices will look the same. Each element stiffness matrix will be multiplied by a nodal displacement vector to equal an external nodal force vector. Now the question is, how is the global stiffness matrix assembled? Well, due to our procedure in solving

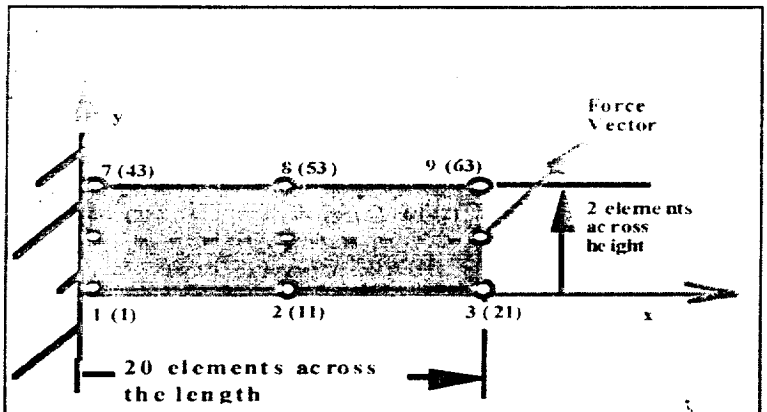


Figure 5. 40 element node scheme for FEA program.

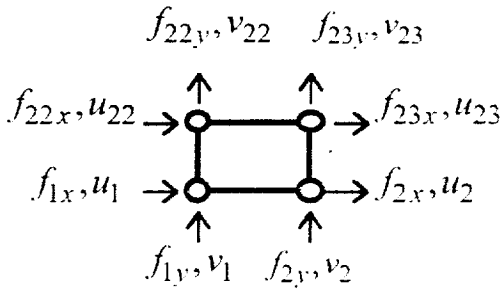


Figure 6. Element 1.

the plane stress equations, the nodal displacement vector for each element is a list of displacements in the x and y direction, for each node in a counter clockwise manner. Also, the nodal force vector for each element is a list of external nodal forces in the x and y direction, for each node in a counter clockwise manner. For example, element 1 of Figure 5, shown in Figure 6, has nodes 1, 2, 23, and 22, associated with it. Therefore, the finite element system of equations for element 1 looks something like $\left[K_{ij}^{\,1}\right]\left\{\delta^1\right\} = \left\{f^1\right\}$, which, when we expand and include (for clarity) the displacement vector terms above the stiffness matrix to account for its columns, we arrive at the following set of equations

$$\begin{matrix} u_1 & v_1 & u_2 & v_2 & u_{23} & v_{23} & u_{22} & v_{22} \end{matrix}$$

$$\begin{bmatrix} K^1_{11} & K^1_{12} & K^1_{13} & K^1_{14} & K^1_{15} & K^1_{16} & K^1_{17} & K^1_{18} \\ K^1_{21} & \cdot & \cdot & \cdot & \cdot & \cdot & \cdot & K^1_{28} \\ \cdot & & \cdot & & & & & \\ \cdot & & & \cdot & K^1_{45} & & & \\ \cdot & & & & \cdot & & & \\ \cdot & & & & & \cdot & & \\ \cdot & & & & & & \cdot & \\ K^1_{81} & \cdot & \cdot & \cdot & \cdot & \cdot & \cdot & K^1_{88} \end{bmatrix} \begin{Bmatrix} u_1 \\ v_1 \\ u_2 \\ v_2 \\ u_{23} \\ v_{23} \\ u_{22} \\ v_{22} \end{Bmatrix} = \begin{Bmatrix} f_{1x} \\ f_{1y} \\ f_{2x} \\ f_{2y} \\ f_{23x} \\ f_{23y} \\ f_{22x} \\ f_{22y} \end{Bmatrix} \qquad \text{Eq.22}$$

This can be done for all 40 elements, except the superscript 1 changes to the element number, and the subscripts 1, 2, 23, and 22 of the nodal displacement and force vector terms respectively change to the 1st, 2nd, 3rd, and 4th node number of the associated element. The 1st node of an element is the lower left node. Proceeding in a counter-clockwise manner one can then obtain the 2nd through the 4th element node number. Note that in equation set 22, any term in the stiffness matrix can be described by its row and column, which is in terms of the nodal displacement vector components. For example, in equation 22,

$$K^{1}{}_{45} = K_{v2,u23} \qquad \text{Eq.23}$$

Therefore, when this term is moved to the global set of equations it is placed in the slot given by the terms of the right hand side of equation 23. After all the terms of the stiffness matrix in equation 22 were assembled in the global set of equations, the result is the following incomplete set of equations

$$\begin{array}{c} \begin{matrix} u_1 & v_1 & u_2 & v_2 & \cdots & u_{22} & v_{22} & u_{23} & v_{23} & \cdots & u_{63} & v_{63} \end{matrix} \\ \begin{bmatrix} K^1_{11} & K^1_{12} & K^1_{13} & K^1_{14} & \cdots & K^1_{17} & K^1_{18} & K^1_{15} & K^1_{16} & \cdots & & \\ K^1_{21} & K^1_{22} & K^1_{23} & K^1_{24} & & K^1_{27} & K^1_{28} & K^1_{25} & K^1_{26} & & & \\ K^1_{31} & K^1_{32} & K^1_{33} & K^1_{34} & & K^1_{37} & K^1_{38} & K^1_{35} & K^1_{36} & & & \\ K^1_{41} & K^1_{42} & K^1_{43} & K^1_{44} & & K^1_{47} & K^1_{48} & K^1_{45} & K^1_{46} & & & \\ \vdots & & & & \ddots & & & & & & & \\ K^1_{71} & K^1_{72} & K^1_{73} & K^1_{74} & & K^1_{77} & K^1_{78} & K^1_{75} & K^1_{76} & & & \\ K^1_{81} & K^1_{82} & K^1_{83} & K^1_{84} & & K^1_{87} & K^1_{88} & K^1_{85} & K^1_{86} & & & \\ K^1_{51} & K^1_{52} & K^1_{53} & K^1_{54} & & K^1_{57} & K^1_{58} & K^1_{55} & K^1_{56} & & & \\ K^1_{61} & K^1_{62} & K^1_{63} & K^1_{64} & & K^1_{67} & K^1_{68} & K^1_{65} & K^1_{66} & & & \\ \vdots & & & & & & & & & \ddots & & \\ & & & & & & & & & & u_{63} & \\ \cdots & & & & & & & & & & v_{63} & \end{bmatrix} \end{array} \begin{Bmatrix} u_1 \\ v_1 \\ u_2 \\ v_2 \\ \vdots \\ u_{22} \\ v_{22} \\ u_{23} \\ v_{23} \\ \vdots \\ u_{63} \\ v_{63} \end{Bmatrix} = \begin{Bmatrix} f_{1x} \\ f_{1y} \\ f_{2x} \\ f_{2y} \\ \vdots \\ f_{22x} \\ f_{22y} \\ f_{23x} \\ f_{23y} \\ \vdots \\ f_{63x} \\ f_{63y} \end{Bmatrix} \qquad \text{Eq.24}$$

where equation 24 becomes the complete set of equations only after this is done in the same manner for all 40 elements. If more than one term appears in the same row and column slot, then the algebraic sum of the numbers is calculated.

Once the complete (global) set of equations are assembled, all of the terms of equation 24 will either be zero or have a numerical value. The next step would be to apply the boundary conditions to the now algebraic differential equation. Recall that for a

cantilevered beam the displacements in the x and y directions are zero at the fixed end. Referring to Figure 5 one can tell that this implies that the terms $u_1, v_1, u_{22}, v_{22}, u_{43}, v_{43}$ are all zero in equation 24. The rest of the terms in the displacement vector $\{\delta\}$ are the unknown displacements of each node in each direction that need to be solved for. Also, the force vector $\{f\}$, which is the list of *external* nodal forces for each direction, contains unknown terms at the same location where the displacements were known. In other words, $f_{1x}, f_{1y}, f_{22x}, f_{22y}, f_{43x}$, and f_{43y} are the external forces to be calculated. The known nodal forces are f_{42x} and f_{42y} which are 500lbs and 1000lbs, respectively. All of the other terms in the force vector are zero, this is verified by referring again to Figure 5 (i.e. the external nodal force in the x direction at node 11 is zero---there is no force applied there).

The next step is to reduce the set of equations. This is done by removing the rows of the force vector, the stiffness matrix, and the displacement vector that correspond to the rows of the displacement vector that have known values (this problem, the ones equal to zero). Then the columns of the stiffness matrix that correspond to the known terms of the displacement are also removed. This forms our reduced set of equations. Using this set the unknown displacements are then calculated in the following manner

$$\{\delta_{REDUCED}\} = \{f_{REDUCED}\}[K_{REDUCED}]^{-1} \qquad \text{Eq.25}$$

The complete set of nodal displacements (global displacement vector) was then obtained by simply expanding its reduced vector in the places where it was reduced and plugging in the terms that were taken out (this case all 0's at nodes 1,22,43). The global force vector can then be calculated using the complete set of equations (equation 24, complete)

$$[K]\{\delta\} = \{f\}$$

where K is the global stiffness matrix (before reduction). Note that the only new terms that will be obtained are the reaction forces at the fixed end of the beam.

Once the nodal displacements and forces are known, other needed items like the stresses or strains at the nodes can be calculated. For this report, we are concerned with

the stresses within the beam. Recall that the first equation we dealt with in this FEM by weighted residuals section was the governing equation for plane stress

$$[L]^T([C][L]\{\delta\}) = \begin{Bmatrix} 0 \\ 0 \end{Bmatrix}$$

where L, C and δ were expanded in equation 9. This equation comes about by substituting the strain-displacement equations of plane stress into the stress-strain equations of plane stress and finally that result into the equilibrium equations for plane stress. However, we can obtain an equation for the stress as a function of displacement by substituting the strain-displacement equations into the stress-strain equations for plane stress. The result is the following set of equations

$$\begin{Bmatrix} \sigma_{xx} \\ \sigma_{yy} \\ \tau_{xy} \end{Bmatrix} = \frac{E}{1-\nu^2} \begin{bmatrix} 1 & \nu & 0 \\ \nu & 1 & 0 \\ 0 & 0 & \frac{1-\nu}{2} \end{bmatrix} \left(\begin{bmatrix} \frac{\partial}{\partial x} & 0 \\ 0 & \frac{\partial}{\partial y} \\ \frac{\partial}{\partial y} & \frac{\partial}{\partial x} \end{bmatrix} \begin{Bmatrix} u(x,y) \\ v(x,y) \end{Bmatrix} \right) \qquad \text{Eq.26}$$

The displacement vector is then replaced by equation 12 and the result is the following equation that can be used to calculate the stress at any point within the beam.

$$\begin{Bmatrix} \sigma_{xx} \\ \sigma_{yy} \\ \tau_{xy} \end{Bmatrix} = \frac{E}{1-\nu^2} \begin{bmatrix} 1 & \nu & 0 \\ \nu & 1 & 0 \\ 0 & 0 & \frac{1-\nu}{2} \end{bmatrix} \left(\begin{bmatrix} \frac{\partial}{\partial x} & 0 \\ 0 & \frac{\partial}{\partial y} \\ \frac{\partial}{\partial y} & \frac{\partial}{\partial x} \end{bmatrix} \begin{Bmatrix} \sum_{i=1}^{4} N_i u_i \\ \sum_{i=1}^{4} N_i v_i \end{Bmatrix} \right) \qquad \text{Eq.27}$$

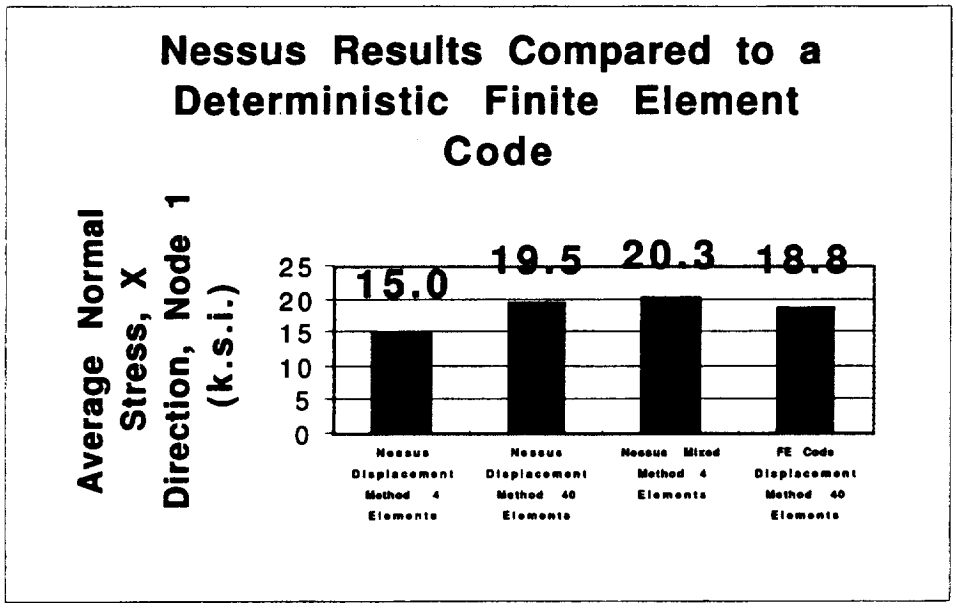
For the beam shown in Figure 5, the maximum average normal stress in the x direction was calculated to be 18.8 k.s.i. It was found to occur at node 1 of the beam. Since the maximum stress did not exceed the tensional yield stress of 36 k.s.i. for the material, the beam did not fail by permanently deforming.

Comparing NESSUS to a Finite Element Code

Since the maximum average normal stress in the x direction was the most significant stress within the beam, we shall compare its values obtained from the three

NESSUS runs to the value obtained from my finite element code. Figure 7 shows the maximum average stress in the x direction obtained from all three runs as well as my finite element code.

Figure7. NESSUS results compared to a deterministic finite element code.



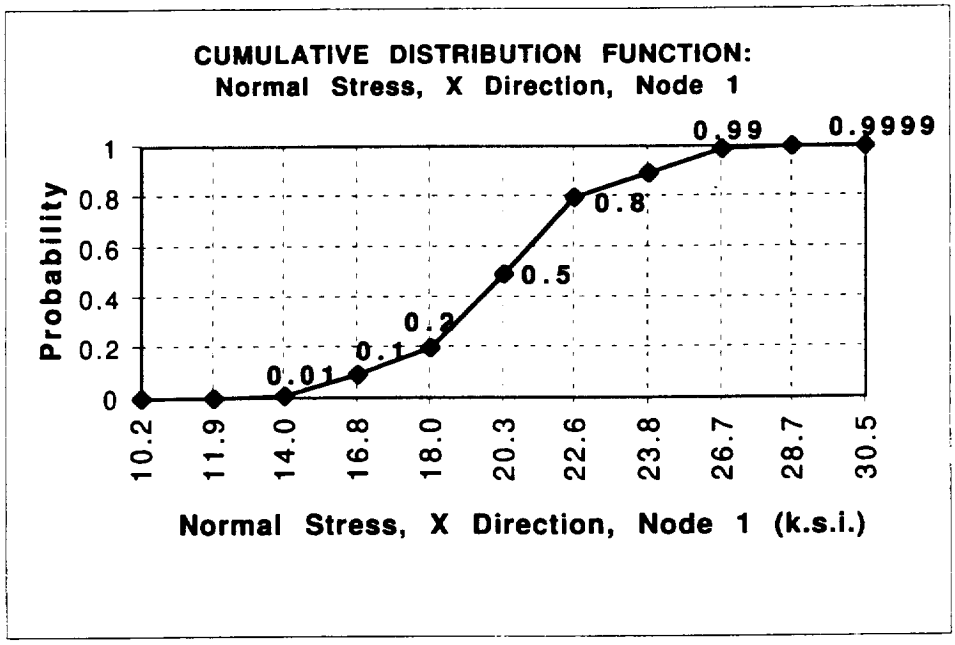
The percent difference between the NESSUS 40 element displacement run and the deterministic FE code 40 element run was calculated to be 3.59%. Now that confidence has been gained with the results from the NESSUS finite element code, let us talk about the most important aspect in NESSUS...its probabilistic capabilities.

Probabilistic NESSUS

NESSUS is a probabilistic finite element code. All of the values that we have discussed thus so far have been calculated from the average values of the design variables. If you will recall some of the variables had only one deterministic value, but the probabilistic design variables had a range of values and associated probabilities of occurring. One form of output that a user might request is the probability density function (p.d.f.) for the stresses that were calculated. However, for structural applications, many times it is desirable that the stress at every point within a material stay below that material's yield stress. When stresses exceed their yield values, plastic or permanent deformation has occurred, or will soon occur [3]. Therefore, since many times an analyst is only concerned with the chances of the solution (or *output*, or *field*) variable

being below a certain value, i.e., the stress within the body being less than the material's yield strength, NESSUS can be used to calculate a cumulative distribution function, a c.d.f., for the requested output. A cumulative distribution function for any random variable (this case our stress solution is a r.v. due to the r.v. inputs) is still the same set of values, but there is another value associated with the c.d.f. for a random variable. This value is the probability or chance that the random variable will be equal to or less than that value. The cumulative distribution function for the normal stress in the x direction at node 1 for the 4 element mixed method run was obtained from NESSUS and graphed in Figure 8.

Figure 8. Cumulative distribution function for node 1 σ_{xx} mixed method run.



From Figure 8, one can deduce that, due to the uncertainties in our model, there is a 99.99% probability that the normal, x-directional stress at node 1 will be equal to or less than 30.5 k.s.i. Recall that the yield strength in tension for this material is 36 k.s.i. Therefore, there is *less than* a 1/10000 probability that the cantilevered beam analyzed will fail by permanently deforming or yielding.

Conclusion

The cantilevered beam was analyzed in the probabilistic finite element code NESSUS with three different runs. For the 4 element displacement method run, the maximum average

normal x-direction stress within the beam was found to be 15 k.s.i. For the 4 element mixed method run, the maximum average normal x-direction stress was found to be 20.3 k.s.i. The 40 element displacement method calculated the maximum average normal x-direction stress to be 19.5 k.s.i. All maximum normal stresses were below the yield strength in tension for the material, which was found to be 36 k.s.i. Also, all maximum shear stresses were less than 1 k.s.i, which is well below the material yield strength in shear of 25 k.s.i. It was noted that the displacement method needed 40 elements to converge upon the value obtained using simple beam theory and while the mixed method of analysis needed only 4 elements. Because the normal stress was found to be the most significant stress it was calculated using simple beam theory to be 20.2 k.s.i. A deterministic finite element code was written and used the displacement method of analysis on a 40 element beam. The maximum average normal x-direction stress was calculated to be 18.8 k.s.i. The percent difference between the 40-element displacement NESSUS run and the other finite element code run was found to be 3.59%. NESSUS was observed to yield good results when compared to simple beam theory and another finite element code. The probabilistic aspect of NESSUS let us obtain the cumulative distribution function for the normal stress in the x direction at the same location of the maximum average stress (at the fixed end). From this c.d.f., we observed that the stress at this node would be equal to or less than 30.5 k.s.i. 99.99% of the time. Knowing that the yield stress in tension for the material was 36 k.s.i., it was concluded that the beam had less than a 1/10000 probability of failure by yielding.

REFERENCES

1. Gere, J.M., Timonshenko, S.P., *Mechanics of Materials*, 3rd ed., PWS, Boston, 1990.
2. Huebner, K.H., Thornton, E.A., Byrom, T.G., *The Finite Element Method for Engineers*, 3rd ed., John Wiley & Sons, New York, 1995.
3. Ugural, A.C., Fenster, S.K., *Advanced Strength and Applied Elasticity*, 3rd ed., Prentice Hall, New Jersey, 1995.

REPORT DOCUMENTATION PAGE

Form Approved
OMB No. 0704-0188

Public reporting burden for this collection of information is estimated to average 1 hour per response, including the time for reviewing instructions, searching existing data sources, gathering and maintaining the data needed, and completing and reviewing the collection of information. Send comments regarding this burden estimate or any other aspect of this collection of information, including suggestions for reducing this burden, to Washington Headquarters Services, Directorate for Information Operations and Reports, 1215 Jefferson Davis Highway, Suite 1204, Arlington, VA 22202-4302, and to the Office of Management and Budget, Paperwork Reduction Project (0704-0188), Washington, DC 20503.

1. AGENCY USE ONLY (*Leave blank*)	2. REPORT DATE	3. REPORT TYPE AND DATES COVERED
	July 2001	Final Contractor Report

4. TITLE AND SUBTITLE

Probabilistic Structural Analysis and Reliability Using NESSUS With Implemented Material Strength Degradation Model

5. FUNDING NUMBERS

WU-910-30-11-00
NAG3-2060

6. AUTHOR(S)

Callie C. Bast, Mark T. Jurena, and Cody R. Godines

7. PERFORMING ORGANIZATION NAME(S) AND ADDRESS(ES)

University of Texas, San Antonio
The Division of Engineering
San Antonio, Texas 78249

8. PERFORMING ORGANIZATION REPORT NUMBER

E-12959

9. SPONSORING/MONITORING AGENCY NAME(S) AND ADDRESS(ES)

National Aeronautics and Space Administration
Washington, DC 20546-0001

10. SPONSORING/MONITORING AGENCY REPORT NUMBER

NASA CR—2001-211112

11. SUPPLEMENTARY NOTES

Contents were reproduced from the best available copy as provided by the authors.
Project Manager, Christos C. Chamis, Research and Technology Directorate, NASA Glenn Research Center, organization code 5000, 216-433-3252.

12a. DISTRIBUTION/AVAILABILITY STATEMENT

Unclassified - Unlimited
Subject Category: 39 Distribution: Nonstandard

Available electronically at http://gltrs.grc.nasa.gov/GLTRS

This publication is available from the NASA Center for AeroSpace Information, 301-621-0390.

12b. DISTRIBUTION CODE

13. ABSTRACT ***(Maximum 200 words)***

This project included both research and education objectives. The goal of this project was to advance innovative research and education objectives in theoretical and computational probabilistic structural analysis, reliability, and life prediction for improved reliability and safety of structural components of aerospace and aircraft propulsion systems. Research and education partners included Glenn Research Center (GRC) and Southwest Research Institute (SwRI) along with the University of Texas at San Antonio (UTSA). SwRI enhanced the NESSUS code and provided consulting support for NESSUS-related activities at UTSA. NASA funding supported three undergraduate students, two graduate students, a summer course instructor and the Principal Investigator. Matching funds from UTSA provided for the purchase of additional equipment for the enhancement of the Advanced Interactive Computational SGI Lab established during the first year of this Partnership Award to conduct the probabilistic finite element summer courses. The research portion of this report presents the cumulation of work performed through the use of the probabilistic finite element program, NESSUS, Numerical Evaluation and Structures Under Stress, and an embedded Material Strength Degradation (MSD) model. Probabilistic structural analysis provided for quantification of uncertainties associated with the design, thus enabling increased system performance and reliability. The structure examined was a Space Shuttle Main Engine (SSME) fuel turbopump blade. The blade material analyzed was Inconel 718, since the MSD model was previously calibrated for this material. Reliability analysis encompassing the effects of high temperature and high cycle fatigue, yielded a reliability value of 0.99978 using a fully correlated random field for the blade thickness. The reliability did not change significantly for a change in distribution type except for a change in distribution from Gaussian to Weibull for the centrifugal load. The sensitivity factors determined to be most dominant were the centrifugal loading and the initial strength of the material. These two sensitivity factors were influenced most by a change in distribution type from Gaussian to Weibull. The education portion of this report describes short-term and long-term educational objectives. Such objectives serve to integrate research and education components of this project resulting in opportunities for ethnic minority students, principally Hispanic. The primary vehicle to facilitate such integration was the teaching of two probabilistic finite element method courses to undergraduate engineering students in the summers of 1998 and 1999.

14. SUBJECT TERMS	15. NUMBER OF PAGES
Reliability; Turbopump blades; Sensitivities; Distributions; Education; Students User's Manual	164
	16. PRICE CODE

17. SECURITY CLASSIFICATION OF REPORT	18. SECURITY CLASSIFICATION OF THIS PAGE	19. SECURITY CLASSIFICATION OF ABSTRACT	20. LIMITATION OF ABSTRACT
Unclassified	Unclassified	Unclassified	